CHARACTERIZATION

OF

ULTRAFILTRATION MEMBRANES

Pore structure and Top Layer Thickness

F. Petrus Cuperus

17

CHARACTERIZATION

OF

ULTRAFILTRATION MEMBRANES

Pore Structure and Top Layer Thickness

PROEFSCHRIFT

ter verkrijging van
de graad van doctor aan de Universiteit Twente,
op gezag van de rector magnificus,
prof. dr. ir. J.H.A. de Smit,
volgens besluit van het College van Dekanen
in het openbaar te verdedigen
op vrijdag 14 september 1990 te 14.00 uur

door

Folkert Petrus Cuperus

geboren op 28 maart 1963 te Meppel

Dit proefschrift is goedgekeurd door de promotor:
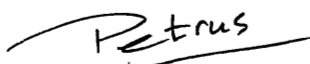prof. dr. C.A. Smolders.
Assistent promotor: dr. D. Bargeman.

Voorwoord

In de afgelopen 4 jaren heeft menigeen me gevraagd wat 'karakteriseren van membranen' inhield. Een, voor deze personen, bevredigend antwoord heb ik volgens mij nooit gevonden! Probeer iemand maar eens uit te leggen dat het opsporen van piepkleine gaatjes van vitaal belang is voor de wetenschap! Zolang een koffiefilter werkt maak je je niet druk om de gaatjes erin! Toch was het juist dit onbegrip, wat mij mede gestimuleerd heeft tot het uitvoeren van het onderzoek en het schrijven van dit proefschrift. Een soort honger naar een niet te verkrijgen waarheid, de ontwikkeling van een 'karakteriseringsfilosofie'. Daarom wil ik een ieder die een dergelijke vraag ooit gesteld heeft bedanken!

Veel support heb ik gehad van mijn kamergenoten: Jaap, Betty, Jaco, Gert, Bart, Herry, Geert-Henk en Hyun-Chai (niet allemaal tegelijkertijd), terwijl de relativerende woorden van de Twentse goeroe Erik Rol me nog lang zullen heugen. De leden van de landelijke karakteriserings- en vervuilingsgroep, alsmede de karakteriserings- en microfiltratie 'cluster'; eveneens bedankt! Het bijna dagelijkse mensa-panel: succes zonder mij! En dan al die DSC uren: dank aan Bert Gebben!

Speciale dank ben ik verschuldigd aan professor Smolders en dr. Bargeman voor de door hen geschapen gelegenheid verschillende aspekten van wetenschappelijk onderzoek te beleven. Gert van den Berg en Arnold Broek: bedankt voor jullie eindeloos geduld tijdens discussies. Patrick Mercera dank ik voor zijn substantiële bijdrage aan hoofdstuk 5, Steven Groot-Wassink voor z'n technical assist, en Zandrie Borneman voor het leveren van de cover van dit proefschrift. Professor Gellings zijn inspanningen om mij de engelse schrijftaal bij te brengen zullen me hopelijk lang bijblijven, net als de tips van dr. Beyer (TEM). Ten slotte dank ik een ieder die op enig andere wijze een bijdrage geleverd heeft aan dit proefschrift!

Petrus

23 Juli 1990

What is the value of this ?
What is the value of science ?
Science has no value..........,
I just enjoy doin' it !

Contents

2 Critical Points in the Analysis of Membrane Pore Structures by Thermoporometry

3 A New Method to Determine the Skin Thickness of
Anisotropic UF Membranes Using Colloidal Gold Particles

4 Permporometry:
Determination of the Size Distribution of Active Pores in UF Membranes

5 Adsorption and Desorption Isotherms Used for the Characterization of UF Membranes

6 Characterization of UF Membranes:
Top Layer Thickness, Pore Structure and Membrane Performance

1

Characterization of UF Membranes
Membrane Characteristics and Characterization Techniques

1.1   Characterization and Membrane History

The Greek word 'charassein' (χαρασσειν) to be translated as 'representing information in a code' is cognate to our word 'character'. It is also the native form of the Greek term 'charac-ter' and 'characteristikos' (χαρακ–τηρ, χαρακτηριστικos) which means 'indicating a peculiar quality' or 'characteristic' [1]. In these terms the meaning of the word 'characterization' is quite obvious, but in reality it is often more cumbersome to define unequivocal and universal characteristics, irrespective whether the definition does pertain to people or to membranes.

Anyway, Lucretius (95-55 BC) who was probably the first European ever writing about filtration in his work 'De Rerum Natura' could have used the word 'characterization' to picture the filtration of water through sand [2]. Although long before Lucretius' time filtration processes were known, exploited and described in the ancient Chinese and Egyptian cultures, one might consider this work as the beginning of separation science in Europe [3]. A very slow start, because it took more than 1500 years before other researchers reported again on the 'new phenomena' of preferential transport of one component through semi-permeable barriers. For instance, La Hire (1640-1718) discovered that, compared to ethanol, water diffused preferentially through a porc bladder. Nollet and Dutrochet (about 1750) used membranes in their osmotic pressure experiments, whereas Graham (1805-1869) used membranes for the separation of crystals from colloids (1854) and accomplished the enrichment of oxygen from air (1863). At the same time, Traube produced the first artificial membranes and many other researchers used membranes in their experiments (Fick, Raoult, van 't Hoff). They also developed the first fundamental theories about membrane structures and transport mechanisms. Graham noted the importance of solubility of components in membranes and, in 1855, Lhermite showed that in principle two different membrane types do exist: porous and

non-porous. Lhermite was also the first who stated the 'solution theory', i.e., permeation as the result of specific interactions between the membrane material and the permeant, but he also recognized that this theory and the 'capillary theories' merge gradually into one another. When Bechhold [4], in 1907, found that the porosity of nitrocellose membranes could be influenced by the manipulation of the collodion concentration in the casting solution, more possibilities became available to study the characteristics of porous membranes thoroughly. Bechhold also developed a technique to evaluate pore sizes in his membranes, which is presently known as the 'bubble pressure method'. Between 1924 and 1926, Zsigmondi systematically investigated porous filter media, which eventually led to the first commercially produced membranes by the Sartorius company [5].

During World War II the development and use of membranes became more important. In Germany, where many cities were being destroyed in air-raids, Sartorius membranes were used in the bacteriological examination of water quality. In the US, the USSR, Great Britain and France, ceramic porous membranes were developed for the enrichment of the gaseous uranium hexafluoride U^{235} isotope. Because the separation efficiency of such membranes for the isotope is very poor, millions of square meters of membrane area had to be used.

(A)　　　　　　　　　　　　　　　(B)

Figure 1. Schematic representation of an isotropic (A) and an anisotropic membrane structure (B).

After the war US-reseachers adopted the knowledge of Sartorius and developed new, better membranes. These polymeric membranes were all of the porous type with pore sizes of at least a few tenths of a micron. Except for the application in isotope enrichment and artificial kidneys, membranes were used only on a small scale for academic and medical purposes. Membranes with different pore sizes or even dense membranes could be made, but showed too poor performance in terms of permeability to be interesting for industrial applications. Only after the development of the anisotropic membrane by Loeb and Sourirajan in 1960, these problems were successfully attacked and a range of new applications became possible. Anisotropic membranes consist of a thin skin layer, which is the essential effective separation layer and a porous sublayer providing the required mechanical stability to the membrane (figure 1). By means of the so-called phase inversion process it became possible to synthesize a variety of porous and non-porous anisotropic membranes from a wide range of polymers. Since then

membrane processes like reverse osmosis (RO), ultrafiltration (UF) and later gas separation and microfiltration (MF) were developed for applications on an industrial scale.

As more complicated membrane systems are developed, the need for consistent theories on membrane structure and membrane performance becomes urgent. A better understanding of the separation mechanism can lead to improved membranes or membrane processes but requires the development of characterization methods and the improvement of models and theories. The characterization of ultrafiltration membranes is the subject of this thesis.

1.2   Characterization: Some Definitions Concerning Porous Membranes

Characterization, as applied to membrane systems, can have different meanings depending on the purpose for which the characteristic data are needed. It may be desirable to have fundamental information about physical properties such as porosity, pore size and pore size distribution but, on the other hand, information concerning the performance of a membrane may be more important. For instance: when the best membrane for a certain separation must be chosen or when the quality of membranes in the manufacturing processes must be controlled. This demands the understanding of the performance properties of the membrane in close relation to the features characteristic for the membrane structure. In addition, the membrane process should be considered with respect to the process streams and the technological features of the whole system [6].

From these considerations, we can define two categories of characteristic parameters: *'performance related parameters'* and *'morphology related parameters'* . The development of consistent theories on membrane structure and performance needs the linkage between the performance and morphology related parameters by a model (figure 2) [7]. For real systems such models may be very complicated. This is not only due to the intricate membrane structures, but also to the complexity of the transport mechanisms and the presence of interfering phenomena like concentration polarization and fouling. The interplay of all these phenomena is responsible for the ultimate membrane performance. From the foregoing recapitulation, it should be clear that characterization involves the development of three main areas:
- accurate determination of the porous structure;
- insight in phenomena which occur during filtration;
- development of models to interpret relationships between preparation, morphology and properties of membranes.
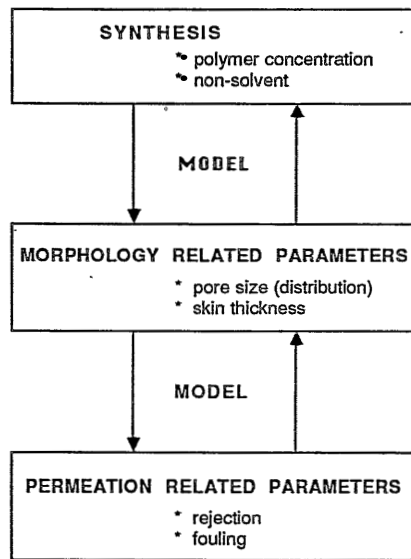
Figure 2. Links between membrane synthesis, morphology related parametrs and permeation related parameters.

In literature several characteristic parameters for membrane performances are enumerated. Permeability, rejection, (effective) diffusion coefficients and separation factors are considered to be the most important ones. Morphology related parameters are pore size, pore size distribution, membrane thickness (for anisotropic membranes: skin thickness), pore shape and various chemical and physical properties like adsorptive and absorptive properties and charge density.

The definition of important membrane characteristics is often a problem, which is not only due to a vague description of such parameters but also is a matter of terminology. For that reason the European Society for Membrane Science and Technology (ESMST) published a list of recommended terms to be used in texts and discussions on membranes [8]. Porous materials have been investigated fundamentally since 1777 (Fontana and Scheel) and consequently the terminology to describe the porous structures has been developed since then. In the following chapters we focus on porous UF membranes and therefore some of these established terms are discussed here.

Ever since the first estimation of pore size in charcoal by Mitscherlich in 1843 [9], the pore size concept has been the most widely used characteristic of porous materials. Dubinin proposed the definition of three pore size classes according to the average width of the pores (which is of course also a little bit arbitrary):

a. macropores: widths exceeding 50 nm (0.05 µm);

b. mesopores: widths between 50 and 2 nm;

c. micropores: widths not exceeding 2 nm.

The elegance of the definition of Dubinin is the fact that the terms are based on clearly different physical adsorption phenomena of gases occurring in pores with a distinct size. Dubinin's definition was considered to be the most expedient by the IUPAC and has been adopted officially in 1972 [10]. According to these definitions microfiltration membranes are porous media

Table 1.   Membrane separation processes and some of their characteristics

membrane process	pore size	other typical characteristics	separation mechanism	remarks
microfiltration	5-0.05 µm	isotropic $\varepsilon \sim 10\text{-}50\%$ [1]	size exclusion	
ultrafiltration	50-2 nm	anisotropic $\varepsilon \sim 0.1\text{-}10\%$	size exclusion	for ceramic types $\varepsilon \sim 10\text{-}50\%$
reverse osmosis	1-0.1 nm [2]	anisotropic	solution diffusion	
dialysis	10-0.1 nm	high porosity $\varepsilon \sim 50\%$	effective diffusion	highly swollen networks
electrodialysis	10-0.1 nm	charge density; ζ- potential	difference in charge	
gas separation	< 0.1 nm	anisotropic;	solution diffusion	
pervaporation	< 0.1 nm	anisotropic;	solution diffusion	volatility required

1) porosity ε: for anisotropic membranes the porosity of the top layer and for isotropic membranes the overall porosity is meant.
2) transition between micropores and intermolecular spaces

with macropores, whereas mesopores are present in skin layers of anisotropic ultrafiltration membranes. Micropores might exist in RO membranes and are certainly present in zeolites, zeolite filled membranes [11] and certain ceramic membranes [12]. The advantage of coupling the well-established IUPAC nomenclature for the pore types to membrane processes like microfiltration and ultrafiltration is the fact that the strong scientific base which other branches of science (catalysis, material science) have already founded, is joined. Since membrane science is expanding rapidly, more overlap with the other branches will occur (e.g., zeolite filled

membranes) and adaptation to the usual terminology is highly desirable.

It is clear that a rough classification of membranes and membrane processes can be made by simply using certain intervals of pore sizes. In some cases, however, a certain overlap exists; e.g., for processes like gas separation, reverse osmosis and pervaporation; so after all the parameter 'pore size' is not a very distinct characteristic. Therefore this classification into pore sizes is often used in combination with other characteristic features (see table 1).

1.3 Characterization of UF Membranes

The major intention of characterization is the prediction of the performance of a membrane from its morphological properties. As mentioned before, this approach requires the use of a model for the pore system and the assumption of a transport mechanism.

There are several reasons for the fact that characterization approaches are not always successful in practice. The problems originate from malfunctions in each of the aspects of characterization:
 a). lack of knowledge of the porous membrane structure,
 b). disturbing phenomena occurring during filtration, like concentration polarization and fouling,
 c). oversimplification of the models used.
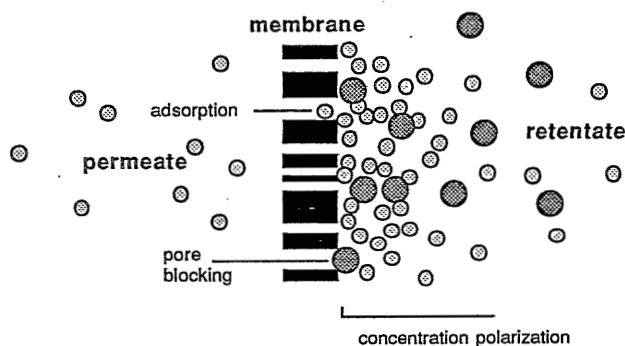
Figure 3. Membrane filtration process (schematic).

Porous media, including UF membranes, usually possess very complicated structures and the models used are gross oversimplifications of the real system. Sometimes it is not even clear which are the most important characteristics of such a porous structure (par. 1.4.2.) and, as a consequence, numerical data which should describe the system are not very precise. During filtration difficulties arise as a consequence of the so-called concentration polarization. This

phenomenon, which is inherent to all pressure driven membrane processes including pervaporation and gas separation [13], is caused by the accumulation of solute near the membrane surface (figure 3). Only for simple systems concentration polarization can be described exactly as is shown by Van den Berg [14]. The situation will be even more complicated when the solutes involved in the ultrafiltration process have a special interaction with the membrane material (adsorption), or block the pores. Although concentration polarization and fouling is primarily induced by the membrane sieving action such anomalous behaviour can hardly be predicted by a pore model, simply because the effects are related to the characteristics of the entire system (solution and membrane) rather than to the actual membrane structure only.

Many researchers [15-17] tried to couple membrane structure and performance. Except for cases where diffusion is the main transport mechanism (dialysis) their efforts had little success. Mason and Wendt [18, 19] suggest a possible reason for these failures: they showed that the commonly used relations between morphology and performance inherently give poor results because the mathematical problem is ill-posed. Mason indicated that a performance related parameter cannot predict membrane structure: one specific performance can be reached by more than one membrane structure. Mason's theory is purely based on mathematical modelling and the results are independent of disturbing effects like concentration polarization. So, a performance characteristic can be useful as an indication, but will not give fundamental information of the membrane process or the membrane structure. From this point of view, the determination of, e.g., the membrane cut-off value[*)] is not a firm basis to predict the performance of real systems but the measurement of structure related parameters should be the first step towards 'total characterization'. The latter can only be reached by using a combination of different morphology and performance related techniques.

1.3.1 Membrane Characteristics and Characterization Techniques

It is clear that for an appropriate modelling of the performance of a porous structure, starting from the morphology, only the parameters relevant for this specific performance are of interest. For instance, for membrane separation the pore size distribution of the interconnected (or active) pores is the important feature whereas for catalysis it is crucial to know the overall porosity, the inner and outer surface area, dead-end and interconnected pores.

Whenever morphology related parameters are to be used to calculate experimental properties it is of great importance to characterize the solid in terms which are related to its performance. So, in a model one should take care to use, e.g., a 'pore size' that is relevant for the actual system and the

---

*) the membrane cut-off value is defined in paragraph 1.3.3.

experimental properties that should be described. For this purpose it is convenient to introduce the term 'active parameter' by which the distinct parameter responsible for the experimental properties is meant. Active parameters can only be measured by a limited number of characterization methods. Generally these parameters are highly model dependent and only in an ideal case the characteristic is an 'active parameter' as well as a parameter describing the overall morphology. For instance, from permeability measurements a hydrodynamic (effective) radius can be calculated (par. 1.4.3), whereas the bubble pressure method of Bechhold (par. 1.4.3. and [4]) yields the least narrow constriction in the interconnected pore channels of the membrane.

The various methods available to analyse porous structures, measure one or more parameters (related to the method) and all the techniques have their distinct advantages and draw-backs. In chapter 1.4 some of the most frequently used characterics are reviewed, followed by a short discussion on some of the methods that can be used to determine these values.

1.3.2 Morphology Related Parameters

Basic morphology related parameters are enumerated in table 2. For an anisotropic membrane, in which the top layer determines the performance, pore size distribution, pore shape (including tortuosity) and top layer thickness are recognized to be complementary parts which should describe all morphological features of the membrane. However, even for simple systems the determination of the parameters mentioned as well as the description of the morphology can turn out to be quite complicated.

Table 2. Some characteristics of UF membranes

morphology related parameters	performance related parameters
pore size (distribution)	(pure water) flux
pore shape	rejection
tortuosity	specific affinity (for adsorption)
surface porosity	hydrophobicity
top layer thickness	charge density
surface roughness	
surface area	

Pore Size
Despite the superficial simplicity of the term, the concept 'pore size' is not always unequivocal. Proper definition is not only troublesome with respect to pore size and pore shape, but also the

'permeation effectiveness' of a pore is a factor that can cause confusion when different characterization methods are compared. The vague definition of pore size is also due to deviations from the assumed pore shape. Generally pores exhibit quite odd shapes, so not only the cross-sectional 'size' is important (as used in cylindrical models, see fig. 4 A), but also the three dimensional pore shape, which influences the resistance of the pore (fig. 4 B). Every model, which couples the membrane structure parameters and the physical phenomena related to that structure, provides a characteristic strictly related to the method and the model (an example has been given in paragraph 1.3.1).
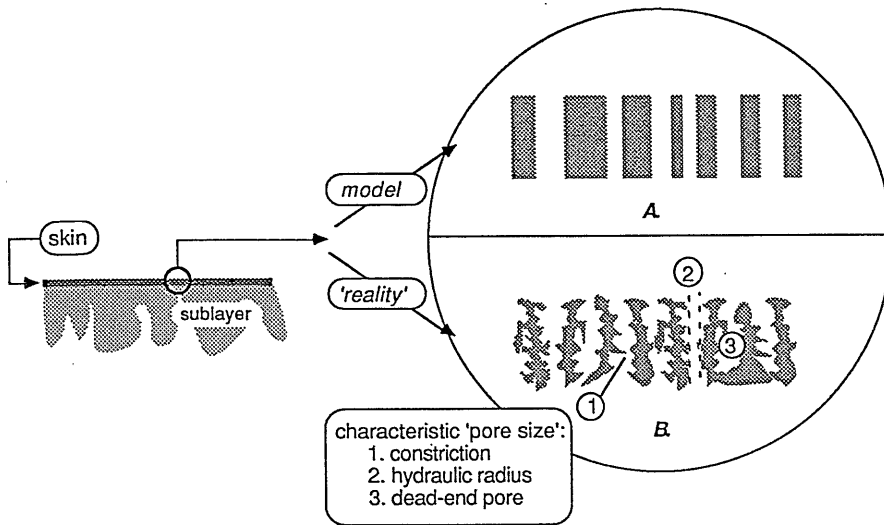
Figure 4. Comparison of ideal model structure (A) and real pore structure (B) in the top layer of an UF membrane.

Surface Porosity

Together with pore size distribution and pore shape, surface porosity is regarded as a very important parameter. With respect to permeability this is only partially true, because the total skin porosity (= surface porosity together with the length of the pore) will determine the membrane resistance. Total skin porosity and surface porosity can deviate to a large extent depending on the structure of the skin, as is illustrated in figure 5.
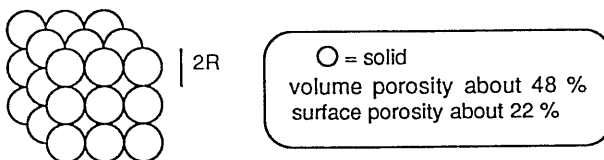
Figure 5. Comparison of surface and volume porosity for a simple model.

Surface porosity can have a severe impact on flux decline during the actual filtration process. As Michaels and others pointed out, sparse surface porosity can aggravate the effect of adsorption and fouling [20, 21]. This is due to a large build-up of solute near the pores. Upon increasing surface porosity, the solute accumulation will be spread more evenly, which also decreases the effect of fouling.

When UF membranes are used as a sublayer for, e.g., composite pervaporation membranes, surface porosity is considered as a key parameter too. In these applications, it is essential to use a supporting membrane which exhibits small pores, a narrow pore size dsitribution and a high surface porosity.

Surface Roughness

Recently, the importance of surface roughness was shown by Fane et al. [21]. Gekas [22] mentioned the probable significance of surface roughness and hydrophobicity. Scanning electron microscopy revealed that surfaces of UF membranes are microscopically rough ('valley'-'hill' differences between 1 and 20 nm), with the pores usually found in the 'valleys'. Roughness on such a small scale does not only increase the surface area (so there are more possibilities for adsorption), but also deteriorates the hydrodynamics near the surface. The latter promotes the effects of concentration polarization and fouling. The accurate determination of surface roughness is difficult. One of the fastest methods available today is the correlation of grey levels of electron micrographs to a certain arbitrary degree of roughness. Though the results are very qualitative, the differences found for the limiting cases: rough and smooth surfaces, at least suggest a relation between surface roughness and fouling [21].

Surface Area

Surface area is important for certain membrane applications, such as affinity membrane systems or catalytic membranes. Also in adsorption studies, the surface area is a crucial parameter. In that respect the ratio of pore area and surface area might be important too [20]. A major point is that one should take care to characterize 'the right surface area'. Adsorption is often due to specific affinity of certain species for certain spots on the membrane surface. Generally it is not possible to compare the surface area determined with a reference molecule like nitrogen and that measured with a protein [9]. Since adsorption of nitrogen is of a physical nature, ruled by van der Waals forces, the whole accessible surface area will be measured. Proteins, however, usually are charged (depending on pH) and specific interaction with charges on the membrane surface occurs. Consequently the surface area measured by protein adsorption is related to the number of active sites. On the other hand, measurements with both sorts of molecules can be used to investigate specific adsorption.

1.3.3 Performance Related Parameters

Pure Water Flux

The pure water flux, which is a measure for the hydraulic permeability of the membrane, is undoubtedly the most extensively used parameter in micro- and ultrafiltration. Although the steady state flux during membrane filtration is a main process feature, the pure water flux itself can hardly be seen as an independent membrane characteristic. It is the result of the interplay of pore size (distribution), tortuosity and thickness of the active part of the membrane and will be influenced very much by fouling and concentration polarization of minor components present in 'pure water'.

Rejection and Selective Permeation

Manufacturers tend to characterize membranes by means of rejection measurements with reference molecules like dextrans, proteins or polyglycols. A parameter extensively used is the cut-off value, which is defined as the lower limit of solute molecular weight for which the rejection is at least 90%. It is argued that these rejection measurements have the closest resemblance to operating conditions. Furthermore, the method can be applied simply to actual membrane devices to be used in practical applications. The latter may be true, but the first argument is at least questionable. Rejection measurements, executed with a single solute like a protein or with molecules having a certain weight distribution, always depend on the type of solute, the membrane (system) and the process parameters used. Especially concentration polarization phenomena will effect rejection measurements very much. Consequently, lab experiments and practical situations are not comparable. As a rule, it is not possible to compare rejection measurements done with the same membrane in different types of equipment, and besides that membranes of different manufacturers with the same claimed cut-off value can show a quite different filtration behaviour.

Specific Affinity, Hydrophobicity and Charge Density

Adsorption and fouling are two of the most persistent phenomena causing flux decline. Adsorption phenomena can be understood from interactions between solute and (pore) surface of the membrane. These interactions can be of physical nature, e.g., hydrophobic interactions, or originate from specific affinity, e.g., when solute and membrane wall are charged. Arguing that adsorption influences the separation process to a considerable extent, specific affinity might be considered as a performance related parameter. On the other hand, one can regard hydrophobicity and charge density as characteristics of the membrane material, but their ultimate effect depends on the conditions in which the membrane is tested or used.

In affinity membranes [23], a special interaction is necessary for an effective process. The most frequently used (but very empirical) way to investigate specific affinity, is measuring the

adsorption of relevant adsorbate-adsorbent pairs. A more fundamental approach concerns the analysis of the molecular groups at the surface of the membranes by, e.g., ESCA, SIMS, NMR or IR-spectroscopy. Such approaches are very time consuming and results mostly are difficult to interpret [24].

Hydrophobicity is suggested to be a very important parameter in membrane fouling and it is expected that a more hydrophobic surface will exhibit a higher degree of fouling. A number of researchers have tried to find a way to express hydrophobicity in a quantitative way. Contact angle measurements are routinely used for dense, flat surfaces but these values cannot be extended to membranes which have a rough surface and contain pores [25, 26]. Recently two methods for the measurement of the 'critical surface tension'[*)] have been published [27, 28]. Although the physical background of these methods is not very clear yet, results do correlate relatively well with expectations concerning grades in degree of hydrophobicity. Despite the extensive research on the subject, the direct relation between hydrophobicity and membrane fouling has not been proven yet. Presumably not only hydrophobicity, but also the interaction between charges present on the membrane surface and the charged species in solution is of great practical importance.

Depending on their molecular structure, membrane surfaces can contain different types of charged spots. But even without such special entities, membrane pore surfaces carry a definite charge [30]. Several species that have to be separated by UF, like proteins, are charged too. In such a case the performance of the membrane will be strongly influenced by the interaction between membrane and solute. The ζ-potential of the membrane, which is correlated with the surface charge of the pores in the membrane, can be measured fairly simply by streaming potential or electro-osmosis measurements [31, 32]. The influence of the interaction between the membrane and the charged solute particles as well as that between particles during filtration can only be described in a semi-quantitative way [14, 33].

1.4   Characterization Techniques

Table 3 shows a number of characterization methods which are presently available. Some of these are still under development, and therefore not (yet) suitable for routine characterization. The majority of these techniques have not been developed specifically for membrane characterization and the interpretation of the results found by these methods needs special care.

---

*)The term 'critical surface tension' is strictly related to the surface tension found using the concept of Zisman [29]. In the case of the 'sticking bubble method' [27] the term 'critical bubble adhesion tension' would be more appropriate.

Table 3. *Characterization methods and characteristic parameters*

method	characteristic	remarks	M / P
gas adsorption-desorption	pore size distribution BET area	dry samples	M
electron microscopy	top layer thickness surface porosity pore size distribution qualitative structure analysis	surface (pore) analysis	M
flux measurements	hydraulic pore radius 'pure water flux'		P
rejection selective permeation	rejection cut-off value		P
bubble pressure method liquid displacement method	pore size distribution	active pores	P/M
mercury porosimetry	pore size distribution	dry samples, measurement of the pore entrance	M
thermoporometry	pore size distribution pore shape	wetted samples	M
permporometry	pore size distribution	active pores	P/M

P: permeation related parameter
M: morphology related parameter

1.4.1 Gas Adsorption-Desorption

This technique can be considered as a standard method in the material science of porous ceramics and catalysts. It is based on the analysis of Thompson (Lord Kelvin) who described the thermodynamics of curved surfaces already in 1855. The theory implies the lowering of the saturated vapour pressure of concave liquid interfaces in comparison with that of a flat surface of the same liquid. This means that inside small pores a gas can condense to a liquid at relative pressures lower than unity. Zsigmondi was the first who used this effect to measure pore sizes and introduced the 'capillary condensation theory' [9].

Gas adsorption isotherms express the relationship between the amount of gas adsorbed, at constant temperature, and the relative pressure. Many (meso)porous systems exhibit a distinct adsorption-desorption behaviour which leads to a characteristic so-called 'type IV-isotherm'. Such isotherms possess a hysteresis loop (figure 6).The origin for the hysteresis effect lies in
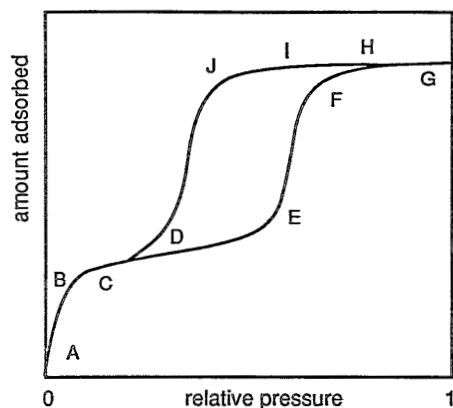
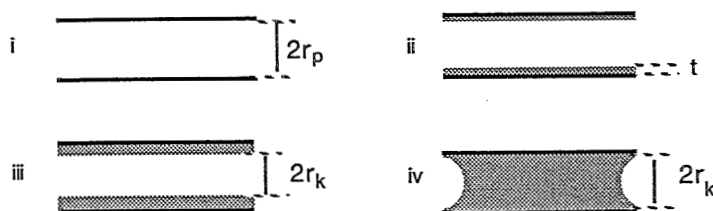*Figure 6. Type IV-isotherm; adsorption branch ACDEFG, desorption branch GHIJDB.*

Figure 7. Several steps in the adsorption analysis; i to iv for increasing relative vapour pressure, iv: capillary condensation has occurred. r_p: pore radius, r_k: Kelvin radius, t: t-layer thickness. Steps are in connection with figure 6: i <--> A, ii and iii <--> BCDE and iv <--> EFG; GHI.

the different geometrical factors which rule the adsorption and desorption process in a mesoporous substrate.

The adsorption-desorption process can be imaged as follows. Due to dispersion forces gas molecules adsorb on the surface of a porous material but this adsorption is restricted to a thin layer on the wall (fig. 6: route ABC). The adsorbed molecules are in thermodynamic equilibrium with the gas phase above the surface and the amount adsorbed is determined by the relative pressure of the gas and the curvature of the interface. At increasing pressure more molecules are adsorbed and layers of adsorbed molecules on the wall form a new liquid-gas interface (fig. 6: point D; fig.7, iii). Because of the curved interface, the vapour pressure of the liquid is lowered. As the curvature of the meniscus passes a certain critical point, pores with a size strictly related to the curvature of the liquid, are filled very quickly: capillary condensation occurs (fig.6, point E). As the pressure is progressively increased the larger pores are filled too (fig.6, EFG).

During desorption the reverse process occurs. At a high relative pressure all pores are filled (fig. 6: GHI) and the equilibrium is governed by the curvature of the meniscus of the liquid at the pore entrance. When the relative pressure is lowered, nothing will happen until the pressure comes below the equilibrium value (given by eq. 1) and the liquid evaporates emptying the entire pore (fig.6, region JD).

When the adsorbed molecules are regarded as a 'normal' fluid with a liquid-gas (l-g) interface, the equilibrium vapour pressure will be determined by the curvature of the (l-g) interface. The most elementary relation in this analysis is the Kelvin equation (1).

$$\ln p_r = (-\gamma v / RT) \cos \Theta * (1/r_{k1} + 1/r_{k2}) \qquad (1)$$

p_r : relative pressure (-) $\qquad\qquad$ Θ : contact angle (°)
γ : interfacial tension (N/m) $\qquad\quad$ r_{ki}: Kelvin radii describing the
v : molar volume liquid (m^3/mol) $\qquad$ curvature of the interface (m)

For capillary pores, with radius r, this equation reads:

$$\ln p_r = (-\gamma v / RT) \cos \Theta * (a/r_k) \qquad (1')$$

with: a = 1 during the adsorption and a = 2 for the desorption process

One has to realize that the radius (r_k) given by the Kelvin equation (1') is the radius of the pore (r_p) minus the thickness (t) of the adsorbed layer (fig. 7), hence:

$$r_p = r_k + t \qquad (2)$$

with: r_p = pore radius (m)
t = thickness of the adsorbed layer (m).

This t-layer thickness has to be determined from adsorption measurements on a flat reference surface. Although in principle incorrect, it is generally accepted to use the t-layer thickness found for silica or to interpolate the t-layer thickness from the experimental data found on the porous sample itself [9].

The Kelvin equation is applicable for pore sizes between about 1 nm and 25 nm, although there is some discussion about the lower limit [7, 9]. The upper limit is set by the experimental difficulty to measure at relative pressures close to unity.

During adsorption and desorption the curvatures of the gas-liquid interface are usually different (which in equation (1') gives rise to the different values for a). Consequently, the condensation and evaporation processes are not the exact reverse of each other and hysteresis arises. The path of this hysteresis curve permits one to work out models about pore structure and shape. Several examples are represented in table 4 and figure 8 [9].

Table 4. *Kelvin radius r_k (in eq. 1'), during the desorption process, compared with pore size characteristics of ideal pore systems (see also figure 8)*

system	size parameters	relationship with r_k and a (eq.1)	
non-intersecting cylindrical capillaries	radius of cylinder = R	a = 2	$r_k + t = R$
parallel plates	slit width = τ	a = 1	$r_k + t = 0.5\,\tau$
packed spheres	sphere radius = R	a = 2	
cubic packing			$r_k + t = 0.414\,R$
rhombohedral packing			$r_k + t = 0.229\,R$

In the gas adsorption-desorption theory the interaction between the solid and the gas is assumed to be very low. But in practice the quantitative description of the adsorption process appears to be influenced by very small differences in interaction energy. Therefore the use of standard adsorption plots determined for a number of classified adsorbent-adsorbate systems, showing different interaction energies, was proposed by Lecloux [34]. However, fundamental aspects in a theoretical as well as in a practical sense are still under development [34].
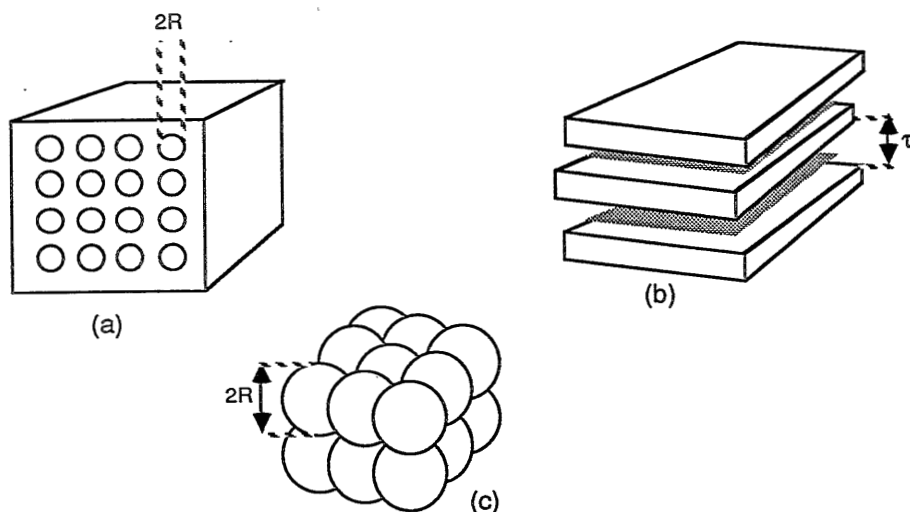
Figure 8. Some idealized pore structures, (a) non-intersecting capillaries, (b) parallel plates and (c) packed spheres, showing different adsorption-desorption hysteresis, see also table 4.

Ceramic membranes can be characterized relatively simply by adsorption-desorption techniques, as shown by several researchers [34, 35]. These membrane systems are quite comparable to the standards used in catalysis (alumina and silica) and the porosity is high

enough to cause a measurable effect. On the other hand only few examples of characterization of polymeric UF membranes by adsorption-desorption studies are known [36-38]. This is probably caused by the low surface porosity usually observed for anisotropic polymeric membranes (see table 5). It is also possible that the pore shape is such that capillary condensation is not found or not recognized [9]. Furthermore, the adsorption-desorption analysis of organic polymers is relatively unknown and phenomena like swelling, caused by the vapour used, do occur. [9, 34].

A general draw-back of the adsorption-desorption method is that the samples have to be dried before the analysis. Therefore the membrane is in a different situation compared to the filtration process. Due to capillary forces, occurring during the drying process, the porous structure may be damaged. Alterations of the structure can also be caused by the de-swelling of the membrane matrix. As a rule, polymeric membranes will be more susceptible to these effects than ceramic membranes.

1.4.2 Electron Microscopy: Qualitative Overall Structure Analysis, Surface Porosity and Top Layer Thickness

Electron microscopy is often used for the observation of membrane structures. Morphological features of microfiltration membranes and, to a lesser extent, of UF membranes can be inspected relatively easily. Especially the Scanning Electron Microscope (SEM) is very suitable for this kind of systems. The ultimate resolution of SEM is about 5 nm which is sufficient for qualitative structure analysis and since the depth of field is high ($\approx$ 150 μm), sharp images of relatively rough surfaces can be obtained. A Transmission Electron Microscope (TEM) in principle has a higher resolving power ($\approx$ 0.3 nm) than SEM has, but the depth of field is only 2 μm (at higher magnifications even smaller). Besides that, very special preparation methods have to be used to make a sample suitable for TEM [39, 40].

In general, the investigation of UF membrane structures by electron microscopy is a delicate and difficult work. This is caused by a number of problems, which in fact, together with the resolution, depth of field and the structure of the sample itself, set the limits of the electron microscopic techniques and determine the suitability of the methods. Furthermore, the interpretation of micrographs may be difficult, analysis is only local and processing of the data may be very time consuming. Some explicit problems are:
1. pores at the surface can be isolated ('blind') and not connected to the porous network.
2. the resolution of the method is too low to detect very small pores.
3. preparation techniques can create artefacts which have a large impact on the final result.

Porous materials are known to be very sensitive to preparation steps such as drying and de-swelling which both can introduce defects in the native membrane structure. These problems are very well known in the biological and medical field and a large number of preparation techniques have been developed to preserve the sample in a state that resembles its native state as closely as possible. One of the newest techniques in this field is cryo-preparation which allows the examination of the membrane structures in the (water-) swollen state. In a microscope (SEM or TEM) equipped with a cryo-unit, preparation as well as examination of the sample at low tempertures is possible (typically -130 °C) [39-41]. The critical step in this preparation method is the freezing of the sample. The cooling rate should be so high that the water is fixed in a glassy state, crystallization should be avoided because this can alter or destroy the structure.

Surface Porosity

The only method which is suitable for the direct estimation of surface porosity is electron microscopy. A major draw-back is that microscopic analysis is very local and that the resolution is insufficient to study finely porous structures. Also, the method becomes very laborious when a reasonable level of precision has to be reached because it is necessary to count and measure a large number of pores. The processing of the data is time consuming, although computer aided image analysis can be used [42]. Consequently, quantitative values of the surface porosity are not much used in practice. The data that are available indicate a very low porosity (0.05-1 %) for the majority of UF membranes, see table 5 [42-49].

It has also been tried to calculate the surface porosity from data found with other characterization techniques. Examples of this approach are the combination of rejection and flux measurements [46] or the liquid-liquid displacement technique and SEM [47]. Starting from the pore size, combined with permeability measurements and assuming a certain skin thickness, tortuosity and pore shape, the number of pores and the surface porosity is calculated. Again the final result will depend strongly on the assumed (and determined) values and the model used.

Top Layer Thickness

Top layer thickness is one of the parameters frequently estimated from electron microscopic pictures. This can give only a rough estimate because the sizes of the pores, present in the top layer, are below the detection level of the EM technique. Also the fact that a clear distinction of the top layer and the support often is not visible, makes a straightforward analysis impossible. In chapter 3 of this thesis a new method for the determination of the skin layer thickness is introduced.

Table 5. *Surface porosity values from literature.*

membrane type and cut-off value (D)	r_p (nm)	r(min-max) (nm)	n (1/m²)	ε_{surf} (%)	method	ref.
XM 100A / 10^5	9	5-12	$30*10^{12}$	0.75	TEM [a]	42
XM 300 / $3*10^5$	12	6-19	$6.7*10^{12}$	0.3	TEM [a]	42
XM 300 / $3*10^5$	12		10^{14}	4.7	TEM [b]	42
Millipore PTSG PSf / 10^4	3	1-15	$4*10^{15}$	7-12	TEM	43
Millipore PSED / $25*10^3$	15	4-75	$2.2*10^{12}$	0.3	TEM	44
XM 50 / $5*10^4$	4	1-12	$5*10^{12}$	0.04	TEM	44
XM 100 / 10^5	7	2-30	$3*10^{12}$	0.54	TEM	44
Millipore VF (10nm)	19	9-70	$2*10^{12}$	0.25	TEM	44
PM 30 / $3*10^4$	6		$2*10^{12}$	2	TEM	45
YM 30 / $3*10^4$				50	TEM	45
UM 10 / 10^4	0.5	0.3-0.8	10^{16}	2.5-4	rejection/flux	46
PM 10 / 10^4	0.8	0.5-1	10^{16}	20	rejection/flux	46
PVDF		3-4	$2*10^{15}$	10	liq. porometry	47
PSf, DDS GR61PP		15-19	10^{14}	1	SEM	48
polyimide UF membranes		1.5-6	$(1-0.1)*10^{15}$	0.7-0.9	TEM	49

r_p: average pore radius   (a): angle sputtered ε_{surf}: surface porosity

n : number of pores   (b): rotary sputtered

1.4.3 Determination of Active Pore Sizes: Permeability Measurements, Bubble Pressure Method and Liquid Displacement Technique

Permeability

Permeability of a membrane for a certain liquid as such can be considered as a characteristic parameter, but often a so-called hydraulic radius is calculated from the measured fluxes. In such an analysis, the permeability is determined, the porosity ε, the tortuosity τ and the membrane thickness 1 are estimated (or preferably determined) and subsequently the pore size can be calculated from the Hagen-Poiseuille equation (3).

$$J = P * (\Delta p / l) \qquad (3)$$

with: $\quad P = n \pi r^4 / 8 \eta \tau \qquad (3')$

J = flux (m/s)	l = membrane thickness (m)
P = permeability (m^{3}s/kg)	Δp = pressure difference
n = number of pores (1/m^2)	across the membrane (N/m^2)
η = viscosity (kg/ms)	τ = tortuosity (-)

It is obvious that such an approach depends largely on the model as well as on the estimated values used. Also, the model cannot discriminate between a system with few large pores and one with a large number of small pores (when, of course n r^4= constant).

The method can be improved by using a gas as the permeating medium instead of a liquid. As the transport mechanism for gases is dependent on the overall pressure in the system <u>and</u> the pore size, discrimination between fine and coarse porous media is possible when the permeability at different pressures is measured. An accurate quantitative description of such systems and therefore the calculation of the hydraulic radius is still ambiguous [50].
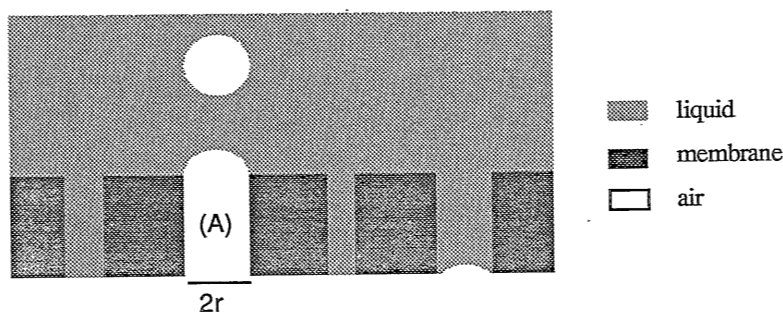

Figure 9. Principle of the 'bubble pressure technique'. In pore (A) the bubble point has just been reached, eq. (4) holds.

Bubble Pressure Method and Liquid Displacement Technique

The bubble pressure method, introduced by Bechhold in 1908, is based on the measurement of the pressure necessary to blow air through a water-filled porous membrane (figure 9). Using Cantor's equation (4) a pore size can be calculated.

$$r = 2\,\gamma\cos\Theta\,/\,\Delta p \qquad\qquad (4)$$

where: r = radius of the capillary (m)
  γ = surface tension (water/air) (N/m)
  Θ = contact angle ($^{\circ}$)
  Δp = pressure difference across the membrane (N/m^2)

Usually complete wetting is assumed, i.e., $\cos\Theta = 1$.

In its most simple form, the moment at which the first bubbles appear, 'the bubble point', is determined visually. The pore size that is related to this 'bubble pressure' represents the largest pore present in the membrane.

When the method is applied to MF membranes with pore sizes between 1.5 and 0.15 µm, typical bubble pressures are between 0.1 and 1 MPa. For UF membranes with pores that are much smaller, higher pressures (about 10 MPa) are necessary. At these pressures the membrane matrix will deform and the structure will be altered, which will consequently lead to erroneous results. To avoid this, Bechhold and Erbe [51] used penetrating systems consisting of two immiscible liquids, which exhibit a low interfacial tension. For the immiscible pair isobutanol/water an interfacial tension of 1.85 mN/m at 20 $^{\circ}$C is found and the system water/isobutanol/methanol(25/15/7 v/v) exhibits an interfacial tension of 0.35 mN/m [51, 52]. With the latter system pores of about 1.5 nm are already 'opened up' at pressure differences of 0.5 MPa.

When this so-called 'liquid-liquid displacement technique' is combined with the permeability method, a pore size distribution rather than the largest pore of the medium is found. For such permeability measurements a set-up similar to the one used for bubble point measurements is used, but now the applied pressure and the flux through the membrane are measured simultaneously. Transport through a pore will start at the moment that the first liquid is displaced by the second one, i.e., at a pressure difference given by equation (4). Once the pore is open, transport will increase upon increasing the pressure difference as described by equation (3). Using a capillary model together with a proper estimation of tortuosity and the thickness of the membrane (or the skin layer thickness), the number of pores can be calculated.

Co-workers of Bechhold found that the observed pore sizes depend on the rate of pressure increase. The faster the pressure was raised, the smaller the measured 'pore size' values appear to be. Schlesinger attributed this effect to the viscosity of the two phases [52], but although he

corrected equation (3) for this effect, the resultant relation did not completely account for all the deviations from the ideal case. It might be that a wetting effect disturbs the measurement [53, 54]. This means that it is not sufficient to determine the 'bubble-pressure curve' of the membrane, but one should also correct for incomplete wetting.

Another disadvantage of the liquid displacement technique is that polymeric membranes may swell or shrink in the alcohol-water system (compared to pure water). As Nikitine pointed out [55], this influences the measured pore sizes. To get an impression of the effect, several permeating media causing a different degree of swelling, should be used. Anyway, the often used argument that during these measurements, the membrane should be in an environment close to 'real' filtration condition does not hold.

To increase reproducibility and accuracy of liquid displacement measurements, researchers nowadays use high precision devices and computerized set-ups [56, 57]. Especially for the UF membranes these are substantial improvements, which permit measuring conditions close to equilibrium so corrections in the sense of Schlesinger [52] are not necessary anymore. Also the technique becomes more suitable for standard measurements.

1.4.4 Mercury Porosimetry

This technique has the same basis as the bubble pressure method: the Cantor equation (eq. 4). But as mercury is a non-wetting liquid, Θ will be higher than 90°. A widely accepted value for Θ is 140°. Originally, mercury porosimetry was mainly used for the characterization of macroporous structures. The technique itself consists in the measurement of the volume of mercury which is forced into the pores of an evacuated porous sample. As the method is simple, it enjoys great popularity among ceramic material scientists. Unfortunately, the method is hardly applicable for UF membranes, since pressures are very high for pores in the nanometer range. A pore of 4 nm corresponds to a pressure of ≈200 MPa, a pressure which may damage ceramic UF membranes and surely will densify the structure of polymeric membranes [58, 59].

1.4.5 Thermoporometry

Thermoporometry, introduced by Brun and Eyraud [35, 60, 61], is based on the microcalorimetric analysis of solid-liquid transformations in porous materials. Since the system of water-filled pores has the closest resemblance with the practical situation of membrane filtration, the solid-liquid transition of water is used for the pore size analysis. Due to the strong curvature of the solid-liquid interface present within small pores, a freezing (or melting) point

depression of the water (or ice) occurs. A full thermodynamic description of this phenomenon is given by Brun et al. [60, 61]. According to this concept, the size of a confined ice crystal (which is set by the size of the pore), is inversely proportional to the degree of undercooling, whereas the pore volume is directly related to the apparent transition energy. With a differential scanning calorimeter (DSC) the transition can be monitored easily and, using the concept of Brun et al., a pore size distribution is calculated. In chapter 2, the determination of pore size distributions of various membranes using thermoporometry is discussed extensively.

1.4.6 Permporometry

Permporometry is a relatively new technique by which the size distribution of the active pores of an UF membrane can be measured [62, 63]. The technique is based on the controlled blocking of pores by condensation of a vapour, present as a component of a gas mixture, and the simultaneous measurement of the gas flux through the membrane. The capillary condensation process is related to the relative vapour pressure (see: Kelvin relation (eq. 1)), so exact control of the relative vapour pressure permits stepwise blocking of pores. Starting from a relative pressure equal to 1, all the pores of the membrane are filled, hence unhindered gas transport through the membrane is not possible. When the vapour pressure is reduced, pores with a size corresponding to the vapour pressure set, are emptied and become available for gas transport. By measuring the gas transport through the membrane upon decreasing relative vapour pressure, the size distribution of the active pores can be found. The possibilities of this technique are investigated and discussed in chapter 4 and 6 of this thesis.

1.4.7 Rejection, Selective Permeation and Fouling

As already mentioned before, rejection measurements are often seen as the 'standard' characterization method. Since phenomena like concentration polarization, pore blocking and fouling will interfere severely with selective permeation measurements, the analysis is less suitable for fundamental characterization purposes. Only by choosing special circumstances, a better defined process may be established and conclusions in relation to the pore structure are possible.

Diffusion processes, the main transport mechanism in, e.g., dialysis, are well-defined and concentration polarization will only have a minor effect on membrane performance (because diffusion through the membrane is a relatively slow process). Klein [15] has shown that hemodialysis membranes can be characterized by simple diffusion models. Bohrer [64, 65], on the other hand, tried to use diffusion measurements to characterize Nuclepore membranes, but

still had to account for boundary layer effects.

Recently, Hanemaaijer [48] introduced a method for estimating an effective pore size from rejection measurements of low molecular weight saccharides. Because the rejection of such species is low, concentration polarization is supposed to be negligible. The elegance of the method is that it is reasonably simple to use and that it is possible to measure clean, fresh membranes as well as fouled membranes. Another possibility for the combined evaluation of rejection and fouling was proposed by Smolders at the workshop on characterization of UF membranes in Örenäs (see table 6) [66]. This approach suggests the measurement of rejection of four different types of substances, differing in molecular weight and hydrophilicity and thus exhibiting different degrees of rejection, fouling and concentration polarization.

Table 6. Possible set-up of combined rejection and fouling studies.

MW	amphipolar	unipolar
low	surfactants	sugar derivatives low MW ethers
high	proteins	carbohydrates polyethers

1.5 Models Describing the Porous Structure

The description of the relation between the pore structure and the observed physical phenomena can be considered as another key-problem in characterization. The first models, which mainly described the pore morphology, originated from the researchers of porous charcoal [9] and were adapted to be used for a wide range of porous media. In these approaches the porous structure is visualized as a network of channels of different size and also dead-end pores are present. Especially for catalysts, such models appear to describe effective diffusion processes quite succesfully [67]. This is partly due to the simple nature of the free molecular diffusion regime which is predominant inside these systems. In fact, the pores are only needed to increase the relative area per volume of catalyst.

The description of transport through (and not only in) porous media appeared to be more complicated, as Mason indicated in his 'Dusty Gas Theory' [68]. Mason pointed out that transport through and in porous media is the resultant of different interfering transport mechanisms (diffusive and convective flow). Only in few situations one transport regime

prevails and a simple model can be applied. Because of the large variety of models describing

different physical phenomena, we will focus on the approaches which are of importance for membrane systems. Already in 1934 Ferry tried to model the transport of small, non-interacting particles through a membrane [69]. In this model the only factor affecting the rejection is the steric hindrance which is, of course, a gross oversimplification. An important conclusion from Ferry's approach is that the separation performance of a membrane process, in which size exclusion is the only separation mechanism, has only limited 'resolution'. This means that the cut-off value is always somewhat diffuse (figure 10). Several extensions of Ferry's theory were introduced which mainly made corrections for the hydrodynamic drag forces on the solute moving inside the pore. An extensive review of similar transport mechanisms has been given by Deen [70].
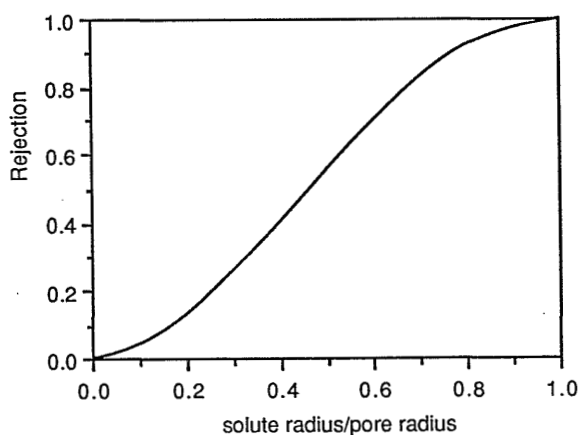

Figure 10. Rejection curve according to Ferry [62]; rejection versus the ratio of solute size and (cylindrical) pore radius.

Percolation Theory

Another 'class' of theories that receives more attention nowadays is the 'percolation approach'. In the percolation models the movement of a particle through a three dimensional network, imagined as a set of diffusion steps, is literally simulated [71, 72]. One of the reasons for the growing interest in this theory is the increased power of computers, which permits the simulation of complex systems, containing three or more permeating components [73]. The elegance of the simulations is that the interference between small and large particles, which together penetrate the porous medium, can be shown. Although the particles have no specific affinity towards each other or to the membrane, their transport through the pores is influenced by the fact that particles cannot 'travel' freely throughout the medium. Besides that, not each diffusive movement will be an effective step 'to the other side' of the membrane and the more

the pores are interconnected, the more the particle can 'get lost' inside the system. The magnitude of the driving force will influence the transport through the network too, because it will change the path of the particle through the network. Altogether this means that at a low degree of interconnectivity, which might be expected for a medium that possesses a very low porosity (like UF membranes), percolation theory can be relatively simply applied.

Fractal Theory

Recently, the fractal nature of a porous medium was recognized. The term 'fractal' [73] refers to purely geometric properties of the objects and means that a structure is built of selfsimilar entities (figure 11). As the transport properties of porous media are determined by the structural geometry, the fractality will have its impact on the hydrodynamic behaviour of the system [74]. The fractal nature of porous media can be approached from three different ways: the pore space, the solid and the solid-pore interface. For characterization the first appears to be the most interesting approach. A major advantage of fractal theories is the possibility to describe very complex systems, as porous media are, in a simple way. Although, until now, fractal geometry has only made conceptual progress in treating complex geometries, prospects for the future are interesting [75].

(a)   (b)
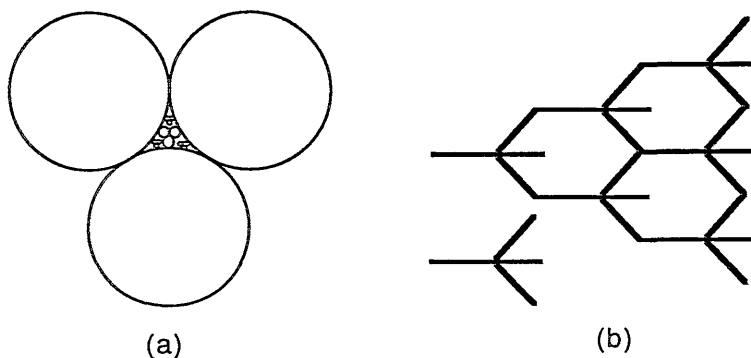
Figure 11. Model of two physical situations described by regular fractals, (a) the solid is fractal, (b) the pore structure is fractal [75].

For UF membranes it is not clear whether a fractal description of the pores can be used. Since the porosity of the top layer is very low, the pore structure itself can be hardly imagined as fractal. It might be possible that the solid exhibits fractal nature, for instance in the form of a 'nodular structure'. But as neither the structures of UF membranes nor that of the nodules have been revealed yet, even this problem is only hypothetical.

1.6   The Structure of This Thesis

From the foregoing it is clear that, for a proper characterization of membranes, a number of conditions should be fulfilled. In the first place the structure of the membrane should be known in relation to the performance or physical parameters that have to be described. In membrane science one is primarily interested in characteristics which can describe the membrane performance, preferably for a wide range of applications. Since the prediction of performance is directly related to the distribution of the active pores and the thickness of the top layer, techniques should focus on the measurement of such active parameters. In this thesis, techniques which measure the pore structure of the membrane as a whole (which in case of anisotropic membranes means: the top and sublayer), as well as techniques measuring the active pore sizes and the top layer thickness are introduced and discussed.

In chapter 2 the analysis of pore size distribution for polymeric and ceramic membranes by means of thermoporometry is discussed. It is shown that thermoporometry can be a very effective method for the characterization of porous media. For anisotropic membranes, however, difficulties can arise which are related to the membrane structure, the anisotropy as well as the pore size distribution.

In chapter 3 a new method for the determination of the skin thickness of anisotropic membranes is presented. This so-called 'gold sol method' is based on the use of well-defined colloidal gold particles, permeating from the sublayer side of the membrane, combined with electron microscopic analysis of the membrane afterwards.
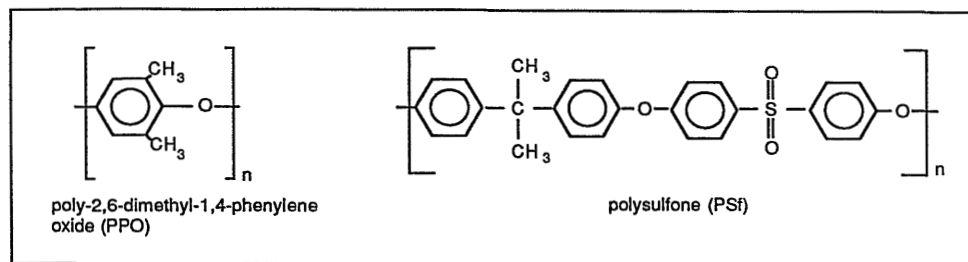

Figure 12. Chemical structures of polymers used in this thesis for membrane preparation.

In chapter 4 another method: 'permporometry' by which the active pore sizes of a membrane can be measured, is introduced. The principle of counter-diffusion of gases is used, in combination with capillary condensation. The capillary condensation phenomenon is well-known and as counter-diffusion measurements are well-defined too, the description of the transport through the membrane is relatively easy. Therefore the permporometry measurements permit one to draw conclusions about the active pore structure.

In chapter 5 the structure of polymeric membranes is studied using gas adsorption-desorption measurements. The concept of classified reference isotherms is used, which provides a better approach for the analysis of porous media other than inorganic materials.

Throughout the work two different polymeric UF membranes, made of polyphenylene oxide (PPO) and polysulfone (PSf), are used as special systems (figure 12). Using the various characterization methods, remarkable differences in membrane structure are revealed. In the last chapter of this thesis these differences are discussed and the impact of the active morphology related parameters on the membrane performance is elucidated.

1.7   Literature

1. Liddel, H.R., Scot, R. in: 'a Greek-English Lexicon', H.S. Jones (ed.), Oxford, Clarendon Press, 1966
2. Audinos, R. in 'Les membranes artificielles', Presse Universitaires de France, Paris, 1983
3. Gelman, C., Analytical Chemistry 37 (1965) 29A
4. Bechhold, H., Z. Phys. Chem. 60 (1907) 328
5. Zsigmondi, A., Z. Anorg. Chem. 71 (1911) 356
6. Trägårdh, G. in 'Characterization of Ultrafiltration Membranes', G. Trägård (ed.), p.9, Lund University, Lund, Sweden, 1987
7. Everett, D.H. in 'Characterization of Porous Solids', K.K.Unger, J. Rouquerol, K.S.W. Sing and H.Kral (eds.), p. 1, Elsevier, Amsterdam, 1988
8. ESMST Report on Terminology for Pressure Driven Membrane Operations 1986, Desalination 68 (1988) 77
9. Gregg, S.J. and Sing, K.S.W. in 'Adsorption, Surface Area and Porosity', 1st edition, 1967; 2nd edition, 1982, Academic Press, London
10. IUPAC Reporting Physisorption Data, Pure Appl. Chem. 57 (1985) 603
11. Te Hennepe, H.J.C., Zeolite Filled Polymeric Membranes, Thesis University of Twente, the Netherlands, 1988
12. a.Keizer, K.K., Burgggraaf, A.J. in 'Porous Ceramic Materials in Membrane Applications in 'Science of Ceramics 14', B. Taylor (ed.), p.83, Institute of Ceramics, Shelton UK, 1988; b.Uhlhorn R.J.R., Ceramic Membranes for Gas Separation, Thesis University of Twente, the Netherlands, 1990.
13. Nijhuis, H.H., Removal of Trace Organics by Pervaporation, Thesis University of Twente, the Netherlands, 1990
14. van den Berg, G.B., Concentration Polarization, Thesis University of Twente, the Netherlands, 1988
15. Klein, E., Feldhof, P., Turnham, T., J. Membrane Sci. 15 (1983) 245

16. Lakshminarayanaiah, N., Chem. Reviews <u>65</u> (1965) 491

17. Michaels, A.S., Sep.Sci. and Techn. <u>15</u> (1980) 1305

18. Mason, E.A., Wendt, R.P., Bresler, E.H., J. Membrane Sci. <u>6</u> (1980) 283

19. Wendt, R.P., Klein, E., J. Membrane Sci. <u>17</u> (1984) 161

20. Michaels, A.S., Preprints ICOM 1987, p.17, June 8-12 1987, Tokyo, invited lecture 5

21. Fane, A.G., Fell, C.J.D. in 'Characterization of UF Membranes', G. Trägårdh (ed.), p.39, Lund University, Lund Sweden, 1987

22. Gekas, V., Zhang, W., Process Biochemistry <u>29</u> (1989) 159

23. Matson, S., US Patent, nr. 4,800,162, Januari 24, 1989

24. Oldani, M., Schock, G., J. Membrane Sci. <u>43</u> (1989) 243

25. Franken, A.C.M., Nolten, J.A.M., Mulder, M.H.V., Bargeman, D., Smolders, C.A., J. Membrane Sci. <u>33</u> (1987) 315

26. Banerji, B.K., Colloid and Polymer Sci. <u>259</u> (1981) 391

27. Keurentjes, J., van't Riet, K., J. Membrane Sci. <u>117</u> (1989) 333

28. Absolon, J., J. Colloid Interface Science <u>117</u> (1987) 550

29. Adamson, A.W. in 'Physical Chemistry of Surfaces', 2nd edition, Chapter vii, Wiley, New York, 1967

30. Cook, M.A. in 'Hydrophobic Surfaces' F.M. Fowkes (ed.), p. 206, Academic Press, New York, 1969

31. Martinez, L., Gigosos, M.A., Hernandez, A., Tejarina, F., J. Membrane Sci. <u>35</u> (1987) 1

32. Nyström M., Lindström, M., Matthiasson, E., J. Membrane Sci. <u>36</u> (1989) 297

33. McDonogh, P.M., Fell, C.J.D., Fane, A.G., J. Membrane Sci. <u>21</u> (1984) 1285

34. Lecloux, A.J., Pirard, J.P., J. Colloid Interface Sci. <u>70</u> (1979) 265 and in 'Characterization of Porous Solids', K.K.Unger, J. Rouquerol, K.S.W. Sing and H.Kral (eds.), p. 233, Elsevier, Amsterdam, 1988

35. Eyraud, C., Betemps, M., Quinson, J.F., Bull. Soc. Chim. France <u>9-10</u> (1984) I-238

36. Smolders, C.A., Vugteveen, E., Polym. Mater. Sci. Eng. <u>50</u> (1984) 177

37. Zeman, L., Tkacik, G. in ' Material Science of Polymeric Membranes', D.R. Loyd (ed.), p.339, ACS Symposium Series no. 269, Am. Chem. Soc.,Washington, DC, 1984

38. Brun, M., Quinson, J.F., Spitz, R., Bartholin, M., Makromol. Chem. <u>183</u> (1982) 1523

39. Lange, R.H., Blödorn, J., Das Elektronen Microskop: TEM & SEM, Thieme Verlag, Stuttgart, 1981

40. Vivier, H., Pons, M., Portala, F., J. Membrane Sci. <u>46</u> (1989) 81

41. Roesink, H.D.W., Microfiltration, Thesis University of Twente, the Netherlands, 1989

42. Fane, A.G., Fell, C.D.J., Waters, A.G., J. Membrane Sci. <u>9</u> (1981) 245

43. Merin, U., Cheryan, M., J. Appl. Pol. Sci. <u>25</u> (1980) 2139

44. Von Preusser, H.J., Kolloid-Z.Z. Polym. <u>250</u> (1972) 133

45. Fane, A.G., Fell, C.J.D., Desalination, <u>62</u> (1987) 117

46. Baker, R.W., Erich, F.R., Strathmann, H., J. Phys. Chem. <u>76</u> (1972) 238

47. Capanelli, G., Vigo, F., Munari, S., J. Membrane Sci. 15 (1983) 289
48. Hanemaaijer, J.H., Robbertson, T., van den Boomgaard, Th., Olieman, C., Both, P., Schmidt, D.G., Desalination 68 (1988) 93
49. Sarbolouki, M.N., J. Appl. Pol. Sci. 29 (1984) 743
50. Altena, F.W., Knoef, H.A.M., Heskamp, H., Bargeman, D. and Smolders, C.A., J. Membrane Sci. 12 (1983) 313
51. Erbe, F., Kolloid Z. 59 (1932) 195
52. Bechhold, H., Schlesinger, M., Silbereisen, K., Kolloid Z. 55 (1931) 172
53. Meltzer, T.H., Bull. Par. Drug Ass. 25 (1971) 165
54. Franken, A.C.M., Membrane Distillation, Thesis, Chapter 3, University of Twente, the Netherlands, 1988
55. Grabar, P., Nikitine, S., J. Chim. Phys. 33 (1936) 50
56. Munari, S., Bottino, A., Moretti, P., Capanelli, G., Becchi, I., J. Membrane Sci. 41 (1989) 68
57. Kujawski, W., Adamczak, P.A., Narebska, A., Sep. Sci. and Techn. 24 (1989) 495
58. Conner, Wm.C., Lane, A.M., J. Catalysis 89 (1984) 217
59. Liabastre, A.A., Orr, C., J. Colloid Interface Sci. 64 (1978) 1
60. Brun, M., Lallemand, A., Quinson, J.F. and Eyraud, Ch., Thermochim. Acta 21 (1977)
61. Eyraud, Ch., Quinson, J.F. and Brun, M. in 'Characterization of Porous Solids', K.K. Unger, J. Rouquerol, K.S.W. Sing and H.Kral (eds.), p. 295, Elsevier, Amsterdam, 1988
62. Mey-Marom, A., Katz, M.J., J. Membrane Sci. 27 (1986) 119
63. Katz, M., Baruch, G., Desalination 58 (1986) 199
64. Bohrer, M.P., I & EC fund. 22 (1983) 72
65. Bohrer, M.P., Patterson, G.D., Carol, P.J., Macromol. 18 (1985) 2531
66. Gekas, V. in 'Characterization of UF Membranes', G. Trägårdh (ed.), p.245, Lund University, Lund, Sweden, 1987
67. Satterfield, C.N., Cadle, P.J., I & EC fund. 7 (1968) 202
68. Mason, E.A., Malinouskas, A.P. in 'Gas Transport in Porous Media: the Dusty Gas Model', Amsterdam, Elsevier, 1983
69. Ferry, Chem. Rev. 18 (1936) 373
70. Deen, W.M., AIChE Journal 33 (1987) 409
71. Shante, V.K., Kirkpatrick, S., Advances in Physics 20 (1971) 325
72. Kirkpatrick, S., Advances in Modern Physics 45 (1973) 574
73. Gyer, R. A., Phys. Rev. 37 (1988) 5713
74. Farin, D., Avnir, D. in 'Characterization of Porous Solids', K.K.Unger, J. Rouquerol, K.S.W. Sing and H.Kral (eds.), p. 421, Elsevier, Amsterdam, 1988
75. Adler, P.M. in 'Characterization of Porous Solids', K.K.Unger, J. Rouquerol, K.S.W. Sing and H.Kral (eds.), p. 433, Elsevier, Amsterdam, 1988

2

Critical Points in the Analysis of Membrane Pore Structures by Thermoporometry

2.1   Introduction

Since the introduction of thermoporometry by Brun et al. in 1973, various porous structures have been examined by means of this technique, mainly by Brun et al. [1-7]. Most of the structures were of inorganic, ceramic nature although in the eighties a few organic swollen and non-swollen resins were investigated [5-6]. These structures are of the isotropic type and the presence of a relatively high pore volume makes the pore size analysis by thermoporometry fairly simple. The success of thermoporometry in the systems used by Brun brought several investigators to apply this technique in the characterization of porous structures in the (wet) environment in which they are actually used. Desbrières et al. [8] measured pore size distributions of hemodialysis membranes whereas Zeman et al. [9] and Smolders et al. [10] reported on the application of the method to characterize ultrafiltration membranes.

Ultrafiltration membranes are generally prepared from polymers; this enables one to manufacture porous membranes in a large area per volume ratio, i.e., in the form of flat sheets or hollow fibres. The main difference between these polymer systems and the porous ceramic media studied by Brun is the superior mechanical and chemical stability and the better definition of the morphological structure (in terms of pore size distribution) of the ceramic materials. Also, polymeric UF membranes are anisotropic: they consist of a thin skin layer with very small pores determining the performance of the membrane and a thicker macroporous sublayer which provides the membrane with mechanical solidity. As the skin layer is very thin and its (surface) porosity generally is in the order of a few percent [11, 12], the pore volume is quite low in comparison with ceramic membranes or catalysts. These aspects can have a large impact on the experimental procedure to be used and on the interpretation of the data found with thermoporometry.

Normally, in the thermoporometry measurements of polymeric membranes, water is used as the liquid imbibed inside the pores, as the system of water filled pores has the closest resemblance with the practical situation. During the measurements, the water inside the pores will undergo a liquid-solid transition at least one time, a change of state which is accompanied by a volume expansion of the water. The question arises whether this phase transition changes the structure of the membrane in a reversible or in an irreversible way. For ceramics such a possible effect has never been mentioned or found which confirms the assumed morphological stability of these materials. On the other hand, Brun suggests [4, 5] that in a swollen resin in which the pore size in principle can change reversibly, different pore size distributions are found depending on the degree of swelling. The swollen membranes show broad distributions with sizes spreading over one order of magnitude, whereas the unswollen dry membranes analysed by the widely used method based on gas adsorption-desorption measurements, exhibit a very sharp pore size distribution.

Brun et al. [6] compared different characterization techniques by applying them to one and the same ceramic system. It appeared that results found with thermoporometry and gas adsorption-desorption hysteresis are consistent with one another. Similar agreement was found by Zeman [9] and Smolders [10] when both methods were applied to polymeric ultrafiltration membranes. On the other hand, the thermoporometry results found by Zeman did not match with his SEM observations and could hardly explain the low cut-off values found for the same membranes, even when concentration polarization effects were taken into account [13]. Consequently, Zeman suggests that by thermoporometry and gas adsorption-desorption the pores in the sublayer of the membrane are measured and therefore these methods do not give relevant information on the pores present in the skin. Smolders and Vugteveen found that the retention of components with molecular weights in the order of 10,000 Dalton was very low, which was not in agreement with the small pores found with thermoporometry. The conclusion must be that, although in some cases thermoporometry is a simple and effective method to determine the pore structure of certain porous media, for a number of particular systems, especially anisotropic polymeric membranes, doubtful results are found. To solve some of the uncertainties mentioned, again measurements with different membranes were performed. In addition these thermoporometry data were compared with membrane characteristics found with other methods to investigate the mutual conformance of the methods.

2.2   Theory

The basic principle of thermoporometry is the freezing (or melting) point depression which is due to the strong curvature of the solid-liquid interface present within small pores. A full thermodynamic description of this phenomenon is given by Brun et al.[1]. According to his

treatise the size of a confined ice crystal is inversely proportional to the degree of undercooling (ΔT). Finely dispersed ice as present in a porous matrix therefore melts at temperatures below the ambient melting point of ice. The smallest size of the ice crystals or the smallest pore size that can be described properly is set by the validity of the assumptions made in the thermodynamic description of curved surfaces. For instance, the approximation of several properties of dispersed water by using values of normal, bulk water is limited to volumes with radii larger than 1-2 nm. According to Defay et al. [15] dispersed water at temperatures below -50 °C cannot be described anymore using normal equilibrium thermodynamics. At such low temperatures any form of liquid water is instable and will become solid. This phenomenon can interfere with the 'normal' equilibrium freezing of water in very small pores ($\approx$ 2 nm). Monitoring cooling effects can also be disturbed by delayed nucleation of the ice phase inside the pores. This will be a minor effect when hydrophilic samples are analysed because the wetted membrane walls can act as nuclei and induce a fast L-S transition [15]. However, for extremely hydrophobic materials delayed nucleation can influence the pore size analysis. Therefore the melting transition is preferred above the solidification for the pore size analysis, although the latter in principle should render identical information.
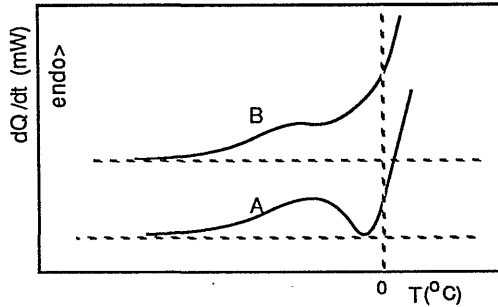

Figure 1. DSC thermogram as found for a narrow pore size distribution (A) and for a broad pore size distribution (B).

For the analysis of a porous substrate, the melting diagram (figure 1) can be monitored in a differential scanning calorimeter (DSC) and the pore size and pore volume are calculated from the equations derived by Brun. For the solid-liquid transition of water inside a cylindrical pore with radius r equation (1) holds. From the heat effect occurring during the transition, the pore volume at a certain undercooling (i.e., pore radius) is calculated. Equation (2) gives the heat of

$$r = 0.68 - (32.33 \, / \, \Delta T) \qquad (1)$$

$$W_a = -0.155 \, \Delta T^2 - 11.39 \, \Delta T - 332 \qquad (2)$$

r : pore radius (nm)
ΔT : undercooling (°C)
W_a : apparent transition energy (J/g)

melting as a function of temperature, used in this procedure. Similar equations can be derived for the solidification process. These are not given here because only the melting process was used in the pore size analysis described in this chapter.

As long as the pores have sizes between 2 nm and 25 nm, the shift of the freezing or melting point is large enough to be measured accurately. A typical example of such a melting curve is given in figure 1 A. Here, water inside the pores and 'free' water outside the membrane give rise to separate peaks and consequently the pore size distribution can be calculated easily. For some membrane types a deviant curve is found (see figure 1B) and distributions calculated from such a curve remain questionable. This problem is discussed in more detail later-on in this paper (see: results and discussion).

2.3   Experimental

Both ceramic and polymeric membranes were investigated by means of thermoporometry. The ceramic γ-alumina systems were supplied by the inorganics group of our department and are described in literature. According to gas adsorption-desorption and transmission electron microscopy these membranes have a well-defined pore structure and a porosity of about 50 % [14]. Furthermore hollow fibre CA membranes used in blood filtration were analysed. According to literature these isotropic membranes exhibit a high porosity [8, 16] which should make analysis by thermoporometry fairly simple.

Lab made anisotropic ultrafiltration membranes were made of poly (2, 6 dimethyl-1,4 phenylene oxide) (PPO), polysulfone (PSf) and cellulose acetate (CA). PPO membranes were prepared from a 10 wt % polymer concentration in a mixture of trichloroethylene and 1-octanol in a weight ratio of 78/22. PSf membranes were casted from a solution composed of 15 wt % PSf (P-3500 Union Carbide) in DMF. Flat CA membranes were made out of a 20 wt % CA solution in 59 wt % aceton, 19 wt % demi-water and 2 wt % magnesiumperchlorate. The solutions were casted on a glass plate at room temperature at thicknesses of 0.2 and 0.03 mm, respectively. In case of PPO, methanol was used as the coagulation bath, PSf and CA membranes were immersed in a water bath.

The calorimetric experiments were performed using a Perkin Elmer DSC 2 or DSC 4. First the sample with a total mass about 50 mg (including water) was cooled at maximum speed to -45 °C. After equilibrium was reached the heat effects during a controlled heating run at a scanning rate of 1 °C/min. were measured.

Pure water flux measurements were performed using freshly filtered RO water and a dead-end

Amicon cell with a membrane area of 35 cm^2, at a pressure of 300 kPa. The steady state flux was determined after 3 hours of permeation.
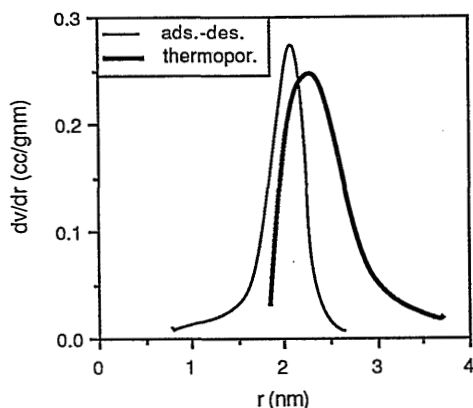

Figure 2. Pore size distributions found for alumina membranes using thermoporometry and gas adsorption-desorption measurements (dv/dr: differential pore volume per g membrane).
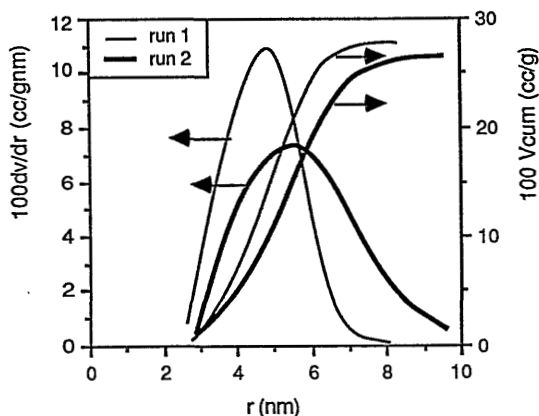

Figure 3. Change in pore size distribution for hollow fibre CA membranes after two succesive runs.

2.4   Results and Discussion

The Effect of Successive Heating Runs

γ-Alumina membranes and hollow fibre CA membranes exhibit a sharp pore size distribution (figures 2 and 3 respectively). The results found for the alumina membranes are in agreement with the data found with gas adsorption-desorption [14]. Alumina samples were analysed during several successive heating runs (up to 8 runs), but differences between the runs were not found. This means that this type of membrane is perfectly stable; the structure does not change during the analysis.

In figure 3, pore size distributions for hollow fibre CA membranes calculated from several consecutive runs carried out with the same sample of membrane material, are shown. It appears that between the first and second run the pore size distribution shifts to slightly larger pore values. Differences between the following experiments are not significant. Obviously, the pore structure of the sample changes during or directly after the first two experiments but is stable thereafter. Probably this alteration has occurred during the cooling of the sample. Since the liquid-solid transition is accompanied by a volume expansion of 8-20 % (dependent on the temperature and the pressure there exist different ice phases) [17, 18], the nuclei deform the porous matrix to some extent. Because the nuclei are induced within the original restricting pore space, the ultimate size of the crystal will only be a little larger than the nascent pore size. During the second cooling run the nuclei again deform the membrane matrix and enlarge the pore. Consequently the pore size measured in the second heating run is larger than that measured in the first run. From the volume expansion of the water the increase in pore size (for an 'original' pore of 5 nm) is calculated to range from 0.1 nm (0 °C and 10^5 Pa) to 0.3 nm (-35 °C and $2*10^8$ Pa). Especially the latter value corresponds quite well with the experimental pore size increase. The fact that the volume expansion has to proceed in a confined pore space makes a transition accompanied by such a high pressure comprehensible. Nevertheless, the deformation appears to have reached its ultimate extent already after the second cooling step, since from the third run no change in the pore size distribution could be observed anymore. Probably the affine deformation caused by the water-ice transition stretches the pore walls to such an extent (reached after 2 transitions) that under the prevailing forces no further deformation is possible. The deformation of the original pore is not reversible because a relaxation phenomenon was not found; even after three days the pore size distribution was identical with the previous (second) analysis run.

The pore size distribution of the thick PPO membranes determined by thermoporometry appears to be very sharp (figure 4). All the pores have sizes between 1.5 and 4 nm and a maximum is found at about 2 nm. Figure 4 shows that the cumulative pore volume found in the first run is significantly lower than the value found (with the same sample) in the following runs. This remarkable difference suggests that not all the water present in the pores has been crystallized upon cooling during this first run and that at -45°C part of the water is presumably present in the glassy state. The so-called vitrification occurs when the cooling rate has been so fast that nuclei could not be formed. However the extreme conditions needed for vitrification (cooling rates $>10^6$ °C/s) are certainly not present in the equipment used here, hence the presence of glassified water is not probable[19]. Since PPO is a hydrophobic material, heterogeneous nucleation induced by, e.g., the polymer wall is less probable than for hydrophilic materials. In the abscence of other nuclei which could induce crystallization, homogeneous nucleation may be important. When homogeneous nucleation indeed should induce crystallization, the water (at -45°C) may be present as an undercooled liquid. According
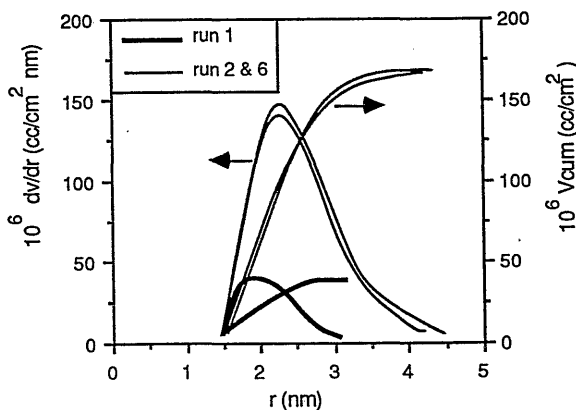
Figure 4. Change in total pore volume (Vcum) for PPO membranes after several successive runs (casting thickness 0.2mm; pore volume expressed as volume per unit membrane area) .

to the analysis of Defay et al. [15], the homogeneous nucleation process at low temperatures is extremely slow and it might need several months to induce crystallization in all the pores of the membrane. This means that after cooling to -45°C, water can be present as an undercooled liquid instead of ice. Hence, phase transition (accompanied by a measurable heat effect) does not occur. The question is why during the second cooling run more ice is formed and crystallization appears to be less delayed. It should be expected that after the heating run, all the ice has become water and the nucleation process then has to start all over again. The only possible explanation is that after the first heating run, conditions are changed (permanently) in a way that heterogeneous nucleation can take place in all the pores.

Another possible explanation for the observed increase in pore volume after the first heating run might be the presence of non-wetted pores, which become wetted after the first run. However, the origin of such non-wetted pores inside the membranes is hard to understand. Pores in UF membranes are formed by liquid-liquid demixing, which for PPO means that, in the native state, all the pores in the membrane are filled with methanol from the coagulation bath. The pores are filled with water by exchanging all the methanol, so in this way dry pores or 'de-wetting' of the membranes cannot occur. It may be that a trace of methanol is still present in some pores and could hinder crystallization. Also then it is not clear why during the second cooling run crystallization is more complete.

The Structure of the Top- and Sublayer
The thermogram of a heating run executed with PPO membranes with a casting thickness of 0.20 mm shows two distinctly separated peaks (figure 1A) and a simple calculation of the pore size distribution is possible. Other UF membranes, like the thick PSf and flat CA membranes, exhibit deviant melting curves like depicted in figure 1B. Although in these latter cases the

calculation of the pore size is possible, the resulting pore size distribution will be more questionable. Not only the impossibility to discriminate fully between 'pore peak' and 'free water peak' gives rise to doubtful results but also the precarious drawing of the base line. Furthermore it is not sure whether the larger pores, related to the higher melting temperatures, are present in the skin or in the sublayer. Especially in case of anisotropic membranes which have relatively thick sublayers it can be imagined that going from the top to the bottom of the membrane a pore size gradient is present which leads to a melting curve with a shape as given in figure 1B.

From the distribution obtained for PPO membranes (figure 4), the cumulative pore volume was calculated. Here, the pore volume is expressed as volume per unit area of the top layer and for the thicker PPO membranes the values ranged from $5*10^{-5}$ till $20*10^{-5}$ cm^3/cm^2 and appeared to be strongly dependent on the casting thickness [10]. Because a PPO membrane is an anisotropic membrane, all this pore volume is expected to be related to pores in the top layer. Consequently, the top layer thickness of the membrane can be calculated when a pore model is assumed. Recently, the top layer thickness of these PPO membranes, directly determined by a new method [20], was found to be about 0.2 µm. This result makes it questionable whether the pore volume measured with thermoporometry is present in the skin only. A simple calculation shows that a porosity value of more than 100% is needed to account for this volume to be present in a skin layer with a thickness of 0.2 µm. Apparently there are also small pores present in the sublayer of the membrane.

It has already been mentioned that the calculation of the pore size distributions of CA and PSf membranes from thermograms of type 1B is cumbersome. From the anisotropic membrane concept one should expect that the small pores of the PSf and CA membranes are present in the skin. If this is really the case it is mainly because of the very low porosity of the skin [11, 12] that the number of the pores or the cumulative volume in the skin cannot be measured. The smallest pore size can be found from the lowest temperature at which the thermogram (figure 1) deviates from the base line but the larger pores in the sublayer make the complete analysis troublesome. Hence, no pore size distribution could be obtained from the PSf and CA membranes.

In order to diminish the influence of the sublayer pores, the ratio of the pore volume present in the skin to that in the sublayer was increased by preparing ultra thin PPO, CA and PSf membranes. For membranes with a casting thickness of 0.03 mm two separate peaks were found again and indeed a pore size distribution could be calculated. The resulting distributions for CA and PSf membranes are given in figures 5 and 6 respectively. The distributions are considerably broader than the pore size distributions found for the thicker PPO membranes (fig. 4). This might be due to the fact that the pore sizes in the top layer of these CA and PSf

membranes really are larger than those in PPO membranes, but it is also possible that the complete membrane structure has changed because of the decreased casting thickness.
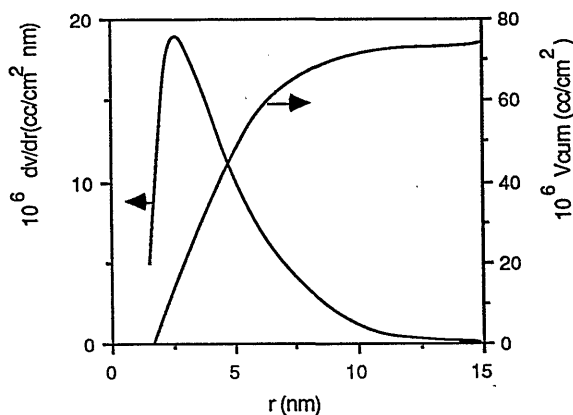

Figure 5. Pore size distribution of thin CA membranes (casting thickness 0.03 mm, pore volume expressed as volume per unit membrane area).
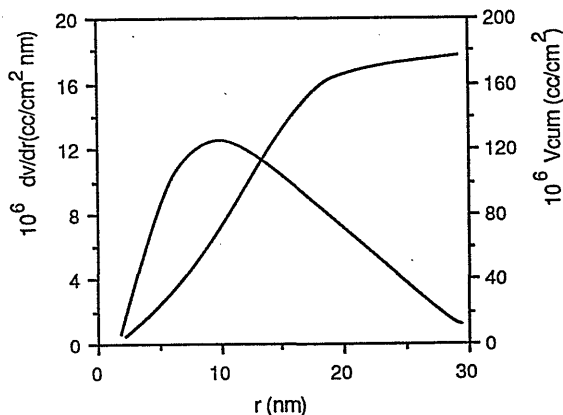

Figure 6. Pore size distribution of thin PSf membranes (casting thickness 0.03 mm, pore volume expressed as volume per unit membrane area).

The broad pore size distribution found for the thin (0.03 mm) PPO membranes (figure 7) completely deviates from the characteristic sharp peak exhibited by the thick (0.20 mm) PPO membranes. This difference in pore size distribution between the thin and the thick PPO membranes also suggests a change in membrane structure caused by a change in casting thickness. To investigate this possibility, the pure water flux of the thin and thick membranes (of CA, PSf and PPO) was measured. The results are given in table 1.
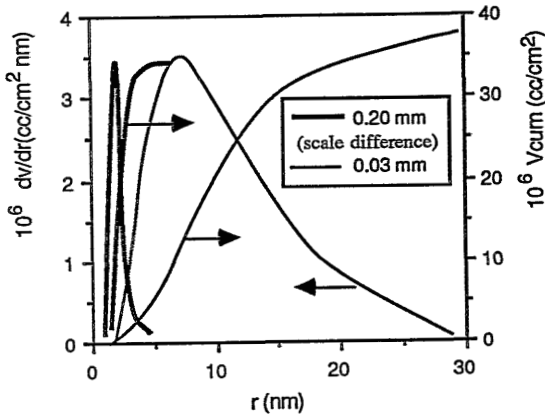
Figure 7. Comparison of PPO membranes with casting thicknesses 0.03 mm and 0.20 mm. (scale dv/dr 0.20 mm membranes should be multiplied by 10, see also figure 4).

The pure water fluxes of both PPO membrane types are surprisingly close to each other. This does not only imply that the pore structure of both types is similar but also supports the idea of the predominant role of the top layer in this case. On the other hand, it can be argued that the large amount of small pores found by thermoporometry in thicker PPO membranes are not related to pores (in the skin) which actually are important for the membrane performance. The number of pores that do determine the performance is so small that they cannot be measured by thermoporometry [11, 12]. The thin membranes used are assumed to have a higher ratio of pore volume in the skin to that in the sublayer than the thick membranes. Therefore the DSC-samples contain about '10 times more' skin which makes the detection of the pores in the skin easier. Consequently the pore size distribution found for the thin membranes is expected to be a better representation of the actual distribution of the pores in the skin. Or in other words: the real pore size distribution in the skin of thick PPO membranes resembles the pore size distribution found for the thin membranes.

Table 1. *Flux and pore volume as determined by thermoporometry for various membranes*

membrane type	PPO		PSf		CA	
casting thickness (mm)	0.2	0.03	0.2	0.03	0.2	0.03
flux (cm/hbar) (± 1)	1	2	3	30	8	4
$10^5 V_{cum}$ (cc/cm^2) (± 30%)	5-20	3	?	4	?	5

For the CA and PSf membranes significant differences in flux values are found for different membrane thicknesses.

The increase in the flux value for thin PSf membranes might imply that the structure of the membrane has been changed, e.g., the average pore size has increased or the skin thickness has decreased or a combination of these two effects has occurred. It can also be argued that for these membranes the sublayer has a substantial resistance for transport. The existence of a pore gradient from the skin to the bottom of the membrane, which could contribute to this resistance was indicated by other methods too [10, 20]. When such a gradient does exist in both thin and thick membranes, the effect of using thin membranes in thermoporometry might be that the larger pores (> 30 nm) which are present at the bottom of the thick membranes are missing in the thin membrane. The tenfold increase of the water flux, however, can hardly be explained in this way and it must be concluded that the decrease in membrane thickness resulted in a change of pore size as well.

The flux of the 0.20 mm CA membranes is higher than that of the 0.03 mm membranes. This can only be explained by a change in pore structure. Consequently, CA membranes of different casting thickness cannot be compared.

2.5   Conclusions

It has been shown that thermoporometry can be a very effective method for the characterization of porous media. However, for anisotropic polymeric membranes the method cannot be used without certain restrictions. Because the whole membrane, i.e., top layer and sublayer structure which both can contain pores of comparable size, is analysed, it is sometimes difficult to discriminate between effects corresponding to pores in the sublayer and pores in the skin. Furthermore, the very low porosity of the skin prevents the accurate determination of the pore size distribution. When the distributions of the skin and the sublayer exhibit such an overlap in pore size, one should prefer a different characterization technique, e.g., permporometry (chapter 4).

The smallest pore that can be analysed properly by thermoporometry is about 2 nm. The limits are set by the assumptions made in the thermodynamic description of the process which are no longer valid at temperatures lower than -40 °C. The upper limit, or the largest pore that can be determined succesfully by thermoporometry, is set by the effect of the curvature on the freezing point depression. For pores of 30 nm or larger the shift from the ambient fusing point is so small that the effect cannot be separated from the free water peak and accurate determination of pore radius and pore volume is not possible anymore.

2.6 Literature

1. Brun, M., Lallemand, A., Quinson, J.F., Eyraud, Ch., J. Chim. Phys. 70 (1973) 973
2. Brun, M., Lallemand, A., Quinson, J.F., Eyraud, Ch., Thermochim. Acta 21 (1977) 59
3. Brun, M., Quinson, J.F. and Benoist, L., Thermochim. Acta 49 (1981) 49
4. Brun, M., Quinson, J.F. and Spitz, R., Macromol. Chem. 183 (1982) 1523
5. Brun, M., Quinson, J.F. and Blanc, R., Macromol. Chem. 181 (1981) 873
6. Eyraud, Ch., Quinson, J.F. and Brun, M. in 'Characterization of Porous Solids',
   K.K. Unger, J. Rouquerol, K.S.W. Sing and H.Kral (eds.), p. 295, Elsevier,
   Amsterdam, 1988
7. Eyraud, Ch., Quinson, J.F. and Brun, M. in 'Characterization of Porous Solids',
   K.K. Unger, J. Rouquerol, K.S.W. Sing and H. Kral (ed.), p.307, Elsevier,
   Amsterdam, 1988
8. Desbrières, J., Rinando, M. and Brun, M., J. Chim. Phys. 78 (1981) 187
9. Zeman, L. and Tkacik, G. in 'Material Science of Synthetic Membranes', D.R. Loyd
   (ed.), p.339, ACS Symposium Series no. 269, Am. Chem. Soc., Washington DC, 1985
10. Smolders, C.A. and Vugteveen, E. in 'Material Science of Synthetic Membranes',
    D.R. Loyd (ed.), p.329, ACS Symposium Series no. 269, Am. Chem. Soc.,
    Washington DC, 1985
11. Fane, A.G., Fell, C.J.D. and Waters, A.G., J. Membr. Sci. 9 (1981) 245
12. Merin, U. and Cheryan, M., J. Appl. Pol. Sci. 2 (1980) 2139
13. Zeman, L. and Tkacik, G., J. Membr. Sci. 32 (1987) 329
14. Leenaars, A., Ceramic Membranes, Thesis University of Twente, the Netherlands, 1984
15. Defay, R. and Prigogine, I., in 'Surface Tension and Adsorption: The Effect of Curvature
    on the Triple Point', p.244, Longmans, New York, 1966
16. Kobayashi, T., Todoki, M., Kimura, M., Fujii, Y., Takeyama, T. and Tanzawa, H. in
    'Membranes and Membrane Processes' E. Drioli and M. Nakayaki (eds.), Plenum Press,
    New York, 1986
17. Handbook of Chemistry and Physics, 58th ed., R.C. Weast (ed.), CRC Press,
    Florida, 1977
18. International Critical Tables, 1st ed., vol. iv, E.W. Washburn (ed.), Mc Graw Hill,
    New York, 1928
19. Lange, R.H., Blödorn, J. in 'Das Elektronenmikroskop', Thieme Verlag, Stuttgart, 1981
20. Cuperus, F.P., Bargeman, D., C.A. Smolders, J. Colloid Interface Sci 135 (1990) 486

3

A New Method to Determine the Skin Thickness of Anisotropic UF Membranes Using Colloidal Gold Particles

3.1 Introduction

The application of ultrafiltration (UF) in industrial processes has gained an increased interest in recent years. In most of these separation processes asymmetric membranes are used. Asymmetric membranes consist of a thin, relatively dense top layer, responsible for the separation characteristics of the membrane and an open sublayer that is supposed not to influence the membrane performance. The size distribution of the pores present in the skin, determines the selectivity of the membrane, whereas the skin thickness is an important parameter when hydraulic permeability of the membrane is concerned.

Pore-size distributions of asymmetric UF membranes can be measured using several independent methods such as thermoporometry, gas adsorption desorption measurements, bubble pressure measurements, and permporometry [1-3]. These sometimes quite sophisticated methods allow the measurement of pore sizes in the range of several nanometers to tens of nanometers. Furthermore, gas and liquid permeation measurements are used extensively [4-6]. When a combination of these techniques is used, a reasonable insight into the pore morphology of the membrane is possible.

For a better understanding of the relation between membrane structure and transport through the membrane, however, more knowledge of another crucial parameter, the skin thickness of an asymmetric UF membrane, is required. Although there are many different methods available for measuring pore size or pore-size distribution, there are only few methods known for measuring the skin thickness of asymmetric porous UF membranes. In most cases the skin thickness of the membrane is estimated by means of scanning electron microscopy (SEM). The size of the pores in the skin however, is too small to be distinguished with SEM and often a certain gradient in pore size from the top of the skin toward the porous sublayer exists. In the

case of asymmetric membranes made by phase inversion the determination of the skin thickness is therefore hardly possible and the analysis is limited to a rough estimation.

Another possibility for obtaining information about the thickness of the skin layer is to calculate it from pure water fluxes or from pore-size/pore-volume distributions as measured by, for example, thermoporometry [7]. Here the assumption of a pore model is necessary and the final result depends strongly on the model used.

The new method presented here is based on the penetration of colloidal particles of well-known size and very narrow size distribution into the 'open' macroporous sublayer of an asymmetric UF membrane. A monodisperse colloidal gold solution, existing of particles with a size slightly larger than the size of the pores present in the skin, is filtered in the reverse way compared to normal filtration. The particles penetrate in the porous support until small pores near or in the skin are reached. When the particles used are only slightly larger than the pores in the skin, a thin layer not permeated by colloids is formed and can be distinguished by means of SEM. By comparing experiments done with different colloidal solutions containing particles of an increasing size, one can obtain information about the pore size in the skin and sublayer.

3.2   Experimental

Preparation and analysis of gold colloids

The synthesis of monodisperse colloidal gold particles is described in the literature [8, 9]. The sizes of these particles are in the 5-50 nm (diameter) range and are dependent on the conditions during synthesis. In this study two sols with different particle sizes were used.

Colloidal solutions containing particles with a mean diameter of 6 nm were obtained in the following way: 10.0 ml of a 1.0 wt% solution of chloroauric acid ($HAuCl_4$) was added to 1000 ml water (filtered by reverse osmosis) and the pH of the solution was adjusted to a value of 7.2 with 0.1 M K_2CO_3 solution. The solution was heated to boiling in a reaction vessel and 10.0 ml diethyl ether saturated with white phosphorus (at 20°C) was added to the well stirred solution. Then the solution was cooled down and a stream of air was lead through the deep red solution during one night to remove the excess unreacted phosphorus.

Sols containing particles with a mean diameter of 50 nm were made by adding a 10.0 ml 1.0 wt% sodium citrate solution to a boiling solution of 1000 ml water (purified by reverse osmosis) and 10.0 ml 1.0 wt% chloroauric acid. During the reaction the solution was stirred vigorously until the color was red. After 5 minutes the heating was stopped and the solution was cooled down. All chemicals used were of analytical grade and supplied by Merck.

The sols were characterized by transmission electron microscopy. Sol droplets were sprayed on coal films and after 1 minute the excess liquid was removed carefully by dipping with a filter paper. Transmission micrographs were made using a Jeol 200 CT device. The resolution of this apparatus is better than 0.5 nm. Particle-size distributions were determined by counting particles and by measurement of their cross section by means of image processing.

Membrane Preparation and Permeation
Poly(2,6 dimethyl-1,4-phenylene oxide) (PPO) and polysulfone (PSf) membranes were investigated. PPO membranes were prepared from a 10 wt% polymer solution in a mixture of trichloroethylene and octanol-1 in a weight ratio 78/22. PSf membranes were made from a 15 wt% PSf solution in DMF. In both cases the solutions were cast at room temperature to a thickness of 0.20 mm on a glass plate. The PPO films were coagulated in a methanol bath and the PSf films in a water bath. All solvents used were of analytical grade.
The membranes were placed with the skin side down in an Amicon cell (membrane area 38.5 cm^2) and permeated at 1 bar with RO water for at least 30 min.. Then a small amount of the dark red colloidal gold solution was added to enter the membrane from the porous side. The colloidal gold solution, containing 100 ppm gold, was permeated through the membrane at 1 bar. In all cases a colorless permeate was obtained, indicating that retention was at least 99%. The amount of solution used was adjusted to obtain a detectable layer in the membrane: in the case of 6 nm particles 100 ml sol solution was needed, and in the case of 50 nm particles 200 ml sol solution was needed. For each membrane only one type of colloidal solution, with 6- or 50-nm particles, was used. The experiments were performed in dead-end filtration and diafiltration modes. Results were identical for both types of filtration.

Scanning Eectron Microscopy
Cross section electron micrographs were obtained with a Jeol JSM 35 CF scanning electron microscope using both the secondary electron image (SEI) and the backscattered electron image (BEI) modes. Micrographs made in the SEI mode are essentially topographical and the rough morphological structure can be examined. The backscattered mode yields not only topographical but also analytical information about the specimen. In this mode the contrast is dependent on the atomic number of the materials present in the sample. In our case the presence of gold particles causes light areas in the dark polymer matrix.

Dry membrane samples were prepared by immersion of the wet membrane for 15 min. in a 50:50 (w/w) ethanol/water bath and another 15 min. in a pure ethanol bath, after which the membrane was dried at room temperature in a vacuum chamber. A thin gold layer (~30 nm) was sputtered on top of the membrane. Again the pores of the membrane were filled with ethanol and fractured at liquid nitrogen temperature. Only in this way a cross section with a

sharp fracture is obtained. The sample was dried as described before. To prevent the sample from becoming charged during electron microscopy, it was covered with a coal layer by using a Balzers BSV 202 coal evaporation unit.

As a result of the entire procedure a sandwich structure is formed, consisting of a 'diffuse' gold layer that results from the permeated particles, a sputtered gold layer on top of the membrane, and an impenetrable skin layer in between.

3.3   Results

TEM micrographs of the colloidal solutions are given in figures 1(a) and (b). Figure 2 shows the particle-size distributions of the sols. The distribution of the sol with the smaller particles is asymmetric and very sharp; 72% of the particles have diameters between 5.6 and 6.4 nm. Particles with diameters smaller than 5.6 nm are not present. The sol with the larger particles has a more Gaussian distribution. In this case the mean particle diameter is 50 nm with a standard deviation of 5 nm.
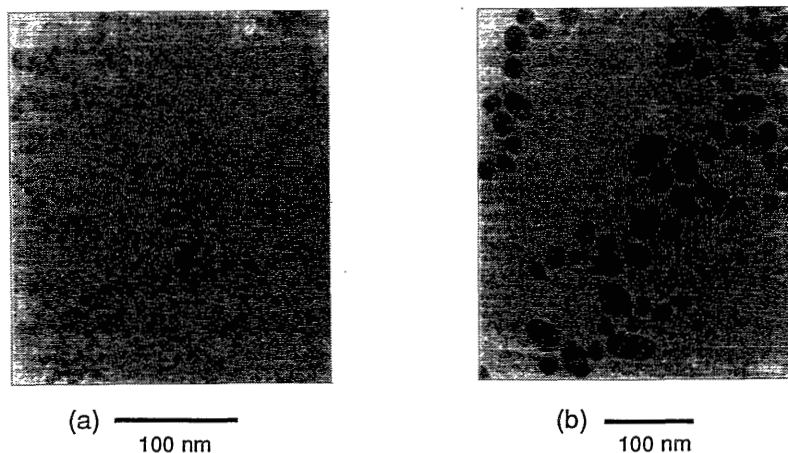

(a) —————   (b) —————
100 nm   100 nm

Figure 1. Typical transmission electron micrographs of gold colloid solutions (a) mean diameter, <d> = 6 nm; (b) mean diameter, <d> = 50 nm.

Figures 3 and 4 show the cross sections of the permeated PPO and PSf membranes, where a and b refer to the two sols used (diameters 6 and 50 nm, respectively) for each polymer. For the examination of these cross sections, the electron microscope is used in the backscattered and 'the normal' secondary electron image modes. The right-hand side of the figures 3 and 4 shows the cross sections of the membranes in the SEI mode. From these pictures it can be seen
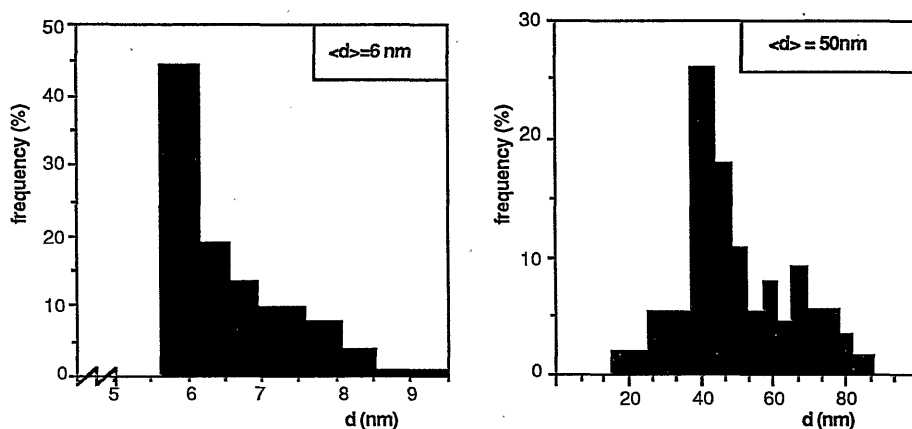
Figure 2. Particle-size distributions of gold colloids. In the case of $<d> = 6$ nm, the size of 500 particles was evaluated, in the case of $<d> = 50$ nm, 300 particles were measured.

that the samples are sharp fractured, as is necessary for proper analysis and interpretation. In the backscattered mode the presence of gold particles can be clearly detected and although the sol particles cannot be seen one by one, the edge formed by the permeated particles can be distinguished easily. From the backscattered image (BEI, left-hand side of figures 3 and 4) three layers can be recognized: a thin light line caused by the sputtered gold layer on top, a more diffuse layer caused by the penetrated gold particles, and in between the two lighter areas is the impermeable (dark) layer in which no particles are present since the pore size is smaller than the particle size of the sol.

Using a sol with particle size of 6 nm, for both membranes an impenetrable layer with a thickness of about 0.2 µm is detected. Although the boundary of the permeated gold particles is somewhat meandering, the thickness of the impermeable layer is defined quite well, showing a skin thickness which is of the same order for PPO and PSf membranes: 0.2 µm.

When a sol with larger particle size is used the two membranes behave in a different way. For PSf membranes a larger thickness of the impermeable layer is found, from 0.2 µm for 6-nm sols to 0.4-0.5 µm for 50-nm sols (fig. 4 b) while the layer still is uniform in thickness.

When a PPO membrane is treated with a sol containing particles of 50 nm (fig 3b) the top layer looks somewhat more frayed and the thickness varies between 0.2 and 0.3 µm. This increase in thickness is very small compared to the situation where 6 nm particles were used.
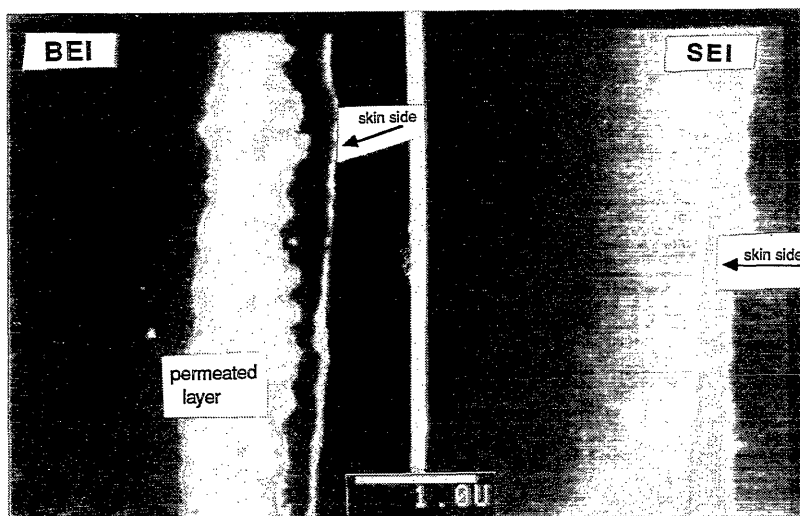
Figure 3a. Cross section of a PPO membrane, using BEI (left-hand side) and SEI(right-hand side) modes, permeated with gold sol solution; mean colloid particle diameter, 6 nm. The cross section of the membrane has been tilted slightly to make the sputtered layer more visible.
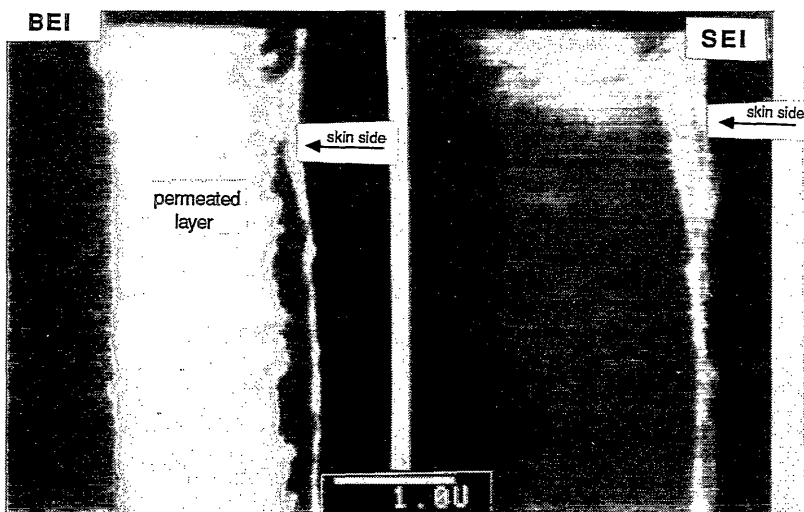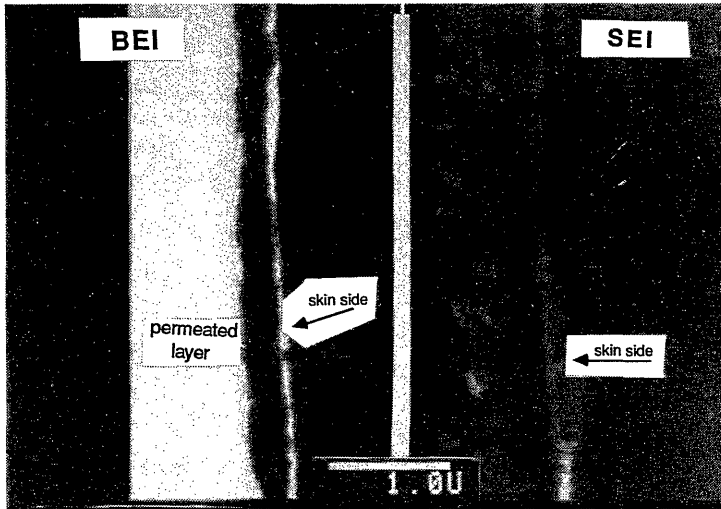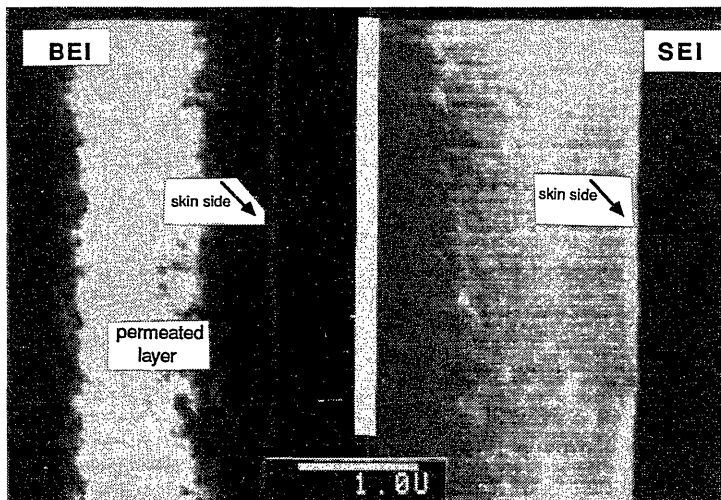

Figure 3b. Cross section of a PPO membrane, using BEI (left-hand side) and SEI(right-hand side) modes, permeated with gold sol solution; mean colloid particles diameter, 50 nm. The cross section of the membrane has been tilted slightly to make the sputtered layer more visible.

Figure 4 a.Cross section of a PSf membrane, using BEI (left-hand side) and SEI (right-hand side) modes, permeated with gold sol solution; mean colloid particle diameter, 6 nm. The cross section of the membrane has been tilted slightly to make the sputtered layer more visible.

Figure 4 b. Cross section of a PSf membrane,using BEI (left-hand side) and SEI (right-hand side) modes, permeated with gold sol solution; mean colloid particles diameter, 50 nm.

We also performed experiments where more sol solution was used (1000 ml). In this case the macrovoids just beneath the skin appeared to be filled with gold. This indicates that the macrovoids take care of a major part of the transport in the sublayer of the membrane (figure 5).
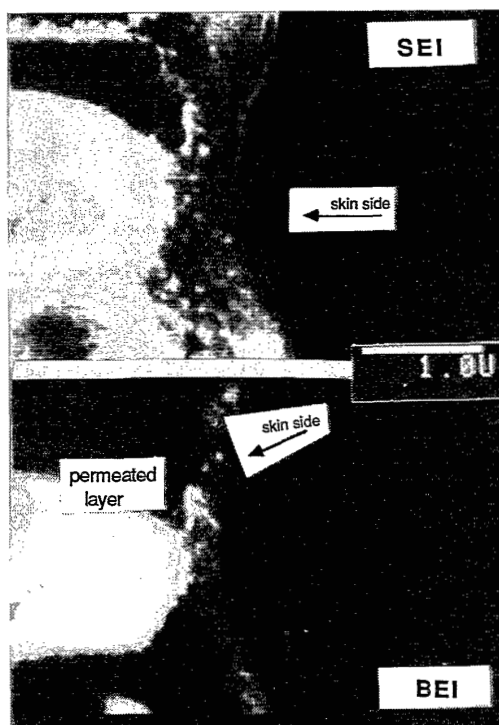

Figure 5. Cross section of a PPO membrane using SEI (top) and BEI (bottom) modes. In this case the membrane was permeated with 1000 ml gold sol solution, mean particle diameter 6 nm. No gold layer was sputtered on top of the membrane, but the position of the membrane on the top (SEI) and the bottom (BEI) of the figure is exactly the same.

3.4   Discussion

Similarly prepared PPO and PSf membranes previously [3, 7] have been characterized by thermoporometry and gas adsorption desorption measurements. It was found that PPO membranes had a very narrow pore-size distribution, with a mean pore diameter of 4.5 nm. The pore-size distribution of PSf appeared to be rather broad, but thermoporometry showed that the smallest pores had a diameter of about 5 nm [3]. It was argued that for PSf membranes no distinct transition could be seen between pores in the top layer and those in the supporting layer, because the pore sizes exhibit a gradual increase.

The small pores, mentioned above, are present in the skin layer and determine the performance of the membranes. The sol particles used have a diameter of 6 nm, which is only slightly larger than that of the pores in the skin. When these sol particles penetrate in the porous support, they will be resisted by pores smaller than 6 nm, present in or very near the skin. In this way the skin layer thickness is defined as a layer in which the pores are of comparable size to the penetrating particles.

From the results described in this paper one can conclude that for PPO membranes the thickness of the impermeable layer, where gold particles are excluded, hardly depends on the size of the particles used (fig. 3). Apparently, in PPO membranes a sharp transition exists between the (macro) pores of the support and the pores in the skin layer, with a size smaller than 6 nm in diameter. So for PPO the skin thickness is well defined as a layer where the pores are much smaller than the continuous pores in the sublayer. These results correspond with the thermoporometry measurements mentioned above indicating that PPO membranes can indeed be described by the simple model of asymmetric membranes, where skin and sublayer are supposed to have independent functions.

For PSf membranes the thickness of the region where particles are excluded increases when larger particles are used. This supports the idea that no discrete skin layer is present here and that the size of the pores gradually increases from skin layer to sublayer.

Some Comments on the Blocking Mechanism

The interpretations given are based on the direct relationship between pore size and particle size, as can be described by a simple sieving mechanism. In this conception the flow of particles is impeded by the difference in size of pores and particles only: a particle cannot penetrate into a pore of a size smaller than its own diameter. As is known from common ultrafiltration transport through the membrane can be influenced by a number of other parameters like adsorption and pore blocking [1,6,10]. The situation described here differs from the normal UF setup. The membrane is permeated from the sublayer side, so the particles move from the large pores in the sublayer into smaller pores in the skin region. Forced by the pressure difference, the particles permeate through the porous structure until the pores are too small and exclusion occurs when the pore size is smaller than the particle diameter. Actually, pore blocking is used here as an indication of the pore size present in the membrane.

Possible Effects of Charges

When colloids are ultrafiltered, coulombic forces between particles mutually and between particles and charged membrane walls may play a role too. The solid particles of a stable colloidal solution carry a definite positive or negative charge. The pore surface of the membrane material may also carry a charge, as is the case for practically every solid-liquid

interface [11, 12]. Because of the occurrence of these surface charges, either repulsive or attractive forces exist between the colloidal particles and the surface of the filter material.

When the interaction between particle and pore wall resulting from van der Waals or coulombic forces is positive, colloidal particles might be captured by the adhesion of the particles in the pores. The retention is then mainly caused by interaction between specific surface sites and particles [11,13] and the size of the pore is of minor importance. If this mechanism prevails, the amount of particles possibly captured by the membrane is limited by the number of specific surface sites. By the time all the sites are occupied, retention can only be caused by differences in size of particles and constrictions. In deep-bed filtration, where the pore size of the filter used is much larger than the particles to be filtered, this phenomenon is known as breakthrough.

Measurements of the electrokinetic charge of colloidal gold particles have shown that the particles carry negative charges [14, 15]. This was confirmed by electrophoretic measurements performed in our laboratory. These experiments were done using a simple Tiselius apparatus. It was observed that the interface between gold sol solution and its dialysate moved in the direction of the cathode, indicating that the particles were negatively charged. The zeta potential of the membrane materials under the conditions used here is expected to be negative[1, 19, 20]. As a result of these charges a repulsive force between pore wall and colloid particle exists, preventing the approach and adhesion of particles at the membrane wall. Since adhesion does not occur, the particles permeate through the porous structure until the pores and the particles are of comparable size.

Mutual interaction due to electrical double layer effects between the particles should be considered too. From literature on permeation of colloids it is known that, for example, during cake formation of filtered colloids, the structure of the cake is determined a great deal by the thickness of the double layer around the cake-forming particles [16-18]. These effects are the result of particle-particle interaction for impermeable particles and the role of membrane structure is limited in that case.

The double layer thickness, however, might increase the effective radius of the particles which do penetrate into the pores, as we are studying. From the DLVO theory the dependence of double layer thickness $(1/\kappa)$ on concentration of counter ions is known [14, 18]. For the sols that have been used here this thickness $(1/\kappa = (10\,cz^2)^{-0.5}$, with $(1/\kappa)$ in nanometers and where c is the counterion concentration in moles/liter and z is the valency of counterions; here c=1.4 $*10^{-3}$ mol/liter and z=1), is calculated to be about 10 nm. Since the double layer is diffuse, it can be deformed very easily, as is known from electrophoretic experiments. Hence only a small part of the diffusive double layer codetermines the hydrodynamic behaviour of the

particle. The distance between the 'hydrodynamic slip plane' and the particle is mainly determined by the size of the hydrated molecules adsorbed in the first layer around the sol particle. This increase in particle size is not more than a few tenths of a nanometer and the effective hydrodynamic size of the sol particles slightly differs from the values found by electron microscopy.

From this discussion it seems fair to assume that the colloidal gold particles are blocked only when the pore diameter and particle diameter are of comparable size. The impermeable layer exists of pores smaller than the size of the particles, whereas the pores at the boundary of the permeated and non permeated regions are of sizes comparable to those of the colloidal particles.

3.5 Conclusion

A new method for the determination of the skin thickness of UF membranes was developed.The method is based on the permeation of colloidal particles of well-known size entering from the macroporous sublayer side of an asymmetric UF membrane. The particles permeate through the large pores of the porous support until small pores near or in the skin are reached. In this way a thin layer is formed through which the colloidal particles cannot penetrate. This layer can be easily distinghuised by scanning electron microscopy.

PPO and PSf membranes were investigated using this method. PPO membranes have a well-defined skin layer with a thickness of about 0.2 μm and a pore size distinctly different from the pore size in the macroporous layer underneath. In case of PSf, a well-defined skin layer cannot be observed. The size of the pores in these membranes increases gradually from skin to sublayer.

3.6 Literature

1. Trågärdh, G. in 'Proceedings, Workshop on Characterization of Ultrafiltration Membranes' G. Trågärdh (ed.), p. 9, Lund University, Lund, 1987.
2. Capanelli, G. ,Vigo, F., Munari, S., J. Membr. Sci. 15 (1983) 289.
3. Smolders, C.A. and Vugteveen, E. in 'Material Science of Synthetic Membranes' D.R. Loyd (ed.), p. 327. ACS Symposium Series, Am. Chem. Soc., Washington, DC, 1985.
4. Kamide, K., Manabe, S. in 'Ultrafiltration Membranes and Applications' A.R. Cooper (ed.), p. 173, Plenum Press, New York, NY, 1980.
5. Altena, F.W., Knoef, H.A.M., Heskamp, H., Bargeman, D., Smolders, C.A., J. Membr. Sci. 12 (1983) 313.

6. Fane, A.G., Fell, C.J.D., Desalination 62 (1987) 117.

7. Bargeman, D., Vugteveen, E., te Hennepe, J., van 't Hof, J., Smolders, C.A., in 'Synthetic Polymeric Membranes' B. Sedlacek and J. Kahovec (eds.), p. 637, de Gruyter, Berlin, 1987.

8. Zsigmondy, R., Z.Anorg. Allg. Chem. 99 (1917) 105.

9. Frens, G., Kolloid Z. Z. Polym. 250 (1972) 73.

10. Fane, A.G., in 'Progress in Filtration and Separation 4,' R. J. Wakeman (ed.), vol. 4, p.101. Elsevier, Amsterdam, 1986.

11. Heertjes, P.M., Lerk, C.F., Trans. Inst. Chem. Eng. 45 (1967) T129.

12. Cook, M.A., in 'Hydrophobic Surfaces' F.M. Fowkes (ed.), p. 206. Academic Press, New York, 1969.

13. Herzig, J.P., Leclerc, D.M., le Cof, P., in 'Flow through Porous Media' R. J. Nunge (ed.), p. 129, ACS Publications, Washington, DC, 1970.

14. Verwey, E.J.W., Overbeek, J.Th.G. in 'Theory of the Stability of Lyophobic Colloids,' Elsevier, Amsterdam, 1948.

15. Glasstone, S., in 'Textbook of Physical Chemistry' p.1239., 2nd ed., McMillan, London, 1951.

16. Porter, M.C., Ind. Eng. Chem. Res. Dev. 11 (1972) 234.

17. McDonogh, R.M., Fane, A.G., Fell, C.J.D., J. Membr. Sci. 21 (1984) 285.

18. Maron, S.H., Lando, J.B., in 'Fundamentals of Physical Chemistry' p. 788. Macmillan, New York, 1974.

19. Lee, C.K., Hong, J., J.Membr. Sci. 39 (1988) 79.

20. Wei, Z. in, 'Proceedings, Workshop on Characterization of Ultrafiltration Membranes' G. Tragardh (ed.), p.234. Lund University, Lund, 1987.

4

Permporometry
Determination of the Size Distribution of Active Pores in UF Membranes

---

4.1   Introduction

For the measurement of pore sizes present in mesoporous media a range of methods is available. The majority of these methods originate from ceramic materials science, where it is of particular interest to know the pore size distribution and the pore volume, irrespective whether it concerns dead-end pores or interconnected pores. The characterization of UF membranes, however, is aimed at the prediction of transport properties from the membrane morphology, if possible. With such a goal in mind, it is crucial to measure the sizes of those pores which really contribute to the permeability. In the case of UF membranes these so-called 'active pores' are present in the skin layer of the membrane.

Most of the routine characterization methods cannot discriminate between the 'active' pores in the skin and 'inactive' pores present in the skin or in the supporting layer. Exceptions are the gas permeability method [1, 2] and the liquid-liquid displacement technique [3, 4]. These methods have other disadvantages and are not always capable to generate accurate, independent data. The significance of the gas permeability method is limited, because only mean pore sizes are measured and, as Altena et al. have shown [2], the quantitative values of these pore sizes are highly ambiguous. With the second method mentioned, the liquid-liquid displacement technique, a pore size distribution of a membrane can be measured, but the results are influenced by the experimental conditions [ref. 3 and chapter 1]. These uncertainties show the need for other characterization methods with which the sizes of active pores can be determined.

Permporometry, introduced by Eyraud [5, 6] and modified by Katz [7, 8], is a quite new characterization method to evaluate the active pores of an UF membrane. It is based on the controlled blocking of pores by condensation of a vapour, present as a component of a gas mixture, and the simultaneous measurement of the gas flux through the membrane. In this

paper we report on permporometry measurements using a set-up which provides a very well-defined (and easy to model) transport regime and a fast adjustment of equilibrium conditions.

4.2 Theoretical

Capillary Condensation

The capillary condensation theory implies the condensation of a vapour in small pores at relative vapour pressure values below one [9]; (relative vapour pressure = {vapour pressure}/{saturated vapour pressure}). At low relative vapour pressures, only adsorption of gas molecules to the pore wall is assumed to occur. This adsorption is restricted to the so-called 't-layer' with a maximum thickness in the order of a few molecular diameters. At higher values of the relative pressure the adsorption process is followed by capillary condensation commencing in the finest pores. As the pressure is progressively increased, wider pores are filled until at the saturation pressure the entire system is filled with condensate. The relative pressure at which pore filling starts depends on the radius of the capillary and can be calculated from the Kelvin relation (1):

$$\ln p_r = (-\gamma v / R T) \cos\Theta * (1/r_{k1} + 1/r_{k2}) \qquad (1)$$

p_r : relative vapour pressure (-) Θ : contact angle (°)
γ : interfacial tension (N/m) r_{ki}: (Kelvin) radius describing the
v : molair volume of the condensate   curvature of the liquid-gas interface (m).
  (m^3/mol)

In the application of the Kelvin relation it is generally accepted that $\Theta=0$. This simplifies equation (1) and permits the direct calculation of a pore radius corresponding to a certain relative pressure.

The desorption shows a similar behaviour as the adsorption. Now a liquid-containing pore will not empty before the vapour pressure falls below the equilibrium pressure given by equation (1). The desorption process is pictured schematically in figure 1.

The adsorption and desorption processes are not necessarily ruled by the same curvature of the liquid-gas interface which often leads to a hysteresis phenomenon. For instance, during adsorption in a cylindrical pore the meniscus has a cilindrical shape (in eq. (1): $r_{k1} = r_k$ and $r_{k2} = \infty$) whereas during desorption the liquid-gas interface is hemispherical (in eq. (1): $r_{k1} = r_{k2} = r_k$).

One has to realize that the Kelvin radius r_k found from equation (1) is the radius of curvature of

the liquid-gas interface, which is equal to the pore radius less the 't-layer' thickness of the adsorbed film on the pore wall (figure 1). The relationship between the true pore radius r_p and the Kelvin radius r_k thus is:

$$r_p = r_k + t \qquad\qquad (1a)$$
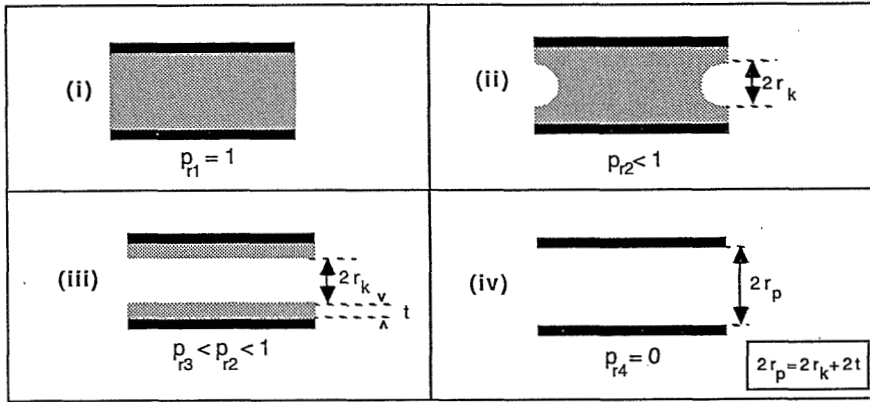
in which t is the thickness of the adsorbed t-layer.

Figure 1. Steps in the desorption process: (i) liquid filled pore, at saturation pressure; (ii): just before desorption starts, pore is still filled; (iii): just after evaporation is complete, t-layer remains; (iv): after complete desorption.

The thickness of the t-layer depends on the relative pressure. In classical adsorption studies this thickness is calculated from separate adsorption experiments which are performed using homogeneous non-porous reference surfaces, preferably made of the same material as the porous medium. This approach is very laborious and therefore we used an approximation to calculate the t-layer thickness directly from permporometry data (see below).

Capillary condensation provides the possibility to block pores of a certain size with a liquid, just by setting the relative pressure. In permporometry this principle is combined with the measurement of the free diffusional transport through the open pores. Starting from a relative pressure equal to 1, all pores of the UF membrane are filled so that unhindered gas transport is not possible. When the pressure is reduced, pores with a size corresponding to the vapour pressure set, are emptied and become available for gas transport. By measuring the gas transport of an inert gas through the membrane upon decreasing the relative pressure of the

condensable gas, the size distribution of the active pores can be found. Of course, similar measurements can be done during the adsorption process, but the equilibrium of the adsorption process is more difficult to reach and therefore quantitative analysis of the desorption process is preferred.

Counterdiffusion

In our approach, the principle of counterdiffusion of two different inert gases, oxygen and nitrogen, in the absence of an overall pressure gradient is used to monitor the transport through the membrane. The driving force for the transport is the concentration gradient of the two gases which, combined with the fact that small pores (< 25 nm) are analysed, assures a well-defined diffusion regime. At an overall pressure of ca. 100 kPa, the main transport mechanism is assumed to be Knudsen diffusion [10], which for a cylindrical capillary structure is described by equation (2):

$$J_{k,i} = \{\pi \, n \, r^2 \, D_{k,i} \, \Delta p_i\} / \{R \, T \, \tau \, 1\} \qquad (2)$$

in which the Knudsen diffusion coefficient $D_{k,i}$ reads:

$$D_{k,i} = 0.66 \, r \, \{(8 \, R \, T) / (\pi \, M_i)\}^{0.5} \qquad (2a)$$

$J_{k,i}$: diffusional flux (mol/s Pa m^2) n : number of pores (1/m^2)
r : pore radius (m) Δp_i : partial pressure gradient (Pa)
1 : thickness of the porous medium (m) M_i : molecular mass of the gas (g/mol)
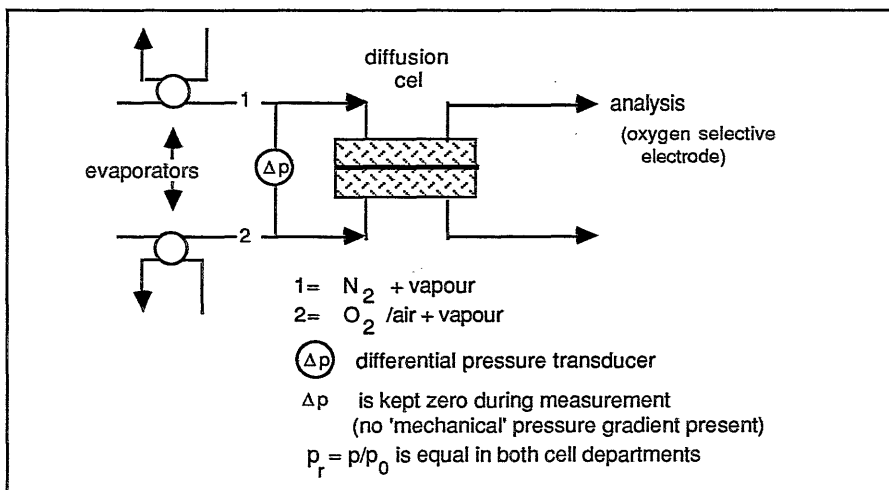τ : tortuosity (-).

Figure 2. Permporometry: experimental set-up

4.3   Experimental

The experimental set-up (figure 2) is derived from those of Eyraud [5] and Katz [7] and adapted to the conditions needed for counterdiffusion measurements. Along both sides of the membrane a mixture of a condensable gas and a non-condensable (i respectively j) gas is flushed. The condensable gas can be any vapour, provided it has a reasonable vapour pressure and is inert with respect to the membranes to be characterized. The relative pressure of the vapour (p_r) is the same in the whole diffusion cell. The main advantage of the apparatus presented here, is the fact that the equilibrium between vapour/gas mixture and capillary condensate is reached faster than with the set-ups described in literature.

The measurements start at a relative vapour pressure equal to one, which means a minimum in diffusional transport. While the membrane is equilibrated at progressively lower relative vapour pressures, the diffusional transport of oxygen through the membrane is measured with an oxygen selective electrode. After reaching a relative pressure of 0, the process is reversed and the adsorption branch is measured. Equilibration times varied from 15 to 30 minutes, depending on the amount of condensate that had to be adsorbed or removed. Using equation (1) and (2), the pore size distribution is calculated from the desorption branch.

Several membranes were characterized by the method described above. Ceramic membranes were kindly supplied by the group of Burggraaf [11], Nuclepore 0.015 µm membranes (lot nr 86A9B14) were purchased from the Nuclepore Corporation and DDS GR61PP, manufactured by DDS Danmark, were supplied by the Dutch Institute for Dairy Research (NIZO).

A more detailed study was made of lab-made anisotropic polymeric membranes, synthesized of poly(2,6 dimethyl-1,4-phenylene oxide) (PPO) and polysulfone (PSf). PPO membranes were prepared from a 10 wt% polymer solution in a mixture of trichloroethylene and octanol-1 in a weight ratio 78/22. PSf membranes were made from a 15 wt% PSf solution in DMF. In both cases the solutions were cast at room temperature to a thickness of 0.20 mm on a glass plate. The PPO films were coagulated in a methanol bath and the PSf films in a water bath. All solvents used were of analytical grade.

In principle, the condensable gas should not change the porous matrix and the vapours must be as inert as possible. To investigate the effect of different vapours, four different adsorbates, i.e., ethanol, methanol, tetrachloromethane and cyclohexane (p.a. quality, Merck) were used.

4.4   Results and Discussion

Ceramic γ-Alumina Membranes

In figure 3 the oxygen flux through an alumina membrane, during the adsorption and desorption of the condensable gas cyclohexane, is shown. This typical plot of flux vs. relative pressure can be divided in three main parts. In the interval $1 \geq p_r > 0.55$ all the pores are blocked with condensate and free gas diffusion is impeded. During desorption, occurring at relative pressures between 0.55 and 0.3, the flux strongly increases with decreasing relative pressure. At lower relative pressures (< 0.3) this increase in flux is less steep.
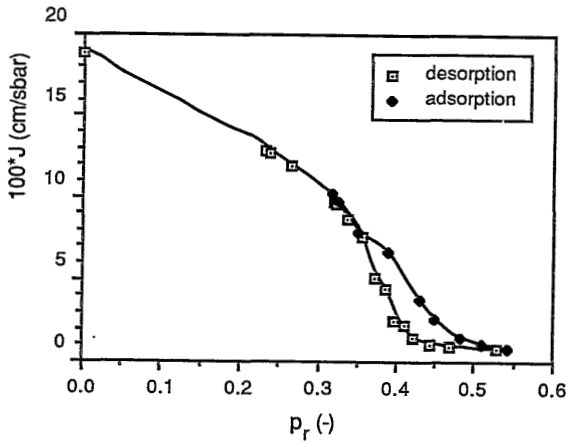

Figure 3. Permporometry: adsorption and desorption curve for a γ-alumina membrane with cyclohexane used as adsorbate

It is clear that in the range of relative pressures between 0.55 and 0.3 the flux behaviour is ruled by the capillary condensation process hence, equation (1) can be applied to calculate the Kelvin pore radii (r_k). The flux vs. pore size plot, given in figure 4 was calculated from the desorption data, assuming a capillary model. From the diffusional flux values and making use of the calculated pore sizes the number of pores is determined from equation (2). In order to find the real pore size the Kelvin radii should be corrected for the adsorbed t-layer. Figure 3 shows that upon lowering the relative pressure beneath 0.3, the flux through the membrane still increases. It can be argued that in this region all pores are already opened and available for transport, but the size of the pores increases a little as the result of the desorption of the t-layer. When a uniform t-layer (with a thickness t) in all pores is assumed at $p_r = 0.3$, the effective pore size will increase from r_k to $r_p = r_k + t$ (equation (1a)) upon decreasing the relative pressure from 0.3 to 0. So, by using the calculated pore size distribution (Kelvin radii) and the experimental values of the oxygen flux at relative pressures 0.3 and 0 respectively, an estimate

of the t-layer thickness can be made. The data found for cyclohexane give a mean t-layer thickness of 0.5 nm (at $p_r = 0.3$).
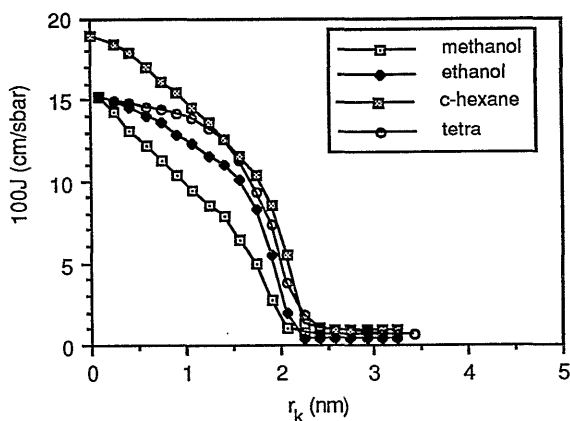

Figure 4. Oxygen flux as a function of the Kelvin radius measured with different adsorbates found for γ-alumina membranes.

In the foregoing analysis only desorption data were used to calculate the pore size distribution. In the case of cyclohexane, in principle, the adsorption branch could be used for the pore size evaluation too. However, the combination of these data with a capillary model gives substantially lower pore sizes than the desorption data. This may indicate that the pore shape in the alumina membrane is not cylindrical. Leenaars [13] concluded from classical adsorption-desorption studies that the alumina membranes contain slit-shaped pores. If the ratio of the length to the width of these slits is not too high, this model indeed may be a better approximation.

To investigate the influence of different adsorbates on the quantitative analysis, measurements using ethanol, methanol and carbon tetrachloride as the condensable gas were carried out. Carbon tetrachloride and cyclohexane are considered as so-called van der Waals gases which means that their molecules are assumed to act as non-interacting hard spheres (similar to an ideal gas) with a finite volume and their physical behaviour is described by the van der Waals equation. Methanol and ethanol are considered to be less ideal which may influence the permporometry measurements [14].

In figure 4 the resulting J - r_k plots for the different vapours used, are shown. The nominal Kelvin radii found with ethanol, tetra and cyclohexane, differ only slightly. When methanol is used it appears that slightly lower pore sizes are found. This shift in Kelvin radius can be attributed to the difference in t-layer thickness. For ethanol, cyclohexane and carbon

tetrachloride the calculated t-layer thicknesses are about the same (~0.4 nm). This value corresponds with 1 or 2 molecular layers which is in good agreement with literature data on physical adsorption of organic molecules [9, 12]. In case of methanol the t-layer is significantly thicker: 0.7 nm, which is an unexpectedly high value especially compared with ethanol.

Table 1. *Pore sizes and t-layer thicknesses found for γ-alumina membranes and using different adsorbates*

adsorbate	r_p (nm) [1]	t (nm)
cyclohexane	2.3	0.5
ethanol	2.2	0.4
methanol	2.3	0.7
carbon tetrachloride	2.2	0.4

1) nominal pore size

In physical adsorption only van der Waals forces account for the interaction, which means that when the molecules of the different adsorbates are of comparable size, the thicknesses of t-layers of these adsorbates is expected to be same. From the latter it follows that the interaction between the alumina pore wall and the methanol molecules is substantially stronger than it is for the other condensable gases. This strong interaction has also been shown in other studies in which γ-alumina is used as a catalyst in the oxidation of methanol [15].

The pore size distributions of the alumina membranes obtained using different vapours and corrected for the t-layer thickness agree very well with each other (figure 5). This indicates that, at least for this type of porous systems, the pore size analysis does not depend on the sort of vapour used. It is clear that the γ-alumina membranes used, exhibit a very well-defined structure which is in agreement with results found with other characterization techniques. For instance, a very sharp pore size distribution (r~2 nm) was also found using the gas adsorption-desorption technique or using thermoporometry (figure 6) [ref. 13, chapter 2]. Because the membranes are of the composite type, the thickness of the active layer is known accurately (5 µm). These particular features should make this membrane a well-suited system to be used in a model study.

Using the determined Kelvin radii and the number of pores, a surface porosity and a volume porosity can be calculated. When the cylindrical capillary model is applied with a tortuosity factor τ=1, the data result in a surface and volume porosity of 0.9-1.2 %. The other techniques
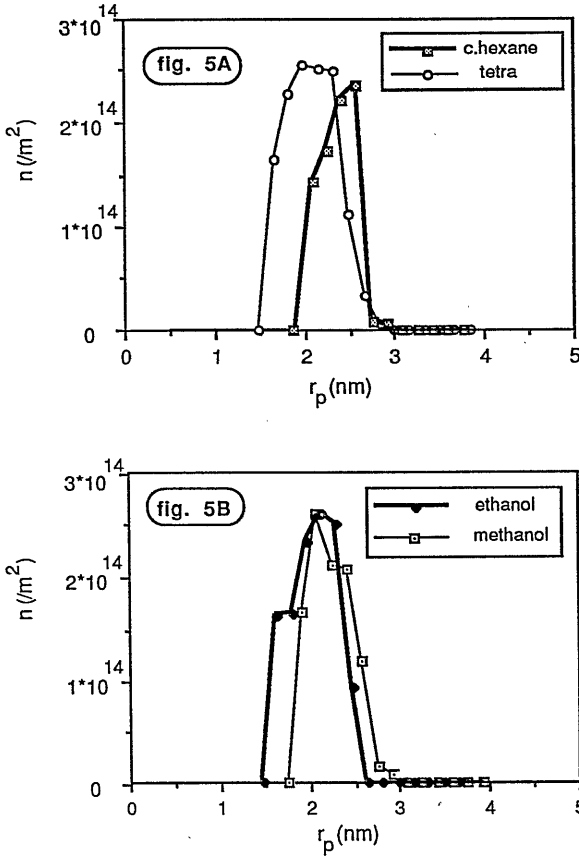
Figure 5A and B. Pore size distributions of active pores of γ-alumina membranes measured with different adsorbents in permporometry.

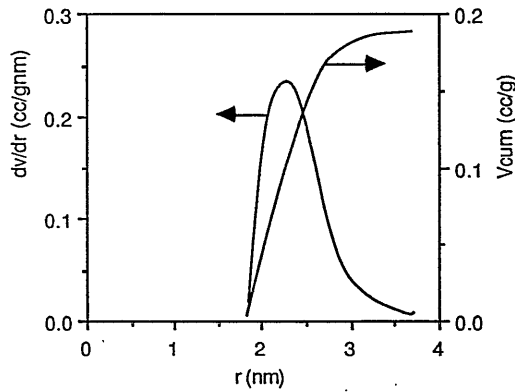*Figure 6. Pore size distribution for a γ-alumina membrane using thermoporometry.*

already mentioned indicate a much higher value for the volume porosity (~45%). One of the reasons for this large deviation is the extremely high tortuosity factor of the alumina membranes. For many porous media the tortuosity factor has a value of 2-3, but for the alumina system a value of 13 was found [13]. Compared to the hypothetical system with $\tau = 1$, the porosity value of the alumina system is 13 times larger.

Another point is that the very thick sublayer of the alumina membranes is responsible for 70% of the resistance of the total system [11]. This means that the effective driving force across the toplayer is only 30% of the total and, the other way around, the porosity of the toplayer is 3 times larger than calculated before. When corrections for the tortuosity ($\tau = 13$ instead of 1) and the resistance of the sublayer are used, the calculated porosity is 35-45 %.

Nuclepore Membranes

Nuclepore membranes are claimed to have a very well-defined capillary structure with a uniform pore size and a tortuosity factor equal to one ($\tau = 1$). Consequently these membranes should be very suitable for model studies. In this work membranes with a claimed pore radius of 7.5 nm were used.

The resulting pore size values found by permporometry (figure 7) are indeed in reasonable agreement with the expected values. The experimental flux, however, appears to be 7 times higher than the value calculated from the data given by Nuclepore (number of pores: $6*10^{12}$ /m^2, tortuosity: 1, pore radius 7.5 nm).
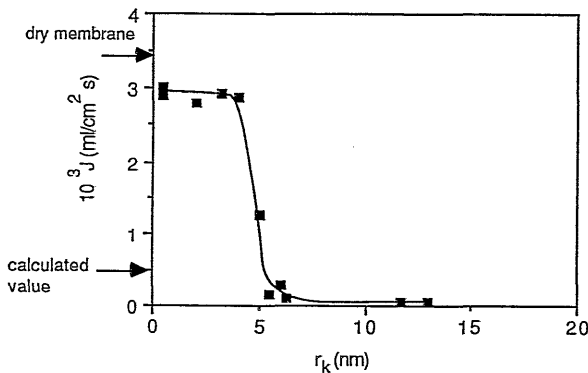

Figure 7. Oxygen flux as a function of Kelvin radius for a Nuclepore 0.015 μ membrane (calculated flux value using data given by Nuclepore: r = 7.5 nm, n = 6 * 10^{12} /m^2, tortuosity = 1.).

Using electron microscopy (EM), the number of pores per unit surface area of similar membranes has been investigated by a number of reseachers [16, 17]. Their results appeared to

correlate very well with the Nuclepore values (also determined by EM). The only possibility to explain the apparent discrepancy is the tortuosity factor, which is obviously too high. A tortuosity factor lower than 1 can be related to a widening of the pores inside the membrane, which accounts for a lower resistance for transport. From the experimental fluxes, the effective pore size (for water and gas transport!) is estimated to be twice the size of the pore opening. Alltogether this means that pores of a Nuclepore membrane have a narrow pore mouth with a size as claimed by the manufacturer and a wider effective pore size inside the membrane which accounts for the reduced transport resistance.

Since the pores of the Nuclepore membrane are relatively large, the thickness of the t-layer is of minor importance (figure 7). A remarkable effect, however, is that the t-layer thickness appears to be unchanged up to very low relative pressures, which might be due to specific interaction (instead of only van der Waals interactions). Going from a relative pressure of ~0.7 to 0.2, the flux through the membrane remains constant, but when the relative pressure is decreased further to 0, a 10% increase in flux is found. This increase corresponds with a t-layer thickness of about 0.5 nm which is about one monolayer of ethanol molecules [12].

PPO Membranes (lab-made)
Pore size distributions of PPO membranes were determined using methanol and ethanol as the condensable component. In figure 8 results for two different samples of a PPO membrane are given. It appears that the largest interconnected pores present in PPO membranes have a size of about 15 nm, although a large number of small pores are present too. Despite their small number, the larger pores mainly determine the performance of the membrane. Consequently the thickness of the adsorbed t-layer is not of decisive significance, it is sufficient to know that it is very small. Using the same treatment as before, the thickness for methanol was found to be 0.25 nm. For ethanol the thickness was estimated to be 0.5 nm. Again these values correspond fairly well with literature data [9, 12].

In order to calculate the number of pores present in the membrane skin, all characteristic parameters in equation (2) are needed, i.e., also the thickness of the skin layer must be known. With the gold sol method ([18], chapter 3), the skin thickness has been determined to be 0.2 μm and assuming that the tortuosity factor equals one, the number of pores can be estimated. From the number of pores and their sizes, the surface porosity has been calculated to be 0.5%, a very low value, as is also found for other UF membranes [19, chapter 1]. Using the skin thickness of 0.2 μm and $\tau = 1$, the volume porosity (per unit membrane area) has been calculated to be about 10^{-7} cc/cm^2.

From thermoporometry and the gas adsorption-desorption technique, it was found that PPO membranes possess a very sharp pore size distribution, with a characteristic mean pore size of
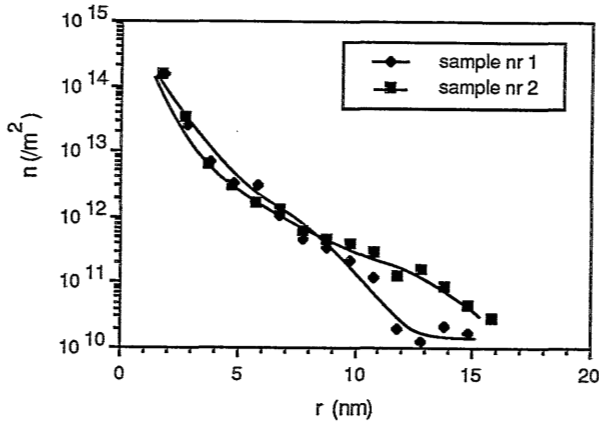
Figure 8. Pore size distribution using permporometry found for two samples of the same PPO membrane (lab-made).

2 nm. This result is in strong contrast with the permporometry data mentioned here. In addition, the porosity value calculated from permporometry is 2000 times smaller than the value found by thermoporometry. This can only be explained by the fact that in the case of gas adsorption-desorption and thermoporometry the membrane is characterized as a whole (top- and sublayer) and small pores which are present in the sublayer are measured too. In the case of PPO membranes, the ratio between the porosity related to active skin pores and the overall porosity indicates that 99.99% of the pores are present in the sublayer and consequently do not influence membrane performance. Hence, the pore volume of the larger pores is so small that their presence cannot be detected by, e.g., thermoporometry.

PSf Membranes (lab-made)
Pore size distributions of two PSf membranes are given in figure 9. Methanol and ethanol, used as the condensable vapours, showed a similar t-layer thickness as in the case of PPO. Also for PSf membranes a broad pore size distribution is calculated (skin thickness 0.2 μm, determined with the gold sol method [18], $\tau = 1$), with a largest pore size of roughly 10 nm. Compared to PPO membranes, the number of the smaller pores (< 5 nm) is substantially lower.

Despite the fact that both membranes were casted out of the same polymer solution, their pore size distributions differ somewhat. One of the membranes appears to have a certain dip in the distribution at a pore size of about 3 nm. This indicates that, even for membranes prepared at nearly the same conditions, from the same polymer solution, differences in pore structure can be present.
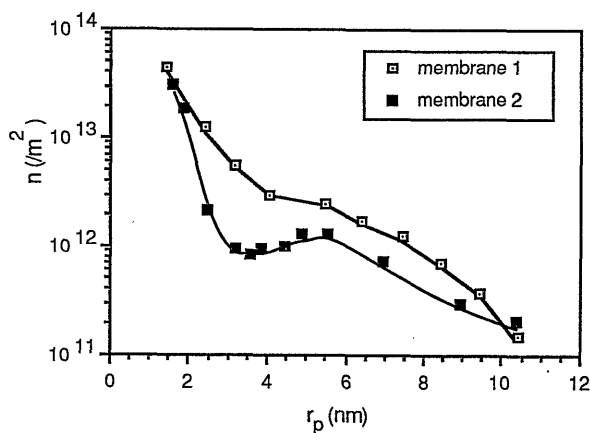
Figure 9. Pore size distribution using permporometry found for two lab-made PSf membranes (cast from the same polymer solution).

The low surface porosity (calculated value ~ 0.3%) is probably the main reason that the pore size distribution of PSf membranes could not be determined by one of the methods already mentioned. The intrinsic independence of skin pore volume in applying permporometry is another advantage of this method, in particular when UF membranes are evaluated which are known to have low skin porosities.

DDS GR61PP Membranes

GR61PP membranes, manufactured by DDS, are made of polyethersulfone (PES) and have a claimed cut-off of 20 kDalton. The pore size distribution as determined with permporometry is remarkably sharp (figure 10), most of the pores have sizes in between 1.5 and 5 nm. When the toplayer thickness of the membranes is estimated at 0.2 μm, the surface porosity is again very low, about 1%. The diffusional fluxes, i.e., the number of pores (fig. 10), found for two samples of the same membrane appear to be significantly different. In the calculations of the number of pores the skin thickness is assumed to be constant. A somewhat varying skin thickness, however, can account for the difference in flux between the two samples as well.

The pore sizes are in agreement with the 'characteristic pore size' found by Hanemaaijer et al. using rejection measurements of low molecular weight sugar molecules [20]. Nilsson [21] determined the pore size distribution of the same type of membranes with the liquid-liquid displacement technique. He found a considerable number of large pores between 25 and 100 nm. Furthermore he found that the porosity (number of pores) of these membranes was inhomogeneously distributed: the pore number for one part of the membrane differs
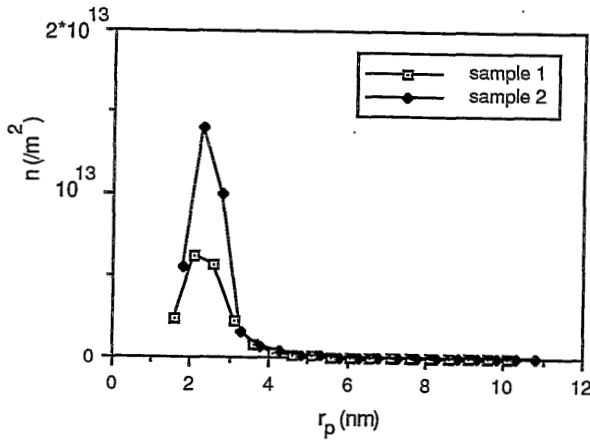
Figure 10. Pore size distributions using permporometry found for two samples of the same DDS GR61PP membrane .

significantly from another part. The latter is confirmed by permporometry measurements (fig.10), but in contrast with Nilsson, pore sizes larger than 5 nm were not detected.

Some Comments on the Pore Size Distribution Determination by Permporometry

The distributions determined for the different polymeric membranes are characterized by an asymmetric shape. For all the membranes, it appears that a relatively large number of small pores (radii smaller than about 2 nm) is present. The question arises whether this porosity really corresponds to such small pores or whether it is an artefact introduced by the characterization technique itself.

One should realize that in the concept used here, the discrimination between t-layer desorption (or adsorption) and capillary condensation is treated quite roughly. In case of ceramic membranes the adsorption and desorption branches can be separated easily, as is shown in figure 3. The lowest relative pressure where the adsorption and desorption process meet, is directly related to the point were capillary condensation and adsorption processes merge. For these membranes this transition is sharp because the pore size is well-defined. The question is what happens when a wider pore size distribution and a relatively large number of small pores are present at the same time. In such a case the t-layer analysis proposed in this work neglects the presence of these small pores in favour of a larger apparent t-layer thickness.

The validity range of the Kelvin relation is not strictly defined, but it is generally agreed that for pores with radii smaller than 1.5 nm, the equation is not valid anymore. This is comprehensible because in these very fine pores, with about the size of a few molecular diameters, the concept

of a meniscus becomes meaningless [9]. In very small pores (micropores), the interaction between molecules and pore wall will be much higher than in mesopores. In such small pores adsorption already occurs at very low relative pressures and molecules present inside the pores can only be removed by using very low relative pressures ($p_r = 0$ or in vacuum). This not only holds for the adsorbates used in this study, but also when the membrane is in the environment where it is actually being used. Together with the fact that in UF membranes the larger pores will mainly determine transport properties and hence the performance of the membrane, it can be concluded that even when very small (micro) pores are present, permporometry indeed gives relevant data on the structure of the membrane, related to its performance.

4.5 Conclusions

Permporometry is a method by which the active pore size distribution can be determined accurately. Characteristic data found by permporometry, sometimes deviate substantially from the characteristics determined by other methods like gas adsorption-desorption or thermoporometry. These discrepancies can be fully understood from the difference in the ability of the methods to detect only the pore structure in the skin.

The pore size distribution of γ-alumina membranes is very narrow, whereas the distributions of lab-made polymeric UF membranes are fairly broad. From the latter it can be concluded that the actual performance of these membranes is governed by the larger pore sizes, i.e., 5 to 10 nm.

DDS GR61PP membranes appear to have a narrow pore size distribution. Differences in permeability observed for different samples may be due to a varying number of pores or local differences of the skinlayer thickness.

4.6 Literature

1. Yasuda, H. and Tsai, J.T., J. Appl. Polym. Sci. 18 (1974) 805
2. Altena, F.W., Knoef, H.A.M., Heskamp, H., Bargeman, D. and Smolders, C.A., J. Membrane Sci. 12 (1983) 313
3. Bechhold, H., Schlesinger, M. and Silbereisen, K., Kolloid Z. 55 (1931) 172
4. Munari, S., Bottino, A., Moretti, P., Capanelli, G. and Becchi, I., J. Membrane Sci. 41 (1989) 61
5. Eyraud, Ch., Betemps, M. and Quinson, J.F., Bull. Soc. Chim. France 9-10 (1984) I-238
6. Eyraud, Ch., lecture presented at the Summer School on Membrane Science,

Cadarache, 1984

7. Mey-Marom, A., Katz, M., J. Membrane Sci. <u>27</u> (1986) 119

8. Katz, M. and Baruch, G., Desalination <u>58</u> (1986) 199

9. Gregg, S.J., and Sing, K.S.W. in 'Adsorption, Surface Area and Porosity', 2nd edition, Academic Press, London, 1982

10. Mason, E.A. and Malinouskas, A.P. in 'Gas Transport in Porous Media: the Dusty Gas Model', Elsevier, Amsterdam, 1983

11. Keizer, K.K. and Burggraaf, A.J. in 'Science of Ceramics 14', B. Taylor (ed.), p. 83, Institute of Ceramics, Shelton, UK, 1988

12. Jones, B.R. and Wade, W.H., in 'Hydrophobic Surfaces', Fowkes, F.M. (ed.), p.206, Academic Press, New York, (NY), 1969

13. Leenaars, A., Thesis University of Twente, the Netherlands, 1984

14. Katz, M. Proceedings of the World Filtration Congress III, p.508, 1982

15. Peri, J.B., J. Phys. Chem. <u>70</u> (1966) 3168

16. Hernandez, A., Martinez-Villa, F., Ibanez, J.A., Arribas, J.I. and Tejerine, A.F., Sep. Sci. and Techn. <u>21</u> (1981) 665

17. Mitchell, B.D. and Deen, W.M., J. Colloid Interface Sci. <u>113</u> (1986) 1

18. Cuperus, F.P., Bargeman, D. and Smolders, C.A., J.Colloid Interface Sci. <u>135</u> (1990) 486

19. Fane, A.G., Fell, C.J.D., Desalination <u>62</u> (1987) 117

20. Hanemaaijer, J.H., Robbertson, T., van den Boomgaard, Th., Olieman, C., Both, P. and Schmidt, D.G., Desalination <u>68</u> (1988) 93

21. Nilsson, J.L., 'A Study of Ultrafiltration Membrane Fouling', Thesis University of Lund, Sweden, 1989

chapter 5

5

Adsorption and Desorption Isotherms Used for the Characterization of UF Membranes

5.1   Introduction

An anisotropic ultrafiltration (UF) membrane consists of a thin top layer (also called 'skin') and a macroporous sublayer. The pores in the top layer are responsible for the separation characteristics of such a membrane, whereas the sublayer acts as a support and in principle does not influence the performance of the membrane. Knowledge of the pore structure of the skin is vital for the understanding of the relation between morphology and performance of these porous membranes and a number of characterization methods have been developed during the past few years [1].

Although the analysis of adsorption and desorption isotherms is one of the most frequently used and best known characterization techniques for porous solids [2], application of this technique to porous polymer samples, like UF-membranes, is scarcely found in literature [3, 4]. One of the reasons for the limited use of this technique is the sometimes deviant adsorption behaviour of polymeric materials compared to inorganic substances [4]. Another reason is that the porosity of UF membranes, at least in the skin, generally is very low (~1%) [5], which makes the determination of a pore size distribution from adsorption or desorption measurements difficult.

It has been shown that for non-porous substances, the thickness of the adsorbed layer (the 't-layer') is a function of relative pressure [2, 6]. According to de Boer [6], this t-layer thickness is nearly independent of the nature of the adsorbent, which leads to the definition of the so-called 'universal t-curve'. In this concept the statistical thickness (t) of an adsorbed layer of nitrogen molecules which is formed on an adsorbent surface is described by:

$$t = \sigma*(v/v_m) = f(p_r) \qquad\qquad (1)$$

t : statistical thickness of the adsorbed layer (Å) p_r : relative pressure (-).
v : adsorbed volume (ml (STP)/m^2)   σ : diameter of the adsorbed
v_m : monolayer volume (ml (STP)/m^2)   molecule; σ(N$_2$) = 3.54 Å.

For the examination of porous materials, the adsorption isotherm of a reference material is needed to separate the 'normal' adsorption from the capillary condensation phenomenon. When, for a given sample, the adsorbed volume (at p_r) is plotted as a function of the thickness t of the adsorbed layer corresponding to the same value of p_r, valuable information about the pore structure of the sample can be deduced. As long as the molecule can adsorb freely and no capillary condensation occurs, the v-t plot is a straight line through the origin. However, when capillary condensation takes place, adsorption is enhanced and an upward deviation from the line occurs.

Lecloux and Pirard [7] pointed out that the universal t-layer concept is only valid in a restricted sense and differences in adsorption isotherms of different materials can be caused by different adsorbate-adsorbent interactions. Consequently, comparison of the isotherms of the reference and the 'unknown' sample is only possible when the adsorbate-adsorbent pairs have approximately the same heat of adsorption. Lecloux et al. classified different reference materials and their adsorption isotherms on the basis of the C_{BET} value, which is a parameter related to the heat of adsorption [2]. This C_{BET} value is determined easily from each adsorption isotherm and thus facilitates the choice of a suitable reference isotherm. As in the classical approaches only reference isotherms of inorganic materials are available, which have a different physical nature than polymeric materials, it appears that Lecloux's broader approach would be more suitable for the analysis of polymeric porous media.

5.2   Experimental

UF membranes were made of poly(2, 6 dimethyl-1, 4-phenylene oxide) (PPO) and polysulfone (PSf). PPO membranes were prepared from a 10 wt% polymer solution in a mixture of trichloroethylene and octanol-1 in a weight ratio 78/22. PSf membranes were prepared from a 15 wt% solution in DMF. In both cases the solutions where cast at room temperature to a thickness of 0.20 mm on a glass plate. The PPO films were coagulated in a methanol bath and the PSf films in a water bath. All solvents were of analytical grade.

Commercial DDS GR61PP membranes, manufactured by DDS Danmark were examined too. According to the manufacturer these membranes are made of polyethersulfone, and have a cut-off value of 20,000 Dalton.

The adsorption and desorption isotherms were determined with an ASAP 2400 apparatus of

Micromeritics Instrument Corporation. Nitrogen was used as the adsorbate.

In order to remove the water from the pores, PSf membranes were immersed in an ethanol bath. The DDS membranes (water filled) were separated from their non-woven support and then immersed in ethanol. Before examination all the membranes were dried at room temperature in a vacuum chamber for at least 48 h.

5.3   Results and Discussion

Figures 1, 2 and 3 show the adsorption and desorption isotherms for the PPO, PSf and DDS membranes respectively. In the case of PPO membranes the isotherms show hysteresis, characteristic for mesoporous media. The hysteresis loop is not closed, i.e., at low relative pressures there still is a considerable volume of adsorbate present. In fact, this adsorbate could be removed only after prolonged time in vacuum (p < 1 mbar). A new adsorption-desorption cycle (with the same membrane) resulted in the same isotherm, including the hysteresis. For PSf and DDS membranes the adsorption and desorption branches are practically identical and the presence of mesopores is not directly evident.
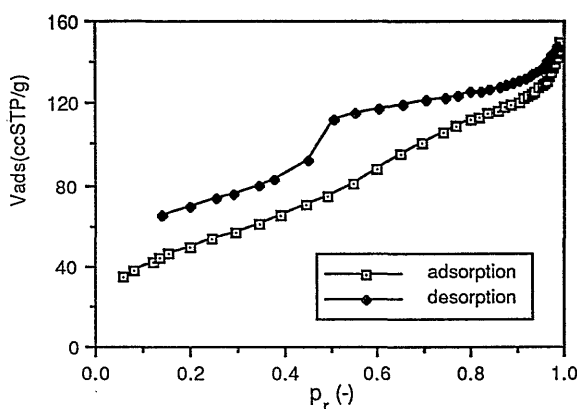

Figure 1. Typical adsorption-desorption isotherm for a PPO membrane.

In order to investigate the occurrence of capillary condensation, the reference isotherms given by Lecloux and Pirard [7] were used. To select the appropriate reference isotherm, the C_{BET} value of the materials had to be determined. Application of the BET-analysis gave the C_{BET} values and the specific surface areas as given in table 1.
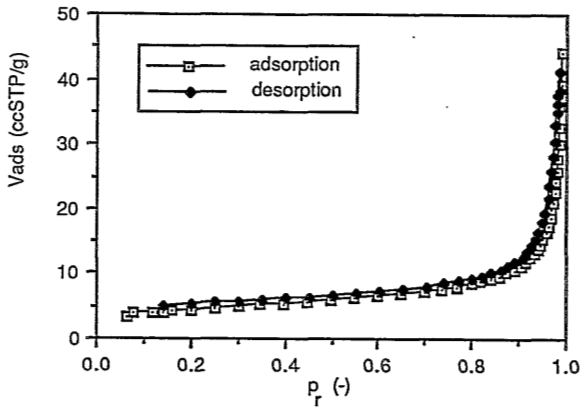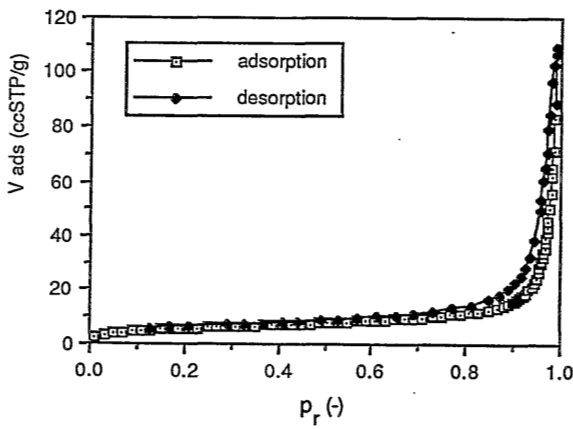
Figure 2. Isotherms found for a PSf membrane.

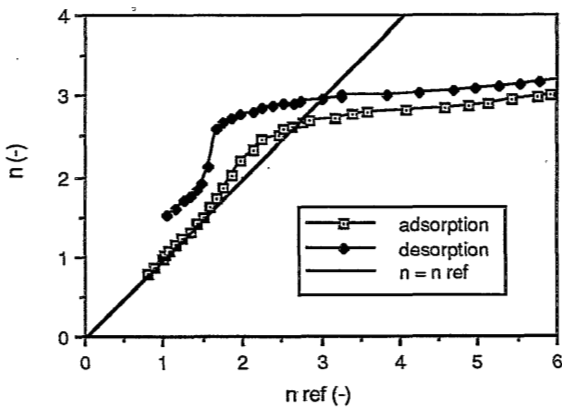Figure 3. Adsorption-desorption isotherms of a DDS membrane.

Figure 4. PPO membranes: measured numbers of adsorbed layers as a function of the number on the reference.

Table 1. *Specific area and C_{BET} values obtained for the different membranes*

membrane	specific area (m^2/g)	C_{BET} (-)
PPO	170	25
PSf	24	77
DDS	17	150

The combination of the reference isotherm and the experimental data, results in the 't-plots' shown in figures 4, 6 and 8 for PPO, PSf and DDS respectively.

PPO Membranes

In figure 4 the number of layers present on the porous PPO membrane is compared with the statistical number of layers of nitrogen molecules adsorbed on a non-porous reference material (both samples at the same p_r). As long as solely adsorption occurs, the increase of the t-layer thickness on the reference and the membrane is the same (so $n = n_{ref}$). At a certain relative pressure the uptake of adsorbate is enhanced (and $n > n_{ref}$) indicating that capillary condensation occurs. Finally, when all the pores are filled with condensate, the amount adsorbed on the porous sample remains practically constant whereas adsorption on the reference proceeds unhindered, so $n < n_{ref}$.

In the case of PPO membranes it is clear that during adsorption, capillary condensation occurs. The desorption branch does not return to the linear part of the plot, related to the pure adsorption of nitrogen. Such phenomena are also found for materials that swell upon adsorption [2]. Since the solubility of nitrogen in PPO is very low (~0.01 cm^3/ gbar at 25 °C [8]), swelling of PPO membranes in nitrogen at 77 K is not probable.

Pore size distributions of PPO membranes were calculated by the BJH method [2, 9], which is based on the combination of the already mentioned t-layer concept [2, 6] and the capillary condensation phenomenon as is described by the Kelvin equation [2, chapter 1]. Both adsorption and desorption branches were used for the pore size analysis. The results are shown in figure 5. The pore size distributions obtained from the adsorption and the desorption isotherm are slightly different. The pore sizes calculated from the adsorption branch are not only slightly larger than those resulting from the desorption branch, but the distribution is
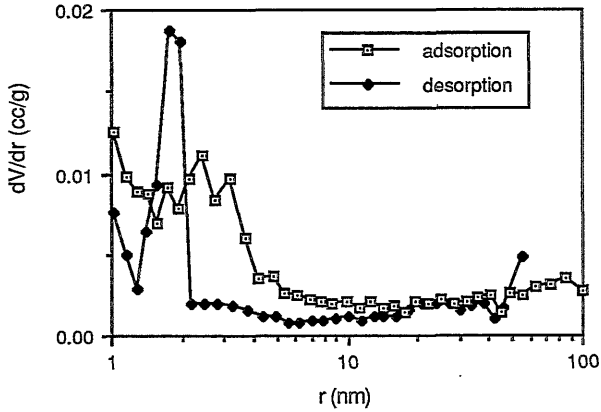
Figure 5. Pore size distribution of a PPO membrane, calculated from the adsorption and desorption branch.
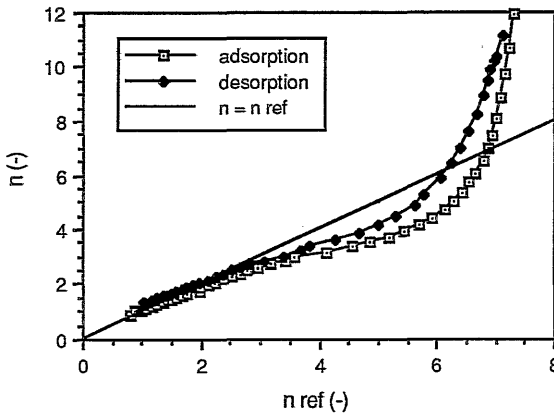

Figure 6. PSf membranes: measured numbers of adsorbed layers as a function of the number on the reference.

broader too. This phenomenon has been recognized as a so-called 'network effect' [2]. In simple capillary structures adsorption and desorption can occur independently of the state of neighbouring pores but in an interconnected network especially the desorption process can be hindered. A simple example is the ink-bottle pore, where the condensate in the 'neck' blocks the pore opening and prevents evaporation of the already unstable condensate in the 'bottle'. In systems where phenomena like pore blocking occur, the pore size distribution derived from the desorption branch tends to be much narrower than it actually is. Since the adsorption process is supposed to be free of blocking effects, this branch is preferred for pore size calculations.

Following the reasoning mentioned above, the pore network of a PPO membrane consists of wider parts connected by narrower channels. According to the pore size distribution calculated

from the adsorption branch, the radius of the largest pores is about 5 nm, but also pores of 2 nm account for a fairly large volume. Network effects can also make the low pressure hysteresis comprehensible. It can be imagined that large pores (> 50 nm) are connected to the outer surface by micropores (< 2 nm). The large pore bodies are filled at high relative pressures, but will not empty before the relative pressure is at the very low equilibrium value common for micropores. As, until now the adsorption processes in micropores are hardly understood, quantification of the micropore size is very difficult.

PSf Membranes

For PSf membranes the t-plot is given in figure 6. As long as n < 3 the experimental and reference t-layer thicknesses agree reasonably well. Also at high relative pressures (n > 6; p_r>0.98) the behaviour of the plot is clear, at these pressures capillary condensation results in the enhanced uptake of adsorbate. The pores related to these relative pressure are very large (> 100 nm) and are probably present in the sublayer of the membrane.

At relative pressures between 0.90 and 0.98 (3<n<6), the amount adsorbed on the porous sample is lower than that on the reference sample, which suggests that hindered adsorption within pores occurs. Such mesopores, however, would cause an enhanced adsorption at lower relative pressure (n < 3), which apparently does not occur. Another explanation is the presence of micropores (radius< 2 nm) which influences the choice of a standard isotherm. As in micropores the molecules are strongly adsorbed, the apparent C_{BET} value is higher than it would be in the absence of micropores. In such a case it is impossible to use the approach of Lecloux.
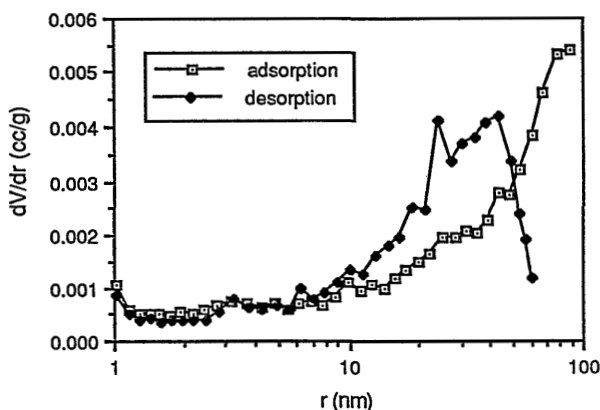

Figure 7. Comparison of the pore size distributions of PSf membranes calculated from the adsorption and desorption branch.
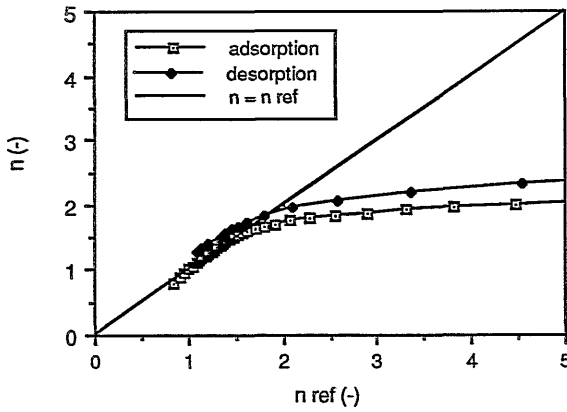
Figure 8. The numbers of adsorbed layers on a DDS membrane compared with the number of layers on a reference.
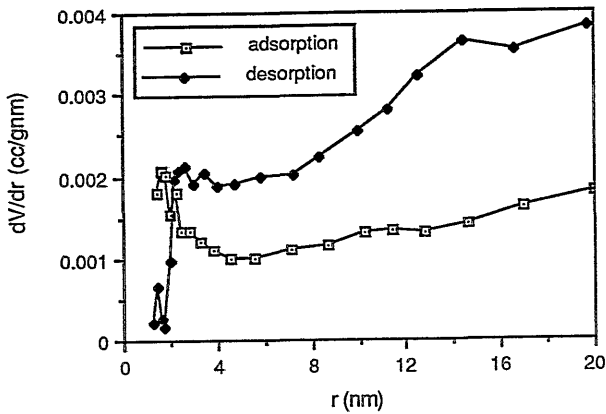

Figure 9. Comparison of the pore size distributions of DDS membranes calculated from the adsorption ads desorption branch.

The pore size distributions obtained for PSf membranes are very broad (figure 7). Since the sizes of the pores are fairly large, it is believed that these pores are present in the sublayer of the membranes. The difference between the distributions calculated from the adsorption and desorption branches again suggest an effect of the pore network. The pore size distribution of the adsorption branch indicates that the size of the pores in these membranes gradually increases from skin to sublayer. The latter fact was confirmed by other methods [10, 11].

DDS Membranes

The t-plot of the DDS membranes is given in figure 8. Obviously, the porosity of the DDS membranes is extremely low. The pore size distributions (figure 9) again suggest a gradual increase in pore size from skin to sublayer, but micropores are not found in a measurable extent. The (meso)pores with radii between 2 and 5 nm presumably are present in the skin, whereas the larger pores found are present in the sublayer of the membrane.

Comparison with Permporometry

The pore size distribution of PPO membranes (figure 5) appears to be fairly sharp, which suggests that the pore structure of the skin of the membrane is well-defined. The same membranes were characterized by permporometry, a technique which exclusively determines pores that are present in the skin [chapter 4, ref. 11]. From these measurements it appears that pores as large as 15 nm are present in the skin of PPO membranes. The skin thickness of PPO membranes was found to be well-defined [10]. From the combined measurements the porosity of the skin was calculated to be less than 10^{-5} cm^3/g, which is far too low to be determined by gas adsorption-desorption measurements. For the other membranes (PSf, DDS) the sizes of the pores in the skin determined with permporometry were ranging from 5 to 10 nm, whereas the skin porosities were again very low. The only way to explain the differences in pore size and porosity values found with these different techniques, is that most of the pores determined by gas adsorption-desorption are present in the sublayer of the membranes.

5.4   Conclusions

It has been shown that the concept of a reference isotherm, given by Lecloux, is not always applicable for the characterization of the pore structures of polymeric UF membranes. The observed discrepancy might be caused by micropores present in these samples.

Differences between the pore size distributions calculated from the adsorption branch and those calculated from desorption measurements can be ascribed to network effects. Micropores present in the network may be responsible for the appearance of the non-closed hysteresis loop which is observed for PPO membranes.

The surface area of UF membranes has been found to vary between 170 m^2/g (PPO) and 17 m^2/g (DDS). Most of this surface area represents pores in the sublayer of the membranes that will not influence membrane performance.

5.5   Literature

1. Trägårdh, G. in 'Characterization of Ultrafiltration Membranes', Trägård, G. (ed), p.9 , Lund University, Lund, Sweden, 1987
2. Gregg, S.J., Sing, K.S.W. in 'Adsorption, Surface Area and Porosity', 2nd edition, Academic Press, London, 1982
3. Smolders, C.A., Vugteveen, E. in 'Materials Science of Synthetic Membranes', D.R. Loyd (ed.), p.329, ACS Symposium Series no. 269, Am. Chem. Soc., Washington DC, 1985
4. Zeman, L., Tkacik, G. in 'Materials Science of Synthetic Membranes', D.R. Loyd (ed.), p.339, ACS Symposium Series no. 269, Am. Chem. Soc., Washington DC, 1985
5. Fane, A.G., Fell, C.J.D., Waters, A.G., J. Membrane Sci.9 (1981) 245
6. De Boer, J.H., Linsen, B.G., Osinger, Th.J., J. Catal. 4 (1965) 643
7. Lecloux, A., Pirard, J.P., J. Colloid Interface Sci. 70 (1979) 265
8. Yasuda, H. in 'Polymer Handbook', 2nd ed., J. Brandrup, E. H. Immergut (eds.), p. III-229, Wiley, New York, 1984
9. Barrett, E.P., Joyner, L.G., Halenda, P.P., J. Am. Chem. Soc. 73 (1951) 373
10. Cuperus, F.P., Bargeman, D., Smolders, C.A., J. Colloid Interface Sci 135 (1990) 486
11. Cuperus, F.P., Bargeman, D., Smolders, C.A., Poster presented at the 6th International Symposium on Synthetic Membranes in Science and Industry, Preprints, p.235 Tübingen, September 4-8, 1989

6

Characterization of UF Membranes
Top Layer Thickness, Pore Structure and Membrane Performance

6.1   Introduction

In commercial membrane separation processes anisotropic membranes are preferentially used because of their high efficiency. Such membranes consist of a very thin layer, the top layer or skin, and a supporting layer. In anisotropic UF membranes the small pores in the thin, relatively dense top layer are responsible for the separation characteristics of the membrane and the open sublayer is supposed not to influence the membrane performance. The size distribution of the pores present in the skin determines the selectivity of the membrane whereas the permeability of the membrane is determined by the pore sizes as well as the skin thickness.

Pore size distributions of anisotropic UF membranes can be measured using several independent methods like thermoporometry, gas adsorption-desorption, liquid-liquid displacement and permporometry [1, chapter 1]. These methods allow the measurement of pore sizes in the range of several nanometers to tens of nanometers. Each technique generates one or more membrane parameters which are related to the morphology of the membrane *and* to the specific physical phenomenon on which the technique is based. Due to this combined, sometimes interfering dependence, different methods may give apparently different characteristics. Consequently, a better insight in the pore morphology of the membrane is only possible when a combination of characterization techniques is used. For instance, for a better understanding of the relation between the morphology of a membrane and the transport through this membrane, knowledge of the thickness of the top layer and the size of the 'active' open pores (i.e., pores contributing to the transport) in the skin is needed. These 'active' parameters can be determined by a limited number of characterization methods, e.g., the skin thickness of UF membranes can be estimated with the gold sol method [2, chapter 3] and the size distribution of the interconnected (active) pores can be determined by permporometry [chapter 4].

The structure and the performance of different types of membranes (porous and non-porous) have been discussed by different authors in relation to membrane formation processes [3-7]. For the preparation of different types of membranes (UF, MF, RO, gas separation membranes) made of various materials (organic or inorganic polymers, ceramics, glasses) different processes (sol-gel technique, immersion precipitation, interfacial polymerisation) are used. All these formation processes are based on phase separation phenomena, which often appear to be extremely sensitive towards very small variations of the conditions present during the coagulation process. The main difference between the formation processes is the extent to which the essential, structure determining phase separation steps can be controlled. A better control of these steps makes a preparation procedure suitable for the formation of well-defined (porous or non-porous) structures.

In this chapter the characteristics of ceramic γ-alumina membranes and of polymeric UF membranes made of polysulfone (PSf) and poly(2,6 dimethyl-, 1,4 phenylene oxide) (PPO) are investigated by means of different characterization techniques. The pore size distributions of these membranes are determined using thermoporometry, gas adsorption-desorption and permporometry. The skin thickness of the anisotropic PPO and PSf membranes is measured with the gold sol method. The results observed using the different methods, their relation to the membrane structure and the specific features of the characterization techniques are discussed. Furthermore, it is shown that a combination of relevant parameters can be used to calculate essential performance related characteristics of the UF membranes.

6.2   Experimental

Ceramic γ-alumina membranes were kindly supplied by the group of Burggraaf [6]. Polymeric membranes were made of PSf and PPO in the way described in chapter 3 and 4. The characterization techniques used are described extensively in chapter 2 (thermoporometry), chapter 3 (the gold sol method), chapter 4 (permporometry) and chapter 5 (gas adsorption-desorption).

6.3   Results and Discussion

Although permporometry, thermoporometry and gas adsorption-desorption all are techniques to measure pore size distributions of porous media, their results are not always directly compatible. In the next section differences between the results and the techniques are discussed.

6.3.1 Gas Adsorption-Desorption, Thermoporometry and the Gold Sol Method

Typical pore size distributions of γ-alumina, PPO and PSf membranes found with gas adsorption-desorption and thermoporometry are shown in figures 1-3. It has been pointed out before that results found with these techniques are compatible, provided that the membrane structure does not change or de-swell upon drying [12, chapter 2].

The results obtained for the γ-alumina membrane given in figure 1, illustrate the compatibility of thermoporometry and gas adsorption-desorption measurements. Pore sizes and pore size distributions found with both methods are similar and also the porosity values (pore volume) are not significantly different (45 %) [6, chapter 2].
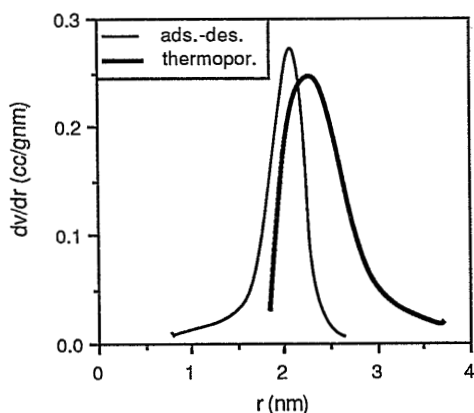

Figure 1. Pore size distributions found for alumina membranes using thermoporometry and gas adsorption-desorption measurements (dv/dr: differential pore volume per g membrane).

Pore size distributions of PPO and PSf membranes are given in figures 2 and 3 respectively. The pore size distribution of PPO membranes found with thermoporometry is very narrow, with a mean pore size of about 2 nm. The analysis of PPO membranes with thermoporometry yielded pore size distributions similar to the ones calculated from gas adsorption-desorption measurements. The pore size distribution calculated from the adsorption branch is somewhat broader than the one calculated from the desorption branch, which is probably due to a network effect, see also chapter 5 [11]. Because thermoporometry and the adsorption isotherm measure real pore sizes and not only necks in pore channels (as are obtained from the desorption branch), the distribution calculated from the adsorption branch agrees better with the thermoporometry data than the distribution calculated from the desorption branch.
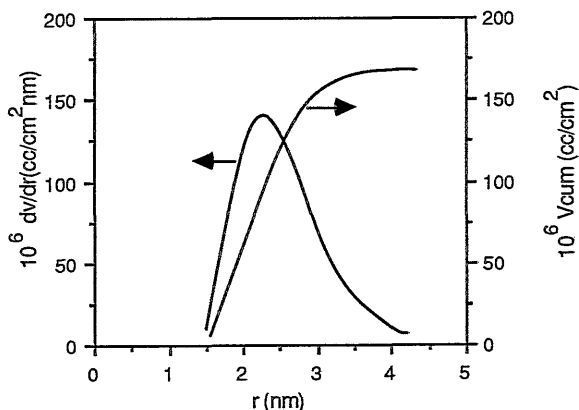
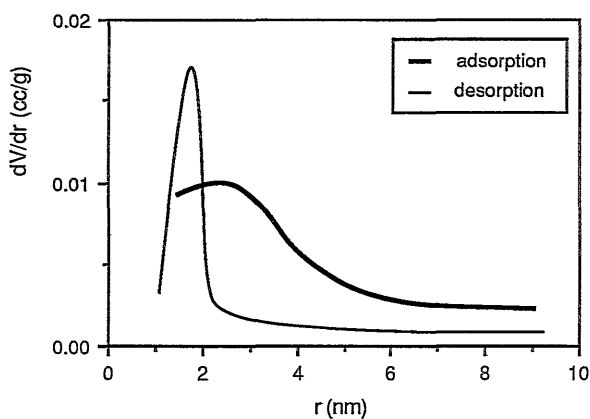*Figure 2a. Pore size distribution of a PPO membrane found with thermoporometry.*

Figure 2b. Pore size distribution of a PPO membrane calculated from the gas adsorption-desorption branch.

The pore size distribution of PSf membranes obtained from thermoporometry as well as from gas adsorption-desorption is fairly broad (fig. 3). The pore volume of the membrane is relatively low, which makes precise measurement of the distribution difficult. Nevertheless, the smallest (meso)pore appears to have a radius of about 5 nm, although the gas adsorption-desorption measurements suggest the presence of micropores (radii< 2 nm) [chapter 5]. Even if these micropores are present, their contribution to the performance (flux) of the membrane is very low and can be neglected in practical situations.

Since PPO and PSf membranes are made by the immersion precipitation method, the skin is assumed to be the most dense part of the membrane which contains the smallest pores. When the pore volume determined by thermoporometry and gas adsorption-desorption is expressed as volume per unit area of top layer (instead of volume per gram of membrane), the skin thickness can be estimated when a pore model of the skin, i.e., a value for the porosity, is assumed. For instance, for PPO membranes a pore volume of $150*10^{-6}cm^3/cm^2$ is found which implies that, when the porosity is set at 100% (so irrealistically, there is *no* polymer present in the skin), the 'skin thickness' would be 1.5 μm.
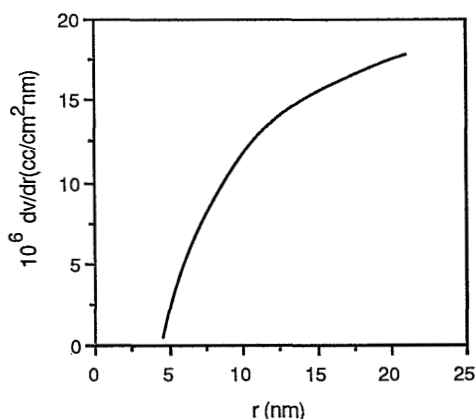

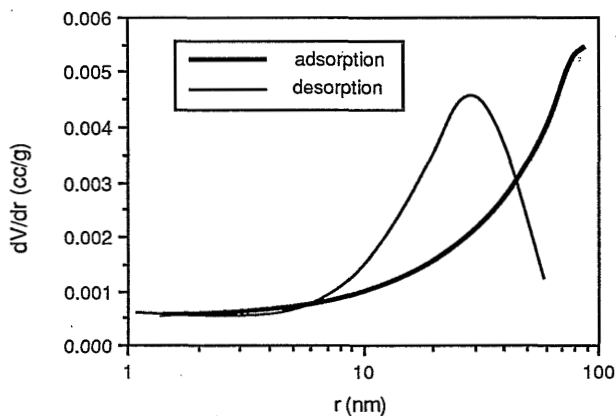*Figure 3a. Pore size distribution of a PSf membrane found with thermoporometry.*

Figure 3b. Comparison of the pore size distributions of PSf membranes calculated from the gas adsorption and desorption branch.

The skin thickness of PPO and PSf membranes was also determined with the more direct technique: the gold sol method [chapter 3, ref. 2]. It was observed that PPO membranes have a

sharply defined top layer with a thickness of 0.2 µm and a pore size very much different from that in the macroporous supporting layer. This thickness does not agree with the smallest thickness that can be calculated from the pore volume (found with thermoporometry or gas adsorption-desorption). It has to be concluded that the pores detected by thermoporometry and gas adsorption-desorption cannot be present in the skin only, but a large part of the pore volume is related to pores in the sublayer.

For PSf membranes the difference between skin and sublayer appears to be less clear. With the gold sol method a distinct skin thickness was not observed and it appears that the size of the pores in these membranes increases gradually from skin to sublayer. This model is supported by the results of thermoporometry and gas adsorption-desorption (fig. 3); the small pores are related to pores in the skin whereas the large pores are present in the sublayer.

6.3.2 Permporometry

Combination of the Techniques
The size distributions of the active interconnected pores obtained for the different membranes are presented in figure 4-6. These pore size distributions have been determined using the concept explained in chapter 4. In this approach the membrane structure is assumed to consist of a bundle of straight capillaries (tortuosity = 1). For the PPO and PSf membranes the number of pores was calculated using a skin thickness of 0.2 µm, as determined with the gold sol method [2]. The thickness of the alumina membrane was 5 µm [6].
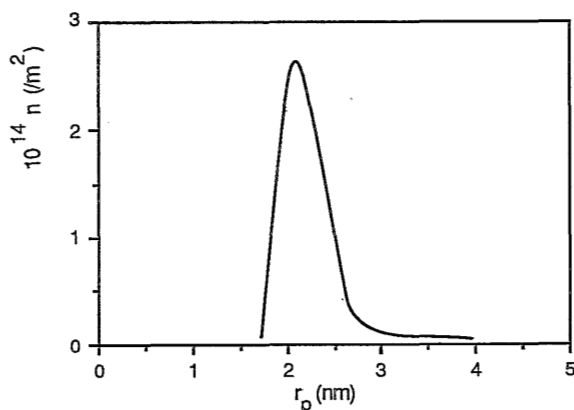

Figure 4. Size distribution of active pores of an alumina membrane measured with permporometry.
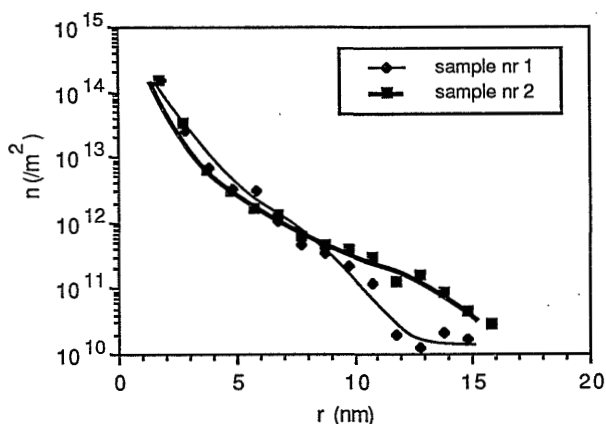
Figure 5. Pore size distributions found for two samples of the same PPO membrane using permporometry.
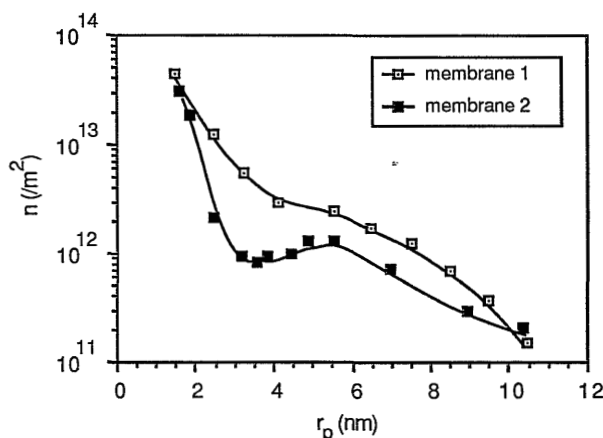
Figure 6. Pore size distributions found for two PSf membranes using permporometry.

The size distribution of the active pores of alumina membranes appears to be very narrow. The average radius agrees well with the values found with the other techniques, i.e., gas adsorption- desorption and thermoporometry. This means that the pores responsible for the performance of the membranes really have a size of about 2 nm. From the number of pores and their sizes, the porosity of the γ-alumina membrane is calculated to be ~1%, a value which is very low compared to the porosity obtained from, e.g., thermoporometry. One of the reasons for this deviation is the very high tortuosity value (τ ~13) of the alumina system which is due to the high aspect ratio of the γ-alumina particles [6, 7]. Furthermore it can be calculated that the thick sublayer of the alumina membrane is responsible for 70 % of the resistance for

diffusional transport of the total system [7]. Since diffusion is the main transport mechanism in permporometry, the effective driving force across the γ-alumina layer is only 30 % of the total during permporometry measurements. When the corrections for the tortuosity (so τ =13 instead of the hypothetical τ =1) and the resistance of the sublayer are used, the calculated porosity is about 40% which agrees with the value found earlier [7].

The size distribution of the open pores in PPO membranes, given in figure 5 is much broader than the pore size distributions determined with thermoporometry or gas adsorption-desorption (figure 2). The largest pore size appears to be ~15 nm, but also pores of a few nanometers are present. For the open pores in PSf membranes a broad distribution was found too, here the largest pore size was about 10 nm. Both membranes exhibit a very low skin porosity; 0.5 % for PPO and 0.3 % for PSf membranes, which are quite normal values for UF membranes [8, chapter 1].

The differences between the pore size distributions measured with permporometry and the ones obtained from thermoporometry and gas adsorption-desorption, can be explained by the pore structure of the membranes and the specific physical phenomena on which the characterization techniques are based. With the two latter techniques all the volume of the (meso)pores present in the whole membrane (skin and sublayer) is measured. Since the volume of the pores present in the skin is very low, it is difficult to detect it with, e.g., thermoporometry. On the other hand, when a considerable number of mesopores is present in the sublayer, these will be measured. Since thermoporometry and gas adsorption-desorption cannot discriminate between pores in the skin and those in the sublayer, the interpretation of the results may be difficult. With permporometry the interconnected open pores present in the skin are detected directly, based on their relative importance for the transport through the membrane. As a consequence, even pores which are present in a very low number (~low pore volume) are detected, provided the gas transport through these pores is high enough.

The Prediction of the Pure Water Flux
From the characterization methods discussed in this chapter, permporometry and the gold sol method are the only techniques which yield characteristic parameters that are really related to the performance of an UF membrane. In order to check the applicability of these characteristics the 'theoretical' pure water flux ($J_{aq,th}$) of the membanes was calculated using the Poiseuille equation (1) and compared with the experimental fluxes.

$$J_{aq,th.} = \{ \pi \, n \, r^4 \Delta p \} / \{ 8 \, \mu \, \tau \, l \} \qquad (1)$$

n : number of pores (1/m^2) $\qquad$ Δp : pressure gradient (Pa)
r : pore radius (m) $\qquad\qquad$ τ : tortuosity (-)
μ : viscosity (kg/ms) $\qquad\qquad$ l : thickness of the active layer (m)

In these calculations the tortuosity factor was assumed to be 1, and for PPO and PSf membranes a skin thickness of 0.2 μm was used (for a cylindrical pore model these assumptions are not necessary; see below). The results of these calculations are summarized in table 1.

One can see that theoretical and experimental pure water fluxes for each type of membrane separately do agree quite well. Also the experimental and calculated pure water fluxes of the alumina membranes agree reasonably well, provided that the data are corrected for the resistance of the sublayer. This indicates that the characteristic parameters of the membranes found with permporometry *and* gold sol method are indeed relevant for the transport properties of the membranes.

Table 1. Comparison of experimental and calculated pure water fluxes

membrane	water flux (l/m^2 hbar)	
	calculated	*experimental*
γ-alumina[*]	2.0-2.5	2.8-3.0
PPO	13-46	15-80
PSf	3-6	3-10

[*] *data corrected for the resistance of the supporting layer, see also text*

The Pore Shape

The agreement between experimental and calculated pure water fluxes, permits one to evaluate the assumed capillary pore shape. With permporometry the contribution of each pore to the diffusional flux is measured. The simplified relation between diffusional transport and pore size for a cylindrical capillary structure, reads:

$$J_{diff.} = \{K \, n \, r^3 \, \Delta p_i\} / \{\tau \, l\} \qquad (2)$$

Δp_i : partial pressure (driving force for transport) (Pa)
K : constant (at constant temperature).

Only in the hypothetical case of a structure with straight capillary pores the tortuosity factor really is 1, and permporometry data can be easily transferred into characteristic membrane parameters. So, provided the thickness of the membrane is known, calculation of the number

of pores is possible, hence the surface and volume porosity can be obtained. However, when the real tortuosity factor of the pores in the membrane is higher than 1, while $\tau = 1$ is still used to calculate the number of pores (see also chapter 4) the pore number, and consequently the porosity, will be underestimated. An observed tortuosity factor lower than 1, of course, leads to a too large number of pores. Depending on the actual 'meaning' of the tortuosity, these two cases can lead to different interpretations of the membrane characteristics and have different implications on calculated performance data (i.e., the pure water flux).

When the number of pores is calculated from permporometry data, a tortuosity factor (τ) of 1 is used. In practice, however, τ is unknown and consequently not the number (n) of pores, but that number divided by the tortuosity factor $(n/\tau) = n_{apparent} < n$ is determined. When the tortuosity is higher than 1 and the apparent number of pores ($n_{apparent}$) is substituted for n, the surface porosity (ε_s) as well as the volume porosity (ε_v) will be underestimated (eq. 3).

$$\varepsilon_s = n \pi r^2 \tag{3a}$$
$$\varepsilon_v = n \pi r^2 \tau \tag{3b}$$

On the other hand, when $n_{apparent}$ as obtained from equation (2), is used to calculate a pure water flux, the actual tortuosity value is of minor importance since the assumed tortuosity values in $n_{apparent} = (n/\tau)$ and in equation (1) cancel and the theoretical pure water flux data should agree with experimental value. However, when the pores differ too much from the cylindrical shape, e.g., the pore consists of wide and narrow parts or has a lot of side-channels (fig. 7), the tortuosity factor no longer has the same value for convective and diffusional transport [10]. Consequently, in that case the theoretical and the experimental flux values are different and the prediction of membrane performance then becomes much more difficult.
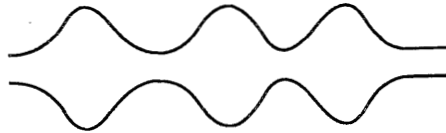
Figure 7. Pore of circular cross-section and varying radius; in such pores the tortuosity values for diffusional and convective transport are not equal.

So from the comparison of *porosity data* found with different techniques one can evaluate whether τ equals 1 or not. For instance, the different porosities obtained with thermoporometry and permporometry for the alumina membranes indicate that the tortuosity is higher than 1 ($\tau=13$; [6]). Agreement of experimental and theoretical *pure water fluxes*, indicates that the

pore shape is at least approximately cylindrical. For all the membranes analysed in this work this approximation appears to be valid, even for the γ-alumina membranes which are supposed to have slit-shaped pores [6].

6.3.3 Pore Characteristics and Membrane Structure

The characteristics presented in the foregoing discussion indicate that ceramic γ-alumina membranes are well-defined, i.e., these membranes have a sharp pore size distribution and a distinct thickness of the active layer. The membranes made by the immersion precipitation technique, i.e., PPO and PSf membranes, exhibit wider size distributions of the active pores and even within one batch of membranes the pore size distributions appear to be significantly different (figure 5 and 6). The gold sol method, on the other hand, indicates that PPO membranes resemble the anisotropic membrane model and indeed have a sharply defined skin in which the pore sizes are much smaller than those in the supporting layer [2]. The large number of small pores found for these membranes using, e.g., thermoporometry, are present in the sublayer of the membrane and do not influence membrane permeability or rejection because of the additional presence of large pores. The PSf membranes studied here do not even have a distinct top layer thickness; the pore size increases gradually going from the top to the bottom of the membrane.

The broad pore size distributions found for the UF membranes made by immersion precipitation, are also reported by other researchers and brought them to the suggestion that this 'indefinite' structure is due to the phase inversion method itself [3, 4, 9]. One of the most popular theories on this subject was developed by Kesting [3], who proposed that the skin layer of membranes made by the phase inversion process basically consists of nodular structures. The difference in structure between several existing types of membranes is related to the packing of the nodules in the skin and the structure of the nodules. For UF membranes the nodule itself is assumed to be dense polymeric material, whereas the interstices between the nodules form the pores of the membrane. Larger pores can be attributed to 'missing nodules'. In this way the structure of the skin can be considered as a defect structure, which inevitably possesses a broad pore size distribution.

One of the questions which arises from the model of Kesting is whether a specific packing of the nodules will occur and to which extent the pore radii depend on the type of packing. The demixing process during which an UF membrane is formed, usually is very fast and when nodules are formed during such a rapid process, a random packing seems more likely than a close packing. Although in a random packing the pore size distribution is not very narrow, very large pores are not expected either. According to Mason [16, 17], who modelled the pore

space in a random packing of non-interacting equal spheres, pores (approximated as cylindrical pores) with radii (r) larger than 0.6 times the radii (R) of the spheres are not present in such a structure. The largest interconnected pore in a network, which is crucial for transport through a membrane, is even smaller (r< 0.3 R) [16]. This means that in a random packed structure the largest pore does not have the size of a nodule, and only when a nodule is missing, pores with a larger size may occur.
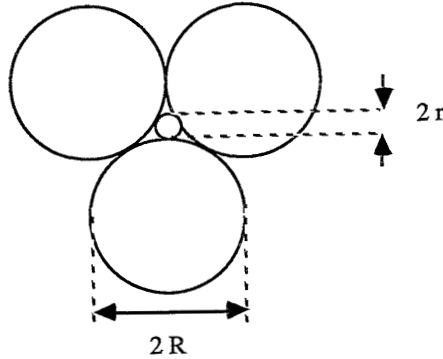

Figure 8. Relation between pore radius (r) in the interstice of a hexagonal packed structure of spheres with a radius (R): r ~ 0.155R.

Following Kestings's concept the size of the pores as well as that of the defects is directly related to the size of the nodule. For instance, the radius of the inscribed circle in an interstice of a hexagonal close-packing of spheres (figure 8) is 0.155 times the radius of the spheres. So, a pore with a radius of 2 nm corresponds which a nodule radius of about 13 nm. These values appear to agree reasonably well with the pore sizes found for the phase inversion membranes analysed in this paper. However, for PPO membranes the number of pores with a size of 2 nm is $\sim 10^{14}$ /m^2 which means that, when the pores are formed by the interstices in a hexagonal packing of nodules, the distance between two pores is about 100 nm. For PSf membranes this distance is even larger (n$\sim$5*10^{13} /m^2 so the distance is about 150 nm). Since the distance between pores is not very dependent on the packing model but is dependent on the size of the nodules, this suggests that, if a nodular structure is present, only a small fraction of the interstices between nodules would act as (small) open pores.

The top layer thickness of PPO and PSf membranes is about 200 nm which corresponds to 8 layers of nodules with a radius of 13 nm. To form an interconnected pore with a size as large as 13 nm in such a skin, at least 8 nodules should be missing on one location. In a packing of non-interacting spheres the presence of pores caused by 'missing nodules' is not very probable because such a structure can reorganize to some extent, and particles are rearranged until a

more perfect packing is reached [18]. Only in a system where the particles 'interact' and cannot move, a defect structure is stable, hence, the maximum pore size can be larger than the limits set by a random packing of equal spheres. This is comprehensible because in that case particles (or nodules) can 'stick together', form aggregates and eventually form a packing of aggregates which contain large pores [18-20]. 'Interaction' between nodules of polymer is likely, e.g., when molecules are part of two or more nodules. On the other hand, the porosity of a compact of equal spheres is about 25 % (hexagonal close packing, [21]) and the porosity of a packing of nodules or aggregates will exceed this value. The porosity of the skin of UF membranes, on the contrary, is very low (~0.5 %). This would mean that during membrane formation, the nascent skin layer is compacted very much and nodules are deformed. The latter would mean that the geometrical considerations, from which the 'nodular structure' is deduced, are no longer valid.

Another point is that a pore in a packed bed does not have a cylindrical shape, but consists of a narrow 'neck' and a wider 'bottle'. Such a pore shape would result in the already anticipated difference between tortuosity factors for diffusional and convective transport. Such a difference is not observed in the analysis of the permporometry data. It has to be concluded that from the characterization data it cannot be deduced clearly whether UF membranes have a nodular structure or not.

It has already been mentioned that membrane formation is prone to very small variations in process parameters. Membrane manufacturers have tried to control the process as closely as possible and the conditions in commercial membrane plants certainly are less fluctuating than those in an ordinary lab. Consequently, the quality of commercial membranes are expected to be at a high level. On the other hand, commercial membranes appear to have broad pore size distributions and fluctuating pure water fluxes too [9, 22], which suggests that these membranes are not well-defined either. Furthermore, Kesting [3, 4] used the data of commercial as well as lab-made membranes and concluded that both 'types' of membranes exhibit a nodular structure, which might be responsible for the 'indefinite membrane structures'. Nevertheless, results obtained with commercial and lab-made membranes should not be compared without further consideration.

6.4   Conclusions

It has been shown that different characterization techniques generate membrane characteristics which are related to the morphology of the membrane and depend on the specific physical phenomenon on which the characterization method is based. Consequently, insight in the membrane structure is only possible when a combination of techniques is used.

Permporometry, a method that measures the size distribution of the active pores, was used to characterize ceramic as well as polymeric membranes. The same type of membranes have been characterized with thermoporometry and gas adsorption-desorption. Using the gold sol method the thickness of the skin layer of PPO and PSf membranes has been determined at about 0.2 µm. It appears that in the case of alumina membranes, results of permporometry and thermoporometry agree very well, whereas for the polymeric membranes large differences in pore size distribution are observed. These differences originate from the structure of the membranes (pores in skin and sublayer) and from the specific features of the characterization methods. Only permporometry measures explicitley skin pores. The different characteristics found with different methods indicate that thermoporometry and gas adsorption-desorption are not always applicable to the characterization of UF membranes. This is due to the very low skin porosities (about 0.5%) of polymeric UF membranes and the mesopores that are sometimes abunemaly present in the sublayer.

From the results observed with permporometry and gold sol method, the pure water flux of the membranes can be predicted appropriately. This indicates that these techniques generate characteristics which indeed determine the performance of the membrane.

The broad pore size distributions of the polymeric membranes found with permporometry can, to some extent, be explained from a nodular structure of polymeric UF membranes.

6.5   References

1. Trägårdh, G. in 'Characterization of UF Membranes', G. Trägårdh (ed.), p. 9, Lund University, Lund, Sweden, 1987
2. Cuperus, F.P., Bargeman, D., Smolders, C.A., J. Colloid Interface Sci. <u>135</u> (1990) 486
3. Kesting, R.E. in 'Proceedings of the Symposium on Advances in Reverse Osmosis and Ultrafiltration', T. Matsuura and S. Sourirajan (ed.), p.3, June 1988, Toronto, Canada
4. Kesting, R.E. in 'Material Science of Synthetic Membranes', D.R. Lloyd (ed.), p.131, ACS Symposium Series 269, Am. Chem. Soc. Washington, DC, 1985
5. Reuvers, B., Membrane Formation, Thesis University of Twente, the Netherlands, 1987
6. Leenaars, A.F.M., Preparation, Structure and Separation Characteristics of Ceramic Alumina Membranes, Thesis University of Twente, the Netherlands, 1984
7. Uhlhorn, R.J.R., Ceramic Membranes for Gas Separation, Thesis University of Twente, the Netherlands, 1990
8. Fane, A.G., Fell, C.J.D., Desalination <u>62</u> (1987) 117
9. Nillson, J.L., A study of Ultrafiltration Membrane Fouling, Thesis Lund University, Sweden, 1989

10. Mason, E. A., Malinouskas, A.P., in 'Gas Transport in Porous Media: the Dusty Gas Model', Elsevier, Amsterdam, 1983

11. Gregg, S.J., and Sing, K.S.W. in 'Adsorption, Surface Area and Porosity', 2nd edition, Academic Press, London, 1982

12. Brun, M., Quinson, J.F., and Spitz, R., Macromol. Chem. 183 (1982) 1523

13. Satterfield, C.N., and Cadle, P.J., I & EC Fund. 7 (1968) 202

14. Eyraud, Ch., Betemps M., Quinson, J.F., Bull. Soc. Chim. France. 9 - 10 (1984) I -238

15. Mey-Marom, A., and Katz M., J. Membrane Sci. 27 (1986) 119

16. Mason, G. J., Colloid Interface Sci. 35 (1971) 279

17. Mason, G. J., Colloid Interface Sci. 41 (1972) 208

18. Hachisu, S., Kose, A., Kobayashi, Y., Takano, K., J. Colloid Interface Sci. 55 (1976) 499

19. Fedors, R.F., Powder Technology 22 (1979) 71

20. Kamide, K., Manabe, S., in 'Material Science of Synthetic Membranes', D.R. Lloyd (ed.), p.197, ACS Symposium Series 269, Am. Chem. Soc., Washington, DC, 1985

21. Rodriguez, J., Allibert, C.H., Chaix, J.M., Powder Technology 47 (1986) 25

22. Fane, A.G. in 'Progress in Filtration and Separation 4', R.J. Wakeham (ed.), vol. 4, p.101, Elsevier, Amsterdam, 1986

Summary

In this thesis various aspects concerning the characterization of anisotropic UF membranes are discussed. Characterization of membrane systems can have different meanings, depending on the purpose for which the data are needed. It may be desirable to have fundamental information about the morphology of the membrane, but certainly the performance is an important aspect of membrane characterization. In this respect two catagories of characteristic parameters are defined: *'morphology related parameters'* and *'performance related parameters'*. Characterization involves the development of three main areas: i) the determination of the porous structure, ii) insight in phenomena which occur during filtration and iii) the development of models to interpret relationships between preparation, morphology and membrane properties. Since the two latter aspects are, at least for a great deal, influenced by the membrane morphology, the determination of the *morphology related parameters* should be the first step in characterizing UF membranes.

The main morphology related parameters of anisotropic UF membranes are: pore size, pore size distribution and thickness of the toplayer. The size distribution of the pores in the skin determine selectivity of the membrane, whereas the permeability is determined by the pore size as well as the skin thickness. There are various methods available for the determination of the pore size, but the data generated are often not very accurate and sometimes characteristics found using different methods are in contradiction with each other. It is pointed out that each characterization method generates one or more characteristic parameters which are related to the membrane structure *and* to the specific physical phenomenon on which the method is based. Consequently, a better insight in the pore morphlogy is only possible when a *combination of techniques* is used.

Pore size distributions measured by means of thermoporometry, gas adsorption-desorption and permporometry are discussed. The first two techniques determine the volume of pores present in the entire membrane, whereas using permporometry the number of pores is determined on the basis of their relative importance for the transport through the membrane, i.e., those pores which are situated in the toplayer of the membrane. Several types of membranes, including

ceramic membranes, are characterized. Throughout the work two different anisotropic polymeric membranes, made of poly(2, 6 dimethyl-1, 4,-phenylene oxide) (PPO) and polysulphone (PSf), are used as special 'standard' systems.

Critical points in the pore size measurement using thermoporometry are discussed in chapter 2. It is shown that thermoporometry can be an effective method for the characterization of porous media that contain pores between 2 and 30 nm. However, when the technique is applied to anisotropic membranes, difficulties arise. Since thermoporometry cannot discriminate between pores present in the top layer and pores of comparable size present in the sublayer, the interpretation of the results with respect to, e.g., membrane performance, needs special care. Furthermore, the skin porosity of UF membranes is so low, that the skin pores cannot be detected by thermoporometry (chapter 6). These two aspects also trouble the characterization of UF membranes by the very well-known gas adsorption-desorption technique. This technique, used extensively for the characterization of inorganic materials, appears to be compatible with thermoporometry, at least when the membrane does not de-swell upon drying. When gas adsorption-desorption measurements are compared with standard reference isotherms, evidence for the presence of micropores (r<2 nm) in (lab-made) PPO and PSf membranes is found (chapter 5). The internal surface area of the membrane, which is also determined from adsorption-desorption analysis, is mainly related to pores present in the sublayer of these membranes.

The size distribution of the active pores is measured using permporometry (chapter 4). For γ-alumina membranes the size distribution of the skin pores is narrow and agrees very well with the data found with thermoporometry and gas adsorption-desorption. The pore size distribution found with permporometry for the lab-made polymeric PPO and PSf membranes, differ substantially from those measured with the two techniques mentioned above. Since the size distributions of the active pores of these membranes are fairly broad, the actual selectivity of the membranes is governed by the larger pores. In chapter 6 it is shown that the pure water flux of the membranes can be estimated appropriately from the permporometry data.

In chapter 3 a new method for the determination of the skin thickness of anisotropic UF membranes is introduced. This method is based on the use of well-defined, uniformly sized colloidal particles, permeated from the rear side of the membrane, combined with electron microscopic analysis of the membrane afterwards. Using this method the skin thickness of the lab-made PPO and PSf membranes is estimated at about 0.2 μm. The skin thickness, together with the size distribution of the active pores form a sound basis from which the surface porosity of the membranes can be calculated (chapter 6). It appears that the surface porosity of the anisotropic membranes is very low (0.5-1 %).

Samenvatting

In dit proefschrift worden verschillende aspekten van het karakteriseren van anisotrope ultrafiltratie membranen behandeld. Het karakteriseren van poreuze media kan vanuit verschillende invalshoeken benaderd worden, maar i.h.a. zal zowel het beschrijven van de morphologische struktuur als ook het bepalen van karakteristieke parameters die gerelateerd zijn aan de uiteindelijke scheidende eigenschappen, de 'performance', essentieel zijn. Er kunnen dan ook twee verschillende typen karakteristieke parameters gedefinieerd worden: *'struktuur beschrijvende parameters'* en *'prestatie gerelateerde parameters'*. Karakterisering van membranen omvat niet alleen de bepaling van deze parameters, maar ook de beschrijving van de relatie tussen beide typen. Omdat de experimentele eigenschappen van membranen primair door de membraanstruktuur worden geinduceerd, is de bepaling van de *'struktuur beschrijvende parameters'* de eerste stap voor het uiteindelijk te beschrijven membraanfiltratie proces.

De belangrijkste karakteristieke eigenschappen van een anisotroop ultrafiltratie membraan zijn de poriegroootteverdeling en de dikte van de toplaag. De selectiviteit van de membranen wordt bepaald door de poriegroootteverdeling in de toplaag, terwijl de weerstand voor vloeistof transport door het membraan bepaald wordt door toplaagdikte én poriegrootte. Ondanks dat de poriegroootteverdeling met diverse technieken bepaald kan worden, schiet het inzicht in de membraanstruktuur vaak te kort. Dit wordt veroorzaakt doordat de technieken gebaseerd zijn op verschillende fysische verschijnselen, zodat de gemeten membraankarakteristiek niet alleen bepaald wordt door de struktuur, maar ook door het meetprincipe zelf. Hieruit volgt dat een groter inzicht in de membraanmorfologie alleen verkregen kan worden wanneer verschillende meetmethoden naast elkaar gebruikt worden.

In dit proefschrift zijn verschillende membranen, waaronder keramische γ-alumina membranen en twee verschillende polymere UF membranen, gekarakteriseerd m.b.v. verschillende methoden. De polymere 'lab-made', membranen werden gemaakt van poly(2, 6 dimethyl-1,4-fenyleen oxide) (PPO) en polysulfon (PSf).

Met behulp van thermoporometrie is het mogelijk de poriegroootteverdeling te bepalen van membranen zonder dat deze gedroogd hoeft te worden (hoofdstuk 2). Er treden echter een

aantal komplikaties op wanneer poriegrootteverdeling in de toplaag van anisotrope membranen bepaald moet worden. De porositeit van de toplaag is in het algemeen erg laag, terwijl in de onderlaag een relatief groot aantal poriën (van vergelijkbare grootte) aanwezig kan zijn. In zo'n geval is het nauwelijks mogelijk om met thermoporometrie poriën in de toplaag aan te tonen.

Dergelijke problemen spelen ook een rol bij het gebruik van gas adsorptie-desorptie (hoofdstuk 5). Het blijkt dat de poriegrootteverdelingen van de verschillende membranen bepaald met thermoporometrie en gas adsorptie-desorptie goed overeenkomen. Verwacht kan worden dat dit alleen geldig is wanneer de membraanstruktuur niet veranderd tijdens drogen. Wanneer de experimenteel bepaalde adsorptie-desorptie isothermen vergeleken worden met standaardisothermen uit de literatuur, zijn er aanwijzingen dat er microporiën (poriestraal<2 nm) in de PPO en PSf membranen aanwezig zijn. Verder blijkt dat het, m.b.v. gas adsorptie-desorptie bepaalde, inwendige oppervlak voornamelijk gerelateerd is aan de poriën in de onderlaag.

De bepaling van de poriegrootteverdeling van de 'aktieve', voor de selectiviteit verantwoordelijke, poriën m.b.v. permporometrie wordt beschreven in hoofdstuk 4. Permporometrie is gebaseerd op het gekontroleerd afsluiten van poriën d.m.v. kapillair kondensatie en het tegelijkertijd meten van het ongehinderde gas transport door het membraan. In tegenstelling tot thermoporometrie en adsorptie-desorptie wordt dus niet het porievolume gemeten, maar de permeabiliteit van de porie (hoe klein het volume ook is). In de skin van de polymere membranen blijken grotere poriën aanwezig te zijn dan werd vermoed op basis van thermoporometrie en gas adsorptie-desorptie. Ondanks hun geringe aantal, zal de aanwezigheid van deze grote poriën van doorslaggevende betekenis zijn voor de membraanprestaties.

De toplaagdikte van de anisotrope PPO en PSf membranen werd gemeten m.b.v. een nieuw ontwikkelde, in hoofdstuk 3, besproken techniek. Beide blijken een toplaag met een dikte van ca. 0,2 µm te bezitten.

De relevantie van de met permporometrie verkregen karakteristieke parameters wordt geillustreerd door het feit dat, uitgaande van deze gegevens, een goede afschatting van de schoonwaterflux mogelijk is (hoofdstuk 6). Wanneer de gegevens van permporometrie gecombineerd worden met de gevonden toplaagdikten, blijkt dat de oppervlakte porositeit van anisotrope UF membranen extreem laag is (ca. 1%). Deze porositeit is inderdaad te laag om met gas adsorptie-desorptie of thermoporometrie gemeten te kunnen worden. Voor γ-alumina membranen komen de poriegrootteverdelingen bepaald met permporometrie en die bepaald met thermoporometrie en gas adsorptie-desorptie goed overeen. Deze keramische membranen zijn goed gedefinieerd en bezitten een zeer nauwe poriegrootteverdeling en hoge porositeit (~45 %). Voor dit soort systemen geven alle drie methoden gelijkwaardige informatie over de voor het transport essentiële poriën.

Curriculum Vitae

Folkert Petrus Cuperus werd geboren op 28 maart 1963, te Meppel. In 1981behaalde hij het VWO-B diploma aan de Rijksscholengemeenschap aldaar. In dat zelfde jaar begon hij de studie Chemische Technologie aan de toenmalige Technische Hogeschool Twente. 'Het modificeren van γ-alumina membranen' was het onderwerp van zijn afstudeerwerk, en na een stageperiode bij Kemira BV, Rozenburg (onderwerp: 'Design of statistical tests to improve CAN quality'), behaalde hij in 1986 het ingenieursdiploma.

Van augustus 1986 tot juli 1990 was hij werkzaam als wetenschappelijk assistent in de groep van professor Smolders, Universiteit Twente. De aldaar verrichtte onderzoek 'Characterization of UF membranes' staat beschreven in het voorliggende proefschrift.

Sinds 1 juli 1990 is F. Petrus Cuperus belast met het membraan technologisch onderzoek bij het ATO, Agrotechnologisch Onderzoeksinstituut, afdeling Agrificatie, te Wageningen.